University of Stavanger

Faculty of Science and Technology

MASTER'S THESIS

Study program/Specialization: **Offshore Technology/Subsea Technology**	Spring semester, 2013 Open
Writer: **Primastono Nugroho**	…… (Writer's signature)

Faculty supervisor:
Prof. Arnfinn Nergaard, Ph.D, University of Stavanger
External supervisor(s):
Leif Hoemsnes, Island Offshore Subsea AS

Titel of thesis:

A Study of Wireline and Downhole Position Control for Riserless Light Well Intervention in Deep Water

Credits (ECTS): **30**

Key words: **Riserless Light Well Intervention** **Monohull Vessel** **Wireline Behavior** **OrcaFlex Software** **Downhole Tool** **Subsea Well**	Pages: 85 pages + enclosure: 33 pages Stavanger, June 15, 2013 Date/year

Abstract

The light well intervention for subsea wells using riserless method has been carried out extensively over the last 10 years to increase the oil and gas recovery from depleted wells. Riserless Light Well Intervention (RLWI) is a relatively new technology that can be used to replace the majority of the well interventions previously done from semisubmersible rigs. RLWI performs subsea well intervention without using a drilling riser package and a subsea BOP. Alternatively, the Well Control Package (WCP) will be installed on top of subsea Xmas Tree as a barrier replacing BOP and then downhole tools can be deployed into the subsea well utilizing wireline from intervention vessel.

The RLWI method is expected to reduce the cost and time in performing well intervention compared to conventional method. But when it comes to lowering down the downhole tool, it has a major issue regarding the accuracy in determining the operational well depth for "in well" work. During RLWI operation in deep water, the environmental conditions will have much influence to the wireline part that is suspended in open water. It is found very difficult to measure part of the cable length that has been submerged into the well since it depends on the "deflection shape" of the cable after it get exposed to the varying sea current from surface to sea bottom. The environmental load from sea current acting along the cable length will be transformed into uplift force on the other end of the cable inside the well. The combination of vertical displacement in upward direction due to uplift force and in downward direction due to cable stretch will affect the accuracy of the well depth measurement and position control of the downhole tool.

Depth accuracy is very crucial in performing work inside the well. This project will study the cable behavior under prevailing dynamic sea environment for RLWI wireline operation in North Sea and will present one approach to correct inaccuracy in determining the exact location of the downhole tool inside the well from marine perspective. The study case was taken from Aasta Hansteen field with 1300 meters water depth in particular. OrcaFlex software will be utilized to perform static and dynamic analysis of the wireline cable under sea current and wave effect. OrcaFlex was developed by Orcina to support a wide range of hydrodynamic and marine structural analysis, including modeling the cable under sea current. During the analysis, the wireline behavior under currents will be observed for different operational well depth cases. The analysis results obtained from OrcaFlex simulations are vertical displacements and forces acting upon the wireline. Then recommended measures are discussed in this thesis to maximize the accuracy during "in well" work with different types of downhole tool weight. In addition, this thesis will also discuss the latest technologies of light well intervention, such as well control equipments used nowadays in RLWI operations.

Acknowledgement

This master thesis is written as final assignment in pursuing two years study Master of Science in Offshore Technology at University of Stavanger. The project was accomplished in the spring semester of 2013 under supervision of Professor Arnfinn Nergaard.

I would like to give my gratitude to him for his guidance, assistance, and willingness during my work. And in this occasion I also would like to thank Mr. Leif Hoemsnes from Island Offshore as my external supervisor for sharing his knowledge and willingness to help me in this master thesis.

I would like to express my gratitude to my lovely girlfriend for her support from far and thanks for waiting for me, to my friends and my brother who always help and care about me. And last but not least, I would like to thank my beloved parents Papa and Mama who always pray, support and encourage me during my study. God bless you always.

Stavanger, 15th June 2013

Primastono Nugroho

Table of Contents

List of Figures

List of Tables

Abbreviations

AHC	Active Heave Compensation
API	American Petroleum Institute
BHA	Bottom Hole Assembly
DHSV	Down Hole Safety Valve
DNV	Det Norske Veritas
DP	Dynamic Positioning
Hs	Significant Wave Height
HXT	Horizontal Xmas Tree
IW	Island Wellserver
LCF	Lower Cursor Frame
LLP	Lower Lubricator Package
LS	Lubricator Section
LUB	Lubricator Tubular
LWI	Light Well Intervention
MD	Measured Depth
MHT	Module Handling Tower
NCS	Norwegian Continental Shelf
NORSOK	Norske Sokkel Standard
PCH	Pressure Control Head
PSA	Petroleum Safety Authority
RAO	Response Amplitude Operator
RLWI	Riserless Light Well Intervention
ROV	Remote Operated Vessel
SCSSV	Surface Controlled Subsurface Safety Valve
TVD	True Vertical Depth
ULP	Upper Lubricator Package
WCP	Well Control Package
WOCS	Work Over Control System
XT	Xmas Tree

CHAPTER 1

INTRODUCTION

1.1 Background

In recent years, production of oil and gas has moved from shallow water to deeper water. Therefore, the use of subsea wells becomes attractive alternative. Some subsea fields have been developed in North Sea, Gulf of Mexico, Brazil, and West Africa. As shown in **Figure 1**, currently there are approximately 5000 subsea wells spread all over the world and it will continue to grow in the years ahead as the exploration goes to deeper water (Island Offshore, 2012). During the production life, subsea wells need interventions to maintain its production and improve its oil recovery rate before it starts to decline. Therefore, well intervention becomes imperative to extend oil field life. Intervention activities can vary from replacing and monitoring downhole equipments, isolating production zone, and logging flow, pressure and temperature (Statoil, Statoil, 2012).

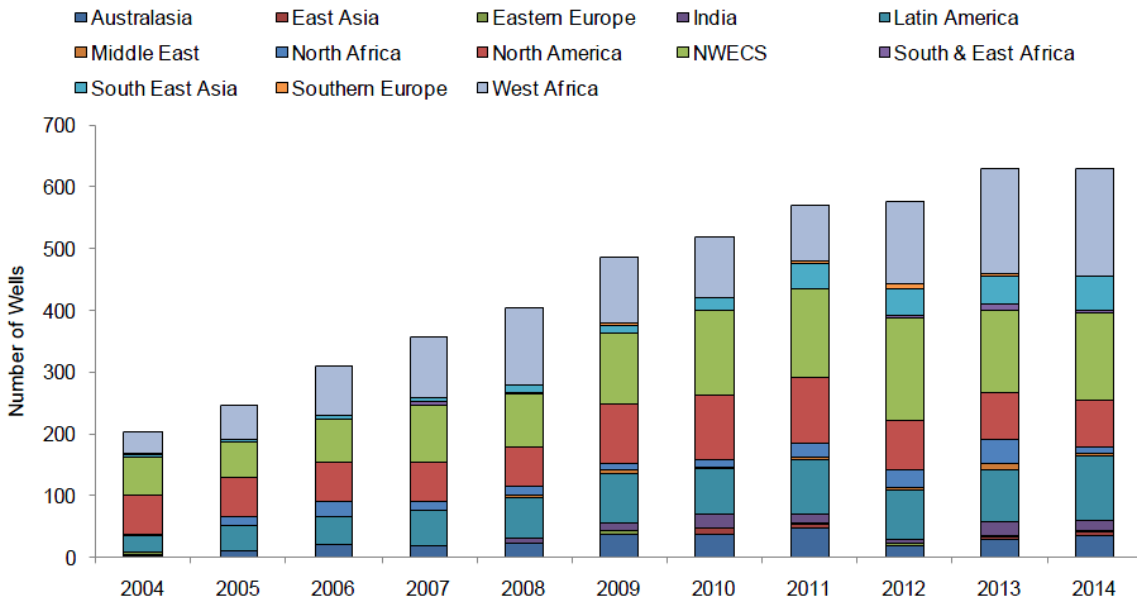

Figure 1. Number of subsea wells starting to produce by region in 2004-2014 according to Infield Systems (Zijderveld, Tiebout, Hendriks, Poldervaart, & GustoMSC, 2012)

A subsea well intervention usually involves very expensive equipment due to more complicated access to the well. Different alternatives needed to be considered to achieve cost efficiency. The conventional well intervention methods utilize drilling rigs which is connected to subsea wells at sea floor using riser and BOP. This method was found time consuming and not cost effective. Anchor handling and anchor tug assistance in addition to the mobilization time was not an ideal solution for efficient well intervention. If the cost can be significantly reduced, intervention and maintenance could be undertaken more often to achieve the targeted oil production rate.

As new technology has been developed, this allows us to carry out light well intervention from monohull vessels instead of semisubmersible rigs. Riserless Light Well Intervention (RLWI) is a relatively new method where well intervention is performed from monohull vessels using wire as a

mean to deploy intervention tools. The deployment system can be guidelineless or using guideline. Guidelines are typically used to guide the RLWI equipment during deployment or retrieval in well intervention. This method can be used to restrict the movement and help the accuracy of well equipment position control during lowering down.

The wireline is used to handle the tool string when performing downhole work in the well bore. During a wireline operation, the effect of sea current on the wireline becomes a major problem, especially for shallow well depth in deep water. In shallower depth of the well, the combined weight of downhole tool and wireline self weight is not large enough to overcome the drag force from sea currents. The force from strong sea currents that acts on the wireline area makes large horizontal and vertical displacements. These displacements can affect the depth accuracy during controlling the downhole tool in deeper water. The operation becomes more susceptible to the environmental condition with increasing of the water depth. Vessel motion with respect to the wave also needs to be further investigated to minimize the lack of accuracy during positioning the downhole tool in the well bore.

1.2 Objectives

This thesis will study the impact of sea currents and well depth in controlling the downhole tool during RLWI operation. The deployment analysis will be modeled using OrcaFlex software. The Aasta Hansteen field is taken as a case of study in this thesis. The main goals of this thesis are:

1. Identifying risks and challenges encountered by RLWI operation in deep water environment.
2. To analyze the behavior of wireline in deep water under strong sea current with respect to vertical position of downhole tool by using OrcaFlex software.
3. Establishing measures required to maximize the accuracy during deployment of the downhole tool.

1.3 Report Structure

This master thesis consists of eight main chapters that can be divided systematically into:

- Chapter 1 Introduction
  This chapter describes brief introduction about well intervention technology, master thesis objectives, and structure of the master thesis report.

- Chapter 2 State of The Art Riserless Light Well Intervention
  This chapter describes the history of Riserless Light Well Intervention technology, its main equipment, its challenges in deepwater operation, and its operation in today's well intervention.

- Chapter 3 Background Theory
  This chapter gives a brief overview of fundamental theory in hydrodynamic forces acting on the RLWI vessel and equipments, tension and deflection, structural design, and marine operation for lifting and subsea operation.

- Chapter 4 Analysis Methodology
  This chapter discusses the methodology used for the analysis and flowchart is provided as guidance for systematically analyzing the problem. In this chapter, OrcaFlex software is also described briefly.

• Chapter 5 Design Case
This chapter contains general description of field being studied and design data required for analyzing the wireline behavior during downhole tool deployment in RLWI operations. The analyses are simulated using OrcaFlex software for wireline types of Sandvik 5R60 Slickline 0.125" and Camesa Monoconductor 7/16". This chapter also describes the design specifications, standards, and regulations that apply in executing well intervention.

• Chapter 6 Analysis Results & Discussions
This chapter discusses the result of analysis from OrcaFlex software and measures that can be taken to improve the accuracy in downhole tool positioning.

• Chapter 7 Summary & Conclusion
This chapter summarizes and concludes briefly the overall analysis results.

• Chapter 8 Recommendation For Future Work
This chapter discusses the possible recommendations for future work in studying RLWI Operation.

CHAPTER 2

STATE OF THE ART OF RISERLESS LIGHT WELL INTERVENTION

2.1 General

Nowadays, there are approximately 5000 subsea wells located all over the world and 1300 of them located in North Sea (Friedberg, Jøssang, Gramstad, & Dalane, 2010). With an increasing demand of oil and gas, subsea field development becomes best alternative to produce oil and gas from larger and deeper field with significantly lower CAPEX compared to conventional oil platform. But all its benefit always comes with a price; subsea equipments located at the sea bottom create another challenge in gaining the access to subsea wet tree for well intervention. There are two main reasons for doing intervention (Zijderveld, Tiebout, Hendriks, Poldervaart, & GustoMSC, 2012):

1. To carry out maintenance on producing well when the production get interrupted.
2. To increase the production recovery rate from mature subsea field.

Since all the subsea activities need to be carried out under the sea, it needs to be supported by sophisticated and advanced tools. It has an impact on higher OPEX compared to fixed platforms. Well intervention is normally intended to extend the life of the subsea wells when the oil production is in declining phase. It means the need to optimize the production from the subsea wells becomes important. Along with the growing number of subsea wells, the need of well interventions increases. Three typical operation categories that can be applied for well intervention are:

1. Light Well Intervention (Category A)
2. Medium Well Intervention (Category B)
3. Heavy Well Intervention (Category C)

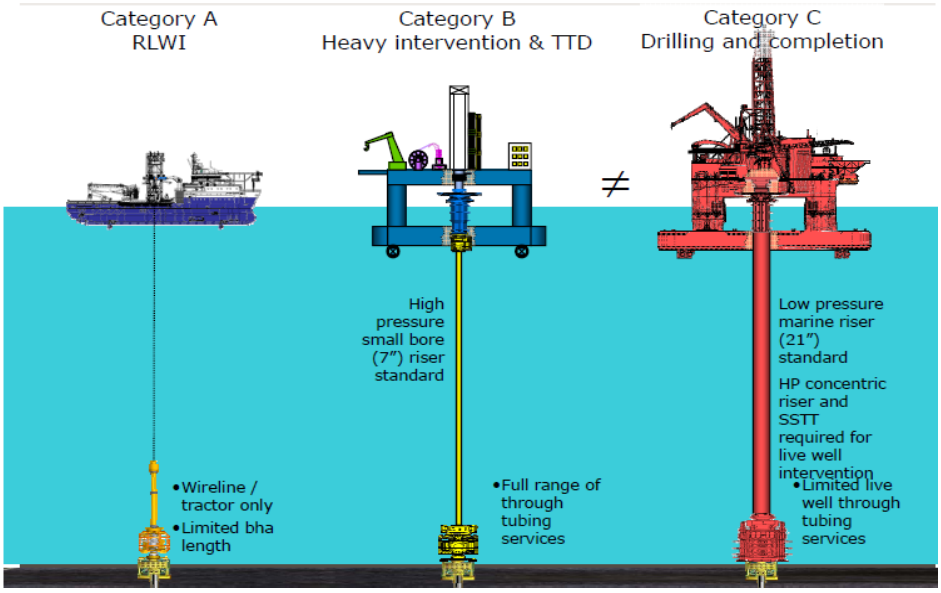

Figure 2. Three categories of well intervention (Jensen, 2008)

2.1.1 Light Well Intervention

Light well interventions are normally type of intervention activities that are performed in existing Xmas Tree and production tubing by using wireline and coiled tubing (Birkeland, 2005). Wireline or coiled tubing can be deployed from a DP-3 class monohull vessel.

2.1.2 Medium Well Intervention

Medium intervention vessels are normally able to attach rigid risers in deeper water and it has bigger deck space to accommodate more complex intervention tools compared to light well intervention.

2.1.3 Heavy Well Intervention

Heavy well intervention is used to perform major workover that need to pull tubing string or re-drill the well. This kind of intervention utilize drilling rig to run marine riser and BOP for containing the pressure from the well bore.

Table 1. Typical operations for different types of well Intervention

Light Well Intervention	Medium Well Intervention	Heavy Well Intervention
- Bore hole logging - Valve repair - Perforating - Fluid displacement - Setting or plugging tubing plugs - Zone isolation - Simulation	- Fishing - Casing leak repairs - Well plugging for abandonment - Sand control - SCSSV repair - Mitigation for paraffin, asphaltenes, hydrates - Cementing improvement	- Tubing packer repair - ESP replacement - Well completion - Re-drilling - Subsea X-mas tree replacement - Well sand control

2.2 Riserless Light Well Intervention

The conventional method can only perform well intervention by using mobile drilling rig. In this case, a riser needs to be connected between the drilling rig and the subsea well tree. Due to size of this drilling rig is big, the mobilization for drilling rig can take a lot of cost and time that prevent the operator to intervene the subsea wells more often for maintenance purpose before it is going towards declining phase. Generally oil platform wells will be intervened at least every 4 years, whereas the subsea well is less frequent (Friedberg, Jøssang, Gramstad, & Dalane, 2010). It causes subsea wells to have lower oil recovery rate compared to platform wells. This problem drives some expertise in this field to come up with new technology that can reduce significantly the time and cost for doing the well intervention.

Riserless Light Well Intervention introduces a system that allows the operator to perform light well intervention regularly and in economical way. This technology provides a way to do well intervention using monohull vessel equipped with dynamic positioning. RLWI has capabilities to perform wireline well intervention instead of riser based intervention.

The UK based “Stena Seawell” completed its first well intervention project in 1998. In 1996 “Stena Seawell” performed what is thought to be the first ever installation of a replacement subsea tree

from a DP monohull vessel. In 1998 they completed the first ever wireline intervention on a horizontal subsea tree.

Figure 3. Subsea Risersless Light Well Intervention (Source: Island Offshore Subsea)

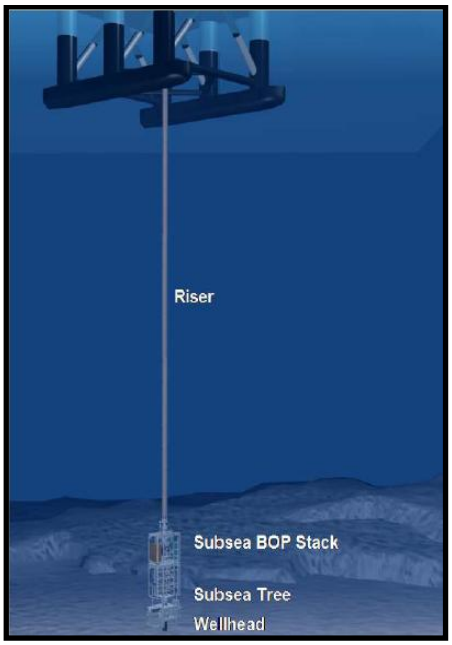

Figure 4. Conventional method for subsea well intervention (Source: Cameron)

RLWI operations from monohull vessels have been done in the Norwegian sector of the North Sea since 2003 and it has been increasing rapidly from 2005 when Island Offshore came into the market with its first monohull vessel. RLWI is normally done for shallow water up to 600 m (Mathiassen, Munkerud, & Skeels, 2008), but recent study has shown that it is possible to do intervention up to 1300 m. With this RLWI operation, oil recovery rate of a subsea well in North Sea is expected to increase from around 45% to 55% (Jøssang, Friedberg, Buset, & Gramstad, 2008). Some of present challenges in nowadays RLWI operation are establishing reliable pressure containment against the wellbore pressure during the well intervention, developing reliable depth control during lowering down the wireline tool strings, increasing the accuracy and control in installation of intervention tools, and avoiding excessive vessel drift off during operation (Crawford & Still, 2010).

2.3 Riserless Light Well Intervention Capabilities

RLWI has capabilities to perform downhole work used to improve production from the existing well. Downhole work for light well intervention includes (Khurana, DeWalt, & Headworth, 2003):

2.3.1 Logging

Well logging is activity to gather some information data from the well by using various sensors and signals that can be transmitted through the electric wireline. The data will be real-time recorded and used for monitoring downhole condition.

2.3.2 Perforating

Perforating is activity to create new perforations in the well casing to make connection to the reservoir and stimulate the oil and gas to easily flow to the well bore. Normally, perforating is done by using electric line to transmit the signal from surface to activate the perforation gun.

2.3.3 Well Cleaning

Well cleaning is used to clean the well bore from scale or sand deposit that can disrupt the well flow. Well cleaning need to be performed regularly to maintain the flow assurance.

2.3.4 Fishing

Fishing operation will be done by using slickline to remove or retrieve unused equipment that is lost in the downhole, such as stuck wireline tools or plugs.

2.3.5 Remedial Cementing/Conformance

Remedial cementing is corrective action to fix the imperfect primary cement job of a well. In addition, cementing can be used to isolate a particular zone for a specific reason such as to shut off the water or gas flow, to re-complete a zone at shallower depth, and to seal a low pressure zone in an openhole before remedial.

2.3.6 Artificial Lift Services

Artificial lift is an effort to increase the flow of oil or gas from an existing well by pumping or injecting gas or water to the reservoir. Artificial lift is needed when there is not enough pressure in the reservoir to transport the product from down the well to the surface.

2.3.7 Surface Controlled Subsurface Safety Valve Repair

Surface Controlled Subsurface Safety Valve (SCSSV) repair is intended to repair or install an insert SCSSV valve.

2.3.8 Tractor Operation

Another challenge that could be faced during well intervention is highly deviated well. For highly deviated well, light well intervention become unfavorable since the wireline is not able to push down the equipment due to the gravity of the equipment is not heavy enough to overcome the friction. For this reason, generally they use coiled tubing for highly deviated wells. But this option was considered expensive and wireline tractor was developed to overcome this problem. The wireline tractor is a new technology that enables the wireline to go through deviated well by using powered motor. The wireline tractor is usually attached to the back of the tool string. The braided electric cable is used for this operation, since an electric power is required to operate the tractor.

2.4 Main System of Riserless Light Well Intervention

2.4.1 Vessel

Riserless Light Well Intervention vessel is designed to have enough space to provide good access for handling the intervention tools. The main component that should be built-in onboard the RLWI

vessel are crane system, heave compensator, skidding system, moonpool as the gate for deploying the equipment, and it has to satisfy Dynamic Positioning Class 3.

Figure 5. The Island Wellserver, delivered in 2008 (Source: Island offshore)

Figure 5 shows one of light well intervention vessel owned by Island Offshore, The Island Wellserver. This vessel was delivered in 2008 and it is a multipurpose vessel that is capable to do light well intervention work, subsea construction, trenching, P&A work, IMR work, and Xmas Tree installation.

2.4.1.1 Dynamic Positioning

Controlling position and motion of the light well intervention vessel is crucial during RLWI operation. Good vessel response with respect to the wave is needed to gain accuracy during lowering down intervention tools. An accurate positioning is required and a computerized DP system becomes a reliable solution. Dynamic position is a computer-controlled system that automatically maintains the position of the vessel and heading by using the vessel's own thruster and propeller. The precision of the positioning is obtained by using thruster, Global Positioning System (GPS), and position reference sensors, such as wind sensors, motion sensors and gyro compasses. These systems will provide accurate information for the computer related to the vessel's position, magnitude and direction of the environmental forces acting on the vessel that affect position of the vessel.

2.4.2 Lower Cursor Frame (LCF)

Lower cursor frame is a special rectangular frame made of steel beams and consists of two prongs and rubber bumper on each side. It will provide horizontal support and control for any equipment that is launched or retrieved through moonpool. A camera and lights are also installed on LCF to give accessibility for the operator to monitor the equipment position when it is entering the moonpool.

Figure 6. Lower Cursor Frame during entering the moonpool
(Jøssang, Friedberg, Buset, & Gramstad, 2008)

Figure 7. Skidding system for equipment handling
(Source: Island Offshore Subsea, 2013)

2.4.3 Moonpool

The moonpool is an open section on the vessel floor that is used to give access for the operator to deploy or retrieve the tools to and from the sea. This system is broadly used on many different vessels. It gives protection and creates sheltered environment; so when the operation needs to be carried out in harsh environment such as in the Arctic, the launched/retreived equipment will not get exposed to surrounding environmental loads. Normally the top of the moonpool will be covered by a hatch system. This hatch system will be closed and locked during mobilization of the vessel and unlocked in open position when the operator needs to run or retrieve equipment through moonpool. The main purpose of the hatch is to protect the equipment on main deck against exposure to slamming wave during vessel mobilization.

2.4.4 Skidding System

Skidding system allows equipment movement or mobilization on deck without using lifting system. The skidding system will enable to handle the equipment horizontally by using skid beam track both in longitudinal and transversal direction. During light well intervention, this system will guide the equipment movement from storage to module handling tower area prior to deployment to sea and vice versa after being retrieved from sea. In addition, this skidding system will restrain the on deck equipment from excessive lateral movement during vessel mobilization.

2.4.5 Module Handling Tower (MHT)

Module Handling Tower is a frame structure made of steel beams used to support vertical handling system for launching or retrieving intervention tools and instruments. The tower is supported by 4 legs standing on the vessel's main deck. Two cursor systems are installed in MHT to ensure safe and reliable deployment/retrieval of the intervention equipment. Upper cursor is utilized to hook up the intervention tools during lifting into the moonpool meanwhile the lower cursor is used as lateral support to restrain the sideways movement of the intervention equipment from the top of the tower all the way down to the vessel's keel.

2.4.6 Heave Compensator

During the operation, vessel will encounter the wave and it will move up and down due to heave. Heave compensator systems are used to compensate the relative vertical movement between the vessel and the tools being deployed. Normally, heave compensator will be installed for crane, wireline system, and umbilical. The wireline compensator is installed at upper wireline sheave wheel located in the Module Handling Tower (MHT).

Umbilical compensation system as shown in the **Figure 8** consists of one compensation sheave and two fixed sheaves. This system will create compensation loop (Friedberg, Jøssang, Gramstad, & Dalane, 2010). The umbilical system is designed to supply hydraulic and electrical function to the subsea well control equipment.

Figure 8. Heave compensation system, control umbilical, and reel installed on MHT (Mathiassen, Munkerud, & Skeels, 2008)

2.4.7 Crane

Crane will provide a support for handling the equipment. The crane will help to transfer the equipment from a supply vessel to RLWI vessel and vice versa.

2.4.8 ROV System

Remote-Operated Vehicle is utilized to assist underwater work without using any divers. It will assist the operator to perform well intervention task and allow the operator to observe the

equipment during deployment underwater. In operation, camera that is attached to the ROV will transmit the images to RLWI vessel to provide monitoring system for the operator to have full control of running and retrieval of subsea equipments.

2.4.9 Well Control Equipment

FMC has invented a RLWI stack that can be deployed from intervention vessel without using any workover riser or a traditional marine riser. This system has used lubricator system that can ensure to insert the tool string without flushing the hydrocarbons back to the vessel or the environment. This new technology from FMC will increase the safety, cost reduction, and integrated operations. The main purpose of RLWI well control equipment is to give safer and reliable tools in entering a subsea well. Well control equipment will create barrier between the well and the environment during performing wireline intervention. The entire system of well control equipment could be deployed from RLWI vessel moonpool equipped with heave compensator. Well control system of RLWI consists of several components that need to be arranged and installed on top of Subsea Tree. The main difference between RLWI system and traditional well intervention is no use of marine riser for rigid connection from subsea tree to topside equipment. There are several RLWI systems available on market in Norway; those are RLWI Mark I and RLWI Mark II. The main differences between RLWI Mark I and Mark II can be listed on below table:

Table 2. Main differences between Mark I and Mark II

RLWI MARK I SYSTEM	RLWI MARK II SYSTEM
It has a heavy assembly of wires shear ram cutting device on top 22 m lubricator tube. It weighs 10 metric tons that needs to be guided on a separate lift line to maintain its stability during lubricator deployment on the seabed	It has smaller and lighter lubricator package. So the deployement of the lubricator can be without guideline. Which in turn, can reduce the possibility of entanglement during deployment
Mark I has a direct hydraulic control system with a surface hydraulic power unit installed. It causes the RLWI Mk I system has bigger diameter of multibore umbilical to accommodate chemical and grease injection.	Due to lighter weight, the length of the lubricator can be increased without affecting the structural stability. The lubricator tube is extended up to 33 meters long
It has a tool trap that can be used to protect the valve located in the well bore and to prevent the tool string from dropping down unintentionally into the well bore.	The RLWI Mark II system uses a smaller electric umbilical combined with a electro hydraulic control and subsea hydraulic power unit.
In case of equipment failure, it can be easily retrieved since most of the control equipment is located on the surface	The Upper Lubricator Pacakge of RLWI Mark II system has a wire shear cutting ball valve that can be used to shear up the 7/16" braided line and seal up the lubricator bore

The RLWI Mark II is more preferable for deepwater operations. It offers easier handling for ROV during the PCH deployment, lighter weight, and reduction of number guidelines used. And the use of a distributed elector hydraulic control system makes the work over control system becomes easier to be monitored and controlled from the surface. The second generation of RLWI stack Mark II was brought to the market on 2009 (Apornsuvan, 2009). Nowadays, RLWI Mark II is mostly used for well intervention operations. **Figure 9** shows common configuration of subsea control system during light well intervention which consists of Well Control Package, Lubricator Section, and Pressure Head Control. This RLWI Mark II is suitable for both subsea Vertical Xmas Tree (VXT) and Horizontal Xmas Tree (HXT). The Work Over Control System on vessel deck will help to control all operations.

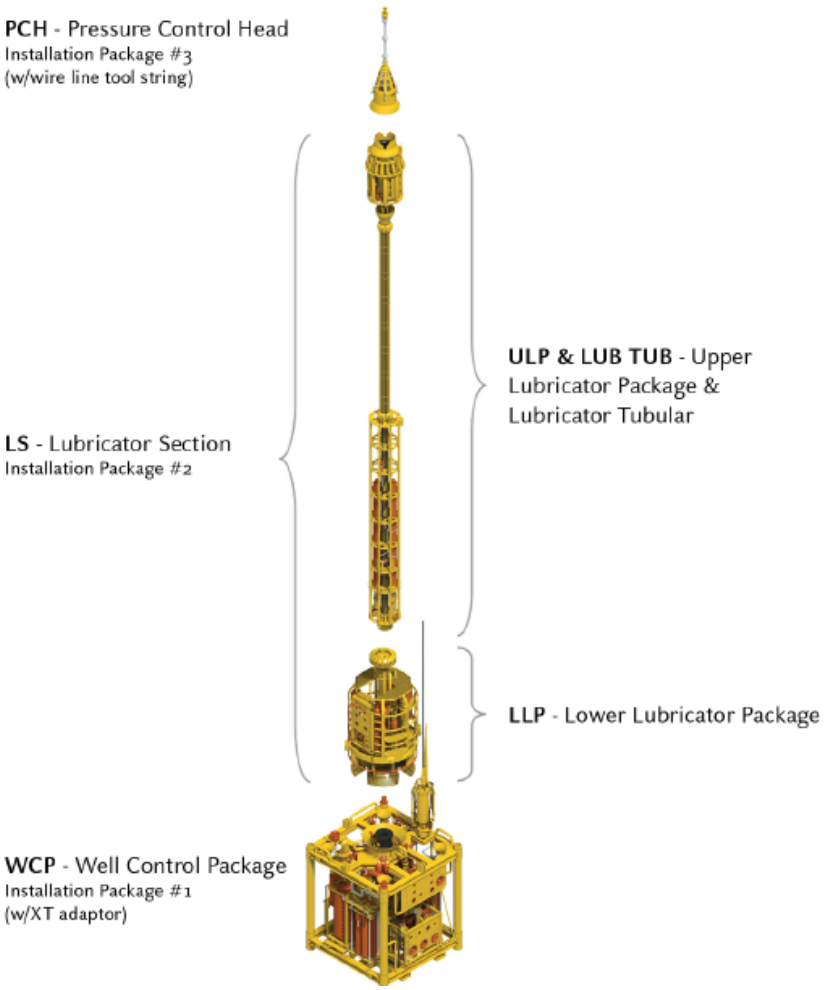

Figure 9. Main configuration of RLWI Mark II system (Source: FMC Technologies)

2.4.9.1 Pressure Control Head (PCH)

Pressure control head is connected directly to lubricator section. The PCH establish subsea well access point for the wireline during well intervention. It is used as a well pressure containment that acts as a seal to allow wireline movement during lowering down the downhole equipment inside the subsea well. It contains grease that is used to lubricate and to create a seal around the moving wireline. The pressure from grease should be higher than well pressure to prevent the oil and gas from coming out of the well and PCH. It also consists of two sealing elements; those are upper and dual stuffing boxes. An upper stuffing box acts as a static seal on a stationary wireline. A dual stuffing box is used as back-up barrier element. The dual stuffing box is equipped with a grease injection point to anticipate gas breakthrough in the flow-tubes. During well intervention using braided wireline, the pressure is created by injecting the viscous grease into the flow tube, making the pressure inside the PCH higher than existing well pressure. To prevent hydrate formation, PCH also provides injection points for MEG. MEG is supplied continuously into the Lubricator from injection point located above the tool catcher. The PCH usually consists of the following components:

- Line wiper
- Upper stuffing box

- Grease injector
- Dual stuffing box with grease injector point
- Tool catcher with ball check valve
- Bend restrictor

Figure 10. Upper left is the PCH, upper right is the ULP, and bottom is Lubricator Tubular (Source: FMC Technologies)

In addition, the PCH can act as a tool catcher to prevent tools from dropping down. This tool catcher is installed below the grease injection point. In case of the wireline being pulled out during returning to its original position in PCH, the tool catcher catches the tool and prevent from losing the tool string downhole. Before the deployment, the PCH is assembled with the wireline and downhole tool string on board. And then it will be guided by means of ROV during lowering down to the seabed.

2.4.9.2 Upper Lubricator Package (ULP)

The Upper Lubricator Package provides safety connection between Lubricator Tubular and Pressure Control Head (PCH) and it also acts as a barrier element during well intervention. The ULP contains wireline Cutting Ball Valve, circulation outlet, and connector to the PCH. The Cutting Ball Valve has capability to shear off 7/16" braided cable and seal up 7" lubricator diameter in case of emergency situation (Mathiassen, Munkerud, & Skeels, 2008). The circulation outlet is used to supply grease.

2.4.9.3 Lubricator Tubular (LUB)

Lubricator Tubular is the mid section of Lubricator Section (LS). The Lubricator Tubular comprises of two grease reservoirs and high pressure grease injection pumps. These two grease reservoirs will provide storage for grease in maintaining well pressure. This Lubricator Tubular also provides temporary storage for tool strings during running in or running out of the well. The Lubricator Tubular holds the entire length of the tool string prior to entering the well. At first the tool string is kept inside the Lubricator Tubular, and then the Lubricator Tubular will be sealed off and pressurized. After the system is pressurized to the well pressure, the tool string can enter into the live well. The lower part of the Lubricator Tubular needs to be designed to bend if it gets exposed to excessive horizontal loads. It will act as weak point in the system that is located in the safety joint above the LLP. This weak point is used to ensure that the excessive horizontal loads will not be transferred to the permanent system.

2.4.9.4 Lower Lubricator Package (LLP)

The LLP assembly is located between Lubricator Section and Well Control Package (WCP). It provides connection point between the Lubricator Tubular and the Well Control Package in the Riserless Well Intervention stack-up. The LLP consists of Subsea Control Module (SCM), Hydraulic Power Unit (HPU), and accumulators.

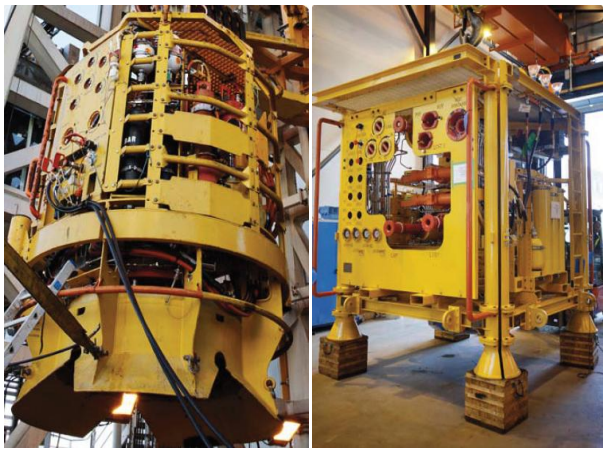

Figure 11. Left is the LLP and right is WCP (Source: FMC Technologies)

2.4.9.5 Well Control Package (WCP)

The WCP is located on top of the subsea Xmas Tree. WCP is primary equipment to control the well flow during performing well intervention. It is used as a main barrier against the pressure from well. It serves same purpose as BOP in drilling and well completions. It comprises of shear /seal ram, upper valve block, and lower valve block. At the lower section of WCP, there is an interface to connect the Xmas Tree re-entry hub and the WCP. The WCP can be installed for both Horizontal Xmas Tree (HXT) and Vertical Xmas Tree (VXT). In case of emergency situation, the shear ram is able to cut the wireline, coiled tubing, or wireline tool string inside the well bore. Main functions of The WCP (FMC, 2012):

- Main well barrier system
- Mounting base for control module and UTH
- Provide quick cutting system for wireline, coiled tubing, and wireline tool string in case of emergency situation

- Provide flushing back system for the hydrocarbon into the well
- To provide hydraulic pressure and supply, and communication with Subsea Tree functions

2.4.9.6 Work Over Control System (WOCS)

The RLWI Control System is responsible to control the RLWI stack and supply required fluids during well intervention services. The control system consists of electro and direct-hydraulic functions. The topside control system is using electric, whereas the subsea part is able to generate hydraulic power. The topside control system in RLWI operation normally consists of following main components:

- Main umbilical
- Chemical Injection Unit (CIU) for flushing of hydrocarbons and hydrate inhibitors
- Grease Injection Unit for providing subsea grease injection

The surface controllers are supported by back-up batteries for autonomous control. All the communication functions between topside and subsea equipment will be provided by 10 Mbit/s Ethernet (FMC, 2012).

2.4.10 Wireline

Wireline is a means to lower the equipment or monitoring devices down to a well to undertake intervention activities. Normally wireline technology will be used to perform various light well intervention tasks including scale removing, perforating, plug retrieval, and logging. The wireline for performing intervention can be categorized into slickline, braided wire, and composite wire.

Table 3. Characteristics of three different types of wireline (Wright, 2011)

Slickline Wire			
Normal Diameter	Material / Type	Breaking Strain	Remarks
0.108"	UHT Carbon	2730 lbs	Poor corrosive resistance sour gas applications
	Supa 75	2100 lbs	
0.125"	UHT Carbon	3665 lbs	Poor corrosive resistance sour gas applications
	Supa 75	2700 lbs	
Braided Wire			
7/32"	Conventional	5400 - 6010 lbs	Dyform considerably stronger
	Dyform	6500 - 8370 lbs	
5/16"	Conventional	11000 - 13490 lbs	Very high breaking force gives the operator better margins when carrying out fishing operations
	Dyform	13560 - 177550 lbs	
Electric Line Wire			
7/32" Poly Cable	Mono conductor cable widely used for e-line operations	Typically 5200 lbs	Cable type will depend of well conditions and operation conducted
5/16" Poly Cable	Mono conductor cable	Typically 11000lbs	Commonly used for logging and perforating

2.4.10.1 Slickline (S-Line)

Slickline is a pure solid wireline without using electric cable that is used to perform only downhole mechanical work. This mechanical work is created by e.g. the operation of jars (hammer). Slickline can be used for retrieving other equipment or wire that has been dropped down into the hole (fishing operation). The size of slickline can range from 3/32", 7/64", and 1/8" diameter (Khurana, DeWalt, & Headworth, 2003). A wireline tool string will be attached to the slickline to perform downhole operation. Normally wireline tool string will consist of:

- Wireline Socket (Rope Socket) for connecting the wireline to the tool string.
- Wireline Stem (Sinker Bar) as an additional weight of the tools in overcoming pressure from the well. So it can make the tool going downward into the well bore by its gravitational weight. It also reduces the friction with elastomers of stuffing box and ensures the wireline is running smoothly against well pressure.
- Wireline Jars is used to generate mechanical shock or hammering effect to the tool string either downwards or upwards. This shock can create locking or unlocking system for certain components such as in plugging operations.
- Wireline Knuckle Joint is located right after mechanical jar and used to give more flexibility to the tool string in deviated wells.
- Different tools that can be attached at the bottom of tool string:
  - Running tools
    These tools are designed to run or retrieve dowmhole devices from the well bore
  - Pulling tools
    These tools are used for retrieving or fishing wireline components that are located in downhole.
  - Gauge cutter
    It can be used to clean inside the tubing from paraffin that might have built up during production.
  - Lead impression block
    It can help to determine the nature of an obstruction that might have been found in the downhole. It is also called wireline camera because it can be used to mark any object inside the well.
  - Bailer
    It is a downhole device that can be used to collect downhole samples such as sand, scale, asphaltene, and debris from well operations.
  - Go devil wire cutter
    This tool is used in situations when the wireline tool string becomes fouled, it will be able to cut conventional wireline
  - Wireline finder
    This tool is used to collect broken wire or cable in the downhole well
  - Broach
    It is used to clean well from wax or scale

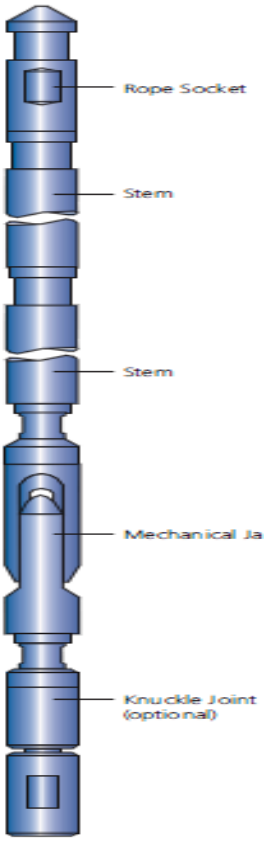

Figure 12. Wireline tool string configurations for downhole work (Source: Leutert)

2.4.10.2 Braided Line

Braided line has two types, which are with electric cable and without electric cable. This type of wireline is stronger than slickline. Normally, the braided line without electric cable is used for heavier fishing operations. The braided line with using electric cable can continuously transmit data to the surface to perform logging task and well tractor operations. The diameter of braided line ranges from 7/32", 5/16", and 7/16" (Harestad, 2009). The larger the diameter, the more height is needed to overcome the well pressure.

2.4.10.3 Composite Cable

The need to develop more cost efficient technology for the light well intervention using wireline becomes important. New type of wireline has been introduced, it is called composite wireline. This kind of wireline is capable of performing all well intervention operation in subsea wells, replacing the use of braided line and slick line. The advantages using composite cable are higher strength, lighter weight, and higher capacity in transmitting the electrical power compared to previous wireline technology. The composite cable consists of three insulated copper conductors wrapped by carbon fibres in a matrix of thermosetting plastic. With this kind of configuration, this cable can sustain in higher temperature and pressure during the well work. And it is expected to reach deeper well sections that cannot be reached by nowadays wireline technology.

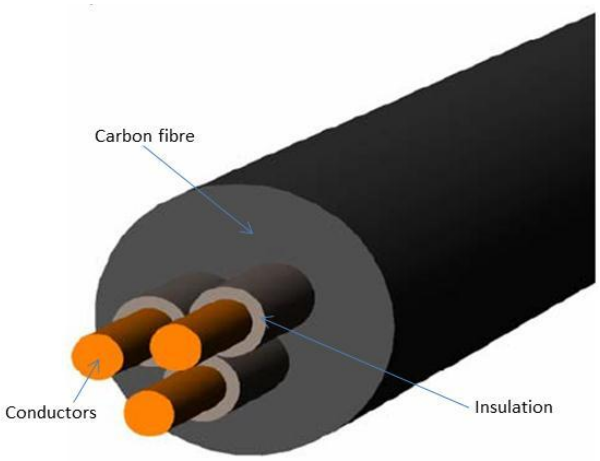

Figure 13. Illustration of composite cable (Munkerud & Inderberg, 2007)

2.5 Riserless Light Well Intervention Operation

The Well Control Package, the Lubricator Section, and the Pressure Control Head are installed one by one. The WCP and the LS are installed first prior to the installation of the sealing section and tool string. The PCH will be installed and lowered down through the vessel moonpool along with sealing section and tool string. The ROV will be utilized to orient and position the tool string when it lands on top of the Lubricator Section. After the deployment of the tool string, the sealing section will be pressurized to the well pressure using glycol. Then the valve in the WCP is opened to allow the tool string entering into the well bore, in the mean time the glycol is flowing to the well. On the surface, winch will pay out wireline from the vessel to lower down the tool string. As the wireline goes through the well, grease is injected into the sealing section to maintain the pressure between well and sea water. The RLWI Stack deployment can be performed with using guideline or guideline less. For the heavy elements can be deployed and retrieved without guide wire, such as WCP. Whereas low weight elements need to be deployed and retrieved using guide wire, such as hoses. Low weight elements especially with a large area will get exposed to the sea currents and it causes a large drift off during deployment. If the drift off is too large, the ROV cannot handle to bring the low weight equipment to its right position. Following is the typical procedure of deployment and retrieval equipments for wireline intervention:

1. ROV survey and removal of debris cap
   - Open hatch using vessel main crane.
   - ROV will retrieve the debris cap.
2. Deployment of the Well Control Package (WCP)
   - Prepare the WCP and WCP Running Tool. Then skid it into the moon pool.
   - Hook up the main wire to WCP RT.
   - Lift WCP, inspect XT connector, and launch the WCP through the moon pool.
   - ROV will guide the deployment
   - Activate the Active Heave Compensator (AHC) on main wire when the WCP is almost closed to the subsea template.
   - ROV helps to orientate and guide the WCP for landing.
   - Land smoothly the WCP onto subsea Xmas Tree.
   - Retrieve and lift WCP Running Tool back into the vessel.

- Secure the WCP Running Tool to the deck, land it out on skid rails, and disconnect the main wire from the WCP Running Tool.
- Close moon pool hatch.
- Mobilize the WCP Running Tool into the WCP hangar.

3. Deployment of the Lubricator Section (LS)
   - Prepare the LS for running.
   - Connect the LS Running Tool to main wire.
   - Lift the LS Running Tool up while the LS is moved into the middle of the Module Handling Tower (MHT).
   - Land the LS Running Tool onto the top of the Upper Lubricator Package (ULP)
   - Secure and lock up the LS Running Tool to the ULP.
   - Run the LS to the sea through the moon pool.
   - Once it is almost close to the WCP, activate the AHC for main winch.
   - During deployment, ROV will help to orientate and position the LS for landing.
   - Land out the LS on top of the WCP.
   - Retrieve and lift back the LS Running Tool into the vessel.
4. Deployment of the Pressure Control Head (PCH) and the Tool String
   - Prepare the PCH and the wire.
   - Assemble the tool string.
   - Connect the PCH Running Tool to the main wire.
   - Mobilize the PCH into center of moon pool area.
   - Lift the PCH and attach the PCH Running Tool.
   - Launch the PCH and the tool string through the moon pool using guide wire.
   - Guide and position the tool string into the Lubricator Tubular.
   - Land out the PCH.
   - Retrieve the PCH Running Tool to the vessel deck.
5. Run in the tool string with the wireline
   - Start injecting the grease into the PCH.
   - Pressure tests the Lubricator Tubular.
   - Open subsea Xmas Tree.
   - Open the WCP.
   - Lowering down the tool string to perform downhole operations.
6. Retrieve the tool string and the wireline
   - Lift the tool string back into Lubricator.
   - Close the barrier elements.
   - Perform inflow test of barriers.
   - Flush hydrocarbons back into the well.
   - Run and connect back the PCH Running Tool.
   - Retrieve the PCH and the tool string.
7. Retrieve the Lubricator Section
   - Launch the LS Running Tool on main wire.
   - Activate the AHC on main wire, once the LS Running Tool is located above the ULP.
   - ROV helps to position and orientate the LS Running Tool for landing into the ULP.
   - Connect the LS Running Tool into the ULP.
   - ROV help to unlock the LLP connector.

- Retrieve the LS to the vessel deck.

8. Retrieve the Well Control Package
   - Connect and run the WCP Running Tool.
   - Deploy the WCP Running Tool through the moon pool.
   - Activate the AHC on main wire, when the WCP Running Tool is closed to the WCP.
   - ROV helps to rotate and position the WCP Running Tool for landing on the WCP.
   - Land the WCP Running Tool and ROV will unlock the connector between the WCP and Subsea Xmas Tree.
   - Retrieve the WCP and the WCP Running Tool to the surface.
   - Land the WCP on the skid and mobilize the WCP from moon pool to hangar.

2.6 Risk and Challenge in RLWI Operation

There are some challenges that present in RLWI operation, especially for deep water. Those risks and challenges are:

1. Experience

There is only limited experience from wireline operation through open water using monohull vessel at deep water till these days. And besides, there are not many investigations and study about how wireline behavior under various sea currents can affect the depth accuracy of downhole tool inside the well. These problems create new challenges in planning and operational activities.

2. Simulation Software

There is no available software for simulation that is capable of incorporating both conditions, open water and in well simulations. It makes the analysis becomes difficult to approach real condition during RLWI operation.

3 Depth Control Accuracy

Deflection and depth accuracy becomes the most important factors in RLWI operations. Large horizontal deflection on cable may lead to excessive friction in top of PCH. It means that downhole weight needs to be increased to reduce the deflection, but this heavier downhole weight will create higher tension at surface while the cable tension must be kept not to exceed the working load limit (WLL).

CHAPTER 3

BACKGROUND THEORY

3.1 Waves Theory

Waves are one of the limiting factors in offshore operations. A vessel that gets exposed to the sea waves will have six degrees of freedom: heave, pitch, roll, surge, sway, and yaw. Unfavorable wave can lead to offshore operation downtime and increase the cost. Wave height and period can be forecasted for some particular areas. The height of the wave is determined by wind speed, duration, and the fetch length. Normally, waves are generated by the wind blowing over the sea surface. Waves will transfer the energy from winds. This energy will be accumulated as the waves propagate. The accumulated energy in a wave is proportional to the square of the wave height. Therefore, long period waves have higher energy. Waves normally have periods of 5-15 seconds, whereas swells may have periods of 20-30 seconds (Gerwick, 2000).

Since ocean waves are generally unpredictable in the nature, there are several theories about wave that can be used to describe wave characteristics. These wave characteristics are important as inputs for designing offshore structures or making decision in marine operations. One of them is regular wave theory. Regular waves will have same form and characteristics in each occurrence. Main parameters that can be used to describe the characteristics of the wave are period (T) which means the time needed for two wave crests to pass through consecutively a point, height (H) which means the vertical height between the crest and the trough, water depth (d) which is the vertical distance from mean sea level to the seabed, and wave length (L) which means the distance between two successive crests or two successive troughs.

3.1.1 Regular Waves

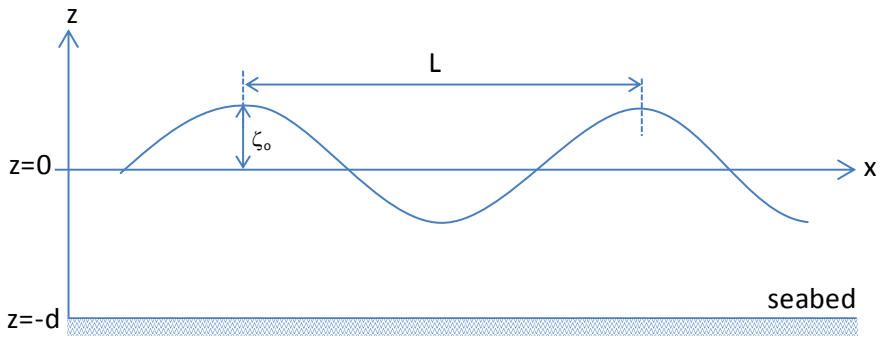

Figure 14. Regular wave profile

Figure 14 above shows a harmonic wave profile; the z-axis is positive for upward direction from mean sea water level, the x-axis is positive in same direction as wave propagation. The crest is the highest point of the wave profile and the lowest point is called trough. The wave amplitude is the distance from mean sea water level to the crest or to the trough. So the wave height H can be measured as:

$$H = 2\xi_a \tag{3.1}$$

If the wave is moving along the x positive direction, the wave profile can be describes as a function of cosines of x and t:

$$\xi = \xi_a \cos(kx - wt) \tag{3.2}$$

Otherwise, if a wave is moving in the opposite direction (x negative), the wave profile can be expressed as:

$$\xi = \xi_a \cos(kx + wt) \tag{3.3}$$

3.1.1.1 Water Particle Kinematics

This subchapter will adopt basic theories from *Gudmestad (2010).* The sea water can be assumed incompressible, inviscid, and irrotational. Based on those assumptions, the water potential velocity needs to satisfy following Laplace equation as follows:

$$\frac{\partial^2 \varphi}{\partial x^2} + \frac{\partial^2 \varphi}{\partial y^2} + \frac{\partial^2 \varphi}{\partial z^2} = 0 \tag{3.4}$$

By solving the Laplace equation with using three boundary conditions, those are sea bed boundary condition, free surface dynamic boundary condition, and free surface kinematic boundary condition; we can find wave potential velocity. The sea water is assumed not be able to penetrate the sea bed, it means the vertical water velocity at the bottom should be zero all the times:

$$w\big|_{z=-d} = 0 \Rightarrow \left.\frac{\partial \varphi}{\partial z}\right|_{z=-d} = 0 \tag{3.5}$$

Kinematic boundary condition states that motion of the fluid particle at the surface must remain at the surface all the times. The kinematic boundary condition can be expressed as follows:

$$w = \frac{\partial \varphi}{\partial t} = \left(\frac{\partial z}{\partial t} + u \cdot \frac{\partial z}{\partial x}\right)\bigg|_{z=\xi(x,t)} = \left(\frac{\partial \xi}{\partial t} + u \cdot \frac{\partial \xi}{\partial x}\right) \tag{3.6}$$

To simplify the kinematic boundary conditions equation, it can be linearized by eliminating the u∂ξ/∂x term. So the expression becomes:

$$\left.\frac{\partial \varphi}{\partial z}\right|_{z=\xi(x,t)} = \left.\frac{\partial \varphi}{\partial z}\right|_{z=0} = \frac{\partial \xi}{\partial t} \tag{3.7}$$

The last boundary that needs to be satisfied is the pressure at the surface must be the same as the atmospheric pressure. This boundary can be derived from Bernoulli's principle:

$$\frac{P}{\rho} + g.z + \frac{\partial \varphi}{\partial t} + \frac{1}{2}\left(u^2 + w^2\right) = C(t) \tag{3.8}$$

By substituting z with ξ (at surface), equation 3.8 can be simplified and linearized as follows:

$$g \cdot \xi + \left.\frac{\partial \varphi}{\partial t}\right|_{z=0} = 0 \Rightarrow \xi = -\frac{1}{g} \cdot \left.\frac{\partial \varphi}{\partial t}\right|_{z=0} \tag{3.9}$$

Hence, the potential velocity φ can be found by solving the Laplace equation with using three boundary conditions. Therefore, the potential velocity function can be given as follows:

$$\varphi(z,x,t) = \frac{\xi_0 \cdot g}{\omega} \cdot \frac{\cosh k(z+d)}{\cosh(kd)} \cdot \cos(\omega t - kx) \tag{3.10}$$

Horizontal direction

The horizontal velocity of the wave can be obtained by taking derivatives of the velocity potential function with respect to ∂x.

$$u = \frac{\partial \varphi}{\partial x} = \frac{\xi_0 \cdot g}{\omega} \cdot \frac{\cosh k(z+d)}{\cosh(kd)} \cdot (-1) \cdot \sin(\omega t - kx) \cdot (-k)$$

$$= \frac{\xi_0 \cdot k \cdot g}{\omega} \cdot \frac{\cosh k(z+d)}{\cosh(kd)} \cdot \sin(\omega t - kx) \tag{3.11}$$

The horizontal velocity function will have its maximum value at crests, when sin (wt-kx)=1 and minimum value at troughs, when sin(wt-kx)=-1. The wave horizontal particle acceleration can be derived from the wave horizontal velocity function as below:

$$\dot{u} = \frac{\partial u}{\partial t} = \xi_0 \cdot k \cdot g \frac{\cosh k(z+d)}{\cosh(kd)} \cdot \cos(\omega t - kx) \tag{3.12}$$

The horizontal acceleration of the wave particle will be maximum when the value of cos(wt-kx)=1, when the wave particle cross through the mean sea water level.

Vertical direction

The vertical velocity of the wave particle can be derived from potential velocity with respect to ∂z. This vertical velocity can be expressed by following equation:

$$w = \frac{\partial \varphi}{\partial z} = \frac{\xi_0 \cdot g}{\omega} \cdot \frac{\cos(\omega t - kx)}{\cosh(kd)} \cdot \frac{\partial}{\partial z}(\cosh k(z+d))$$

$$= \frac{\xi_0 \cdot g}{\omega} \cdot \frac{\cos(\omega t - kx)}{\cosh(kd)} \cdot (\sinh k(z+d)) \cdot k$$

$$= \frac{\xi_0 \cdot k \cdot g}{\omega} \cdot \frac{\sinh k(z+d)}{\cosh(kd)} \cdot \cos(\omega t - kx) \tag{3.13}$$

The wave vertical velocity will be zero at wave crest, when the value of cos(wt - kx) = 0. The wave particle acceleration at vertical direction can be obtained by taking derivatives of the wave vertical velocity as follows:

$$\dot{w} = \frac{\partial w}{\partial t} = -\xi_0 \cdot k \cdot g \frac{\sinh k(z+d)}{\cosh(kd)} \cdot \sin(\omega t - kx) \tag{3.15}$$

At wave crests, the vertical acceleration of the wave will have its maximum since the value of sin(wt - kx) equal to 1.

3.1.2 Irregular Waves

The regular wave theory is suitable for more conservative designs which only consider a single wave. In this theory, a possible extreme wave will be simply represented by a regular wave with certain period and height. However, in the reality the wave cannot be well described by only using simple sinusoidal formula; it is irregular, random, and sum of many different regular waves with various wave lengths, frequencies, or periods. The irregular waves can be approached using wave energy spectrum method. This wave energy spectrum shows the wave energy distribution in many

different wave frequencies of the irregular ocean wave. Fourier series can be used to analyze the irregular wave as a sum of different regular waves as shown in **Figure 15**.

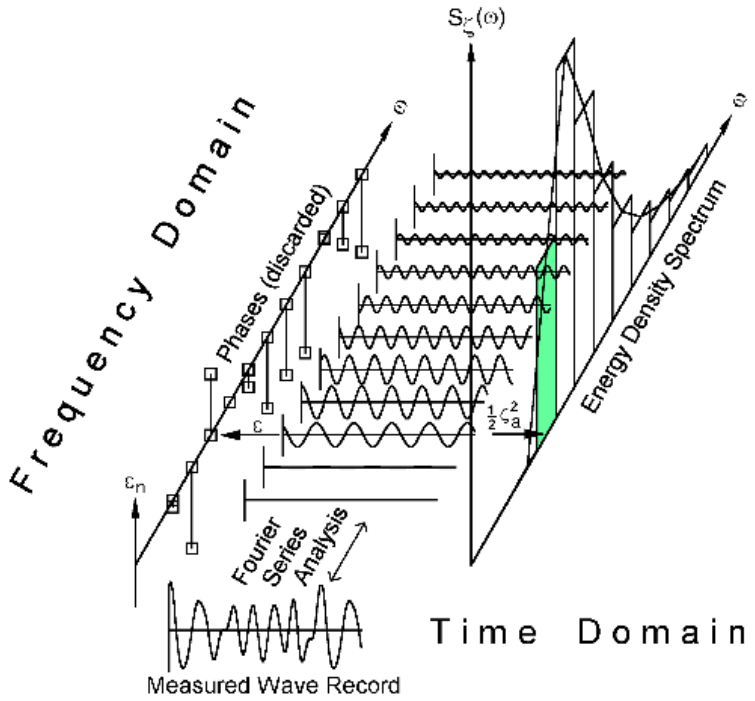

Figure 15. Irregular wave analysis (Journée & Massie, 2001)

According to *Journée & Massie (2001),* an irregular wave profile can be expressed in the following formula as the sum of many regular wave components that travels along positive x-axis during time period –T/2 to T/2:

$$\zeta(t) = \sum_{n=1}^{N} \zeta_{a_n} \cos(k_n x - \omega_n t + \varepsilon_n) \tag{3.16}$$

Where:

ζ_{a_n} = wave amplitude (m)

ω_n = angular frequency (rad/sec)

k_n = wave number (rad/m)

ε_n = random phase angle (rad)

From Fourier analysis, an irregular wave can be broken down into many regular waves. Each regular wave has different characteristic, e.g. wave amplitude, wave length, or wave period. Since the wave energy is proportional to the wave amplitude squared, a wave energy spectrum can be calculated as follows:

$$S(\omega_n) = \frac{1}{2}\frac{\xi_{a_n}^2}{\Delta\omega} \tag{3.17}$$

A graph of spectral density function can be plotted by calculating the wave energy spectrum function for different frequencies:

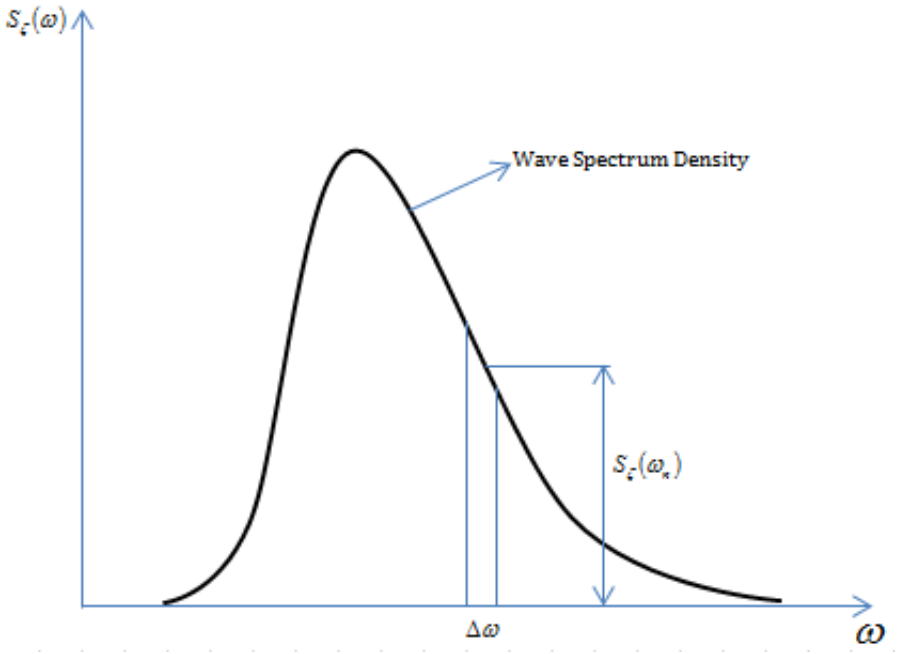

Figure 16. Wave spectral density

Some important characteristics of a wave can be obtained from the wave spectrum. Since the statistics of wave amplitude follow Rayleigh distribution, the integration of the wave spectrum using different powers of wave frequencies will give useful statistical relationship such as significant wave height and mean zero up crossing period that apply on the observation sea area. The nth order of moment can be calculated as follow (Journée & Massie, 2001):

$$m_n = \int_0^\infty \omega^n S(\omega) d\omega \tag{3.18}$$

Significant wave height:

$$H_{1/3} = 4\sqrt{m_0} \tag{3.19}$$

Expected period between zero upcrossing:

$$T_2 = 2\pi \cdot \sqrt{\frac{m_0}{m_2}} \tag{3.20}$$

There are several formulas that can be used to model wave spectrum, but the most commonly used for designing offshore operation are Pierson-Moskowitz(P-M) spectrum and JONSWAP spectrum. These wave spectrum formulas are obtained from statistical observations of ocean wave in particular area and it can be used to represent a sea state in that region for a certain period of time.

Table 4. Typical spectrum based on location (Chakrabarti, 2005)

Location	Operational	Survival
Gulf of Mexico	P-M	P-M or JONSWAP
North Sea	JONSWAP	JONSWAP
Northern North Sea	JONSWAP	JONSWAP
Offshore Brazil	P-M	P-M or JONSWAP
Western Australia	P-M	P-M
Offshore Newfoundland	P-M	P-M or JONSWAP
West Africa	P-M	P-M

3.1.2.1 Pierson-Moskowitz(P-M) Spectrum

The Pierson-Moskowitz formula assumed that the sea wave is fully developed meaning that if the wind blows continuously over a large area for a long time, the wave will reach its maximum regardless the duration of wind blowing (Stewart R. H., 2006). The Pierson-Moskowitz (P-M) spectrum can be expressed as follows:

$$S_{PM}(\omega) = \frac{5}{16} \cdot H_S^2 \omega_p^4 \cdot \omega^{-5} \exp\left(-\frac{5}{4} \left(\frac{\omega}{\omega_p} \right)^{-4} \right) \tag{3.21}$$

Where:

ω_p is the angular spectral peak frequency $2\pi/T_p$

3.1.2.2 JONSWAP Spectrum

The JONSWAP spectrum is obtained by modifying the Pierson-Moskowitz spectrum for a developing sea wave over limited fetch length:

$$S_J(\omega) = A_\gamma S_{PM}(\omega) \times \gamma^{\exp\left(-0.5 \left(\frac{\omega - \omega_p}{\sigma \omega_p} \right)^2 \right)} \tag{3.22}$$

Where:

S_{pm} = Pierson-Moskowitz Spectrumav

γ = Non-dimensional peak shape parameter

σ = Spectral width parameter, which: $\sigma = \sigma_a$ for $\omega \leq \omega_p$ or $\sigma = \sigma_b$ for $\omega > \omega_p$

A_γ = 1-0.287 ln(γ) is a normalizing factor

3.2 Basic Equation for Vessel Motion

A vessel floating on sea has six degrees of freedom and therefore it will have six response motions with respect to the wave. In a open sea, the vessel will respond to a random set of wave magnitude, wave direction, frequency, and phase. Thus, the vessel response motions are a combination of those factors.

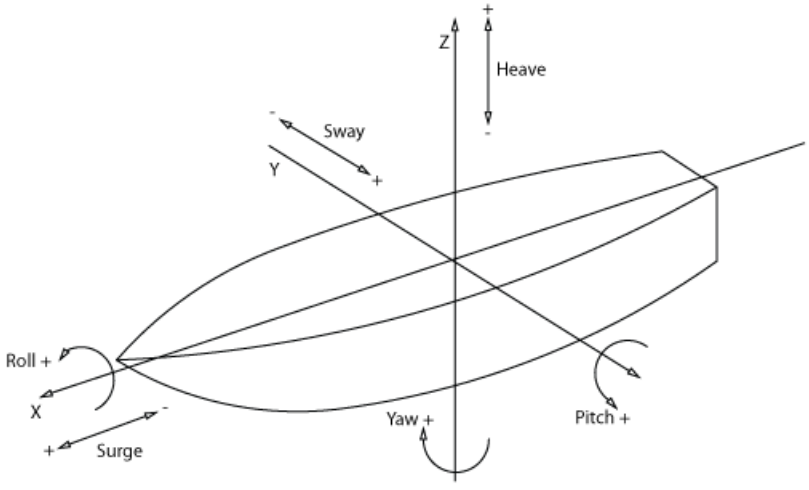

Figure 17. Vessel motions in waves (AT-Marine Oy, 2012)

These six degrees of freedom can be categorized as follows:
Translational Motion: three translational vessel movements along x, y, and z axes. The movements along those axes can be called as:

- Heave: the transitional motion of a vessel along its vertical z axis with positive sign to upward direction.
- Sway: the transitional motion of a vessel along its lateral y axis with positive sign to port side direction.
- Surge: the transitional motion of a vessel along its longitudinal x axis with positive sign to forward direction.

Rotational Motion: three rotational vessel motion about x, y, and z axes. The motion around those axes can be called as:

- Roll: the rotational motion of a vessel around its longitudinal x axis with positive sign for counterclockwise direction.
- Pitch: the rotational motion of a vessel around its lateral y axis with positive sign for counterclockwise direction.
- Yaw: the rotational motion of a vessel around its vertical z axis with positive sign for clockwise direction.

Vessel motions are highly influenced by the hydrodynamic forces working on vessel body. A vessel response depends on the wave frequency and it can be described using response spectrum. The response spectra of the vessel can be generated from the wave spectrum by using a transfer function. This response spectrum is useful for determining the behavior of the vessel on the ocean during marine operation when it gets exposed to the wave. A Response Amplitude Operator (RAO) is a transfer function between wave loads and vessel response with respect to that wave. A RAO can be obtained by simulating the vessel in wave tank or in software (e.g. MOSES). The vessel's behavior is very important in planning deep sea operation. In harsh environment operation, a vessel with a "good" RAO is required to maintain its stability during operation. Since most of the intervention tools will be deployed through moon pool located on the ship's center of gravity, the heave motion will become the most governing aspect to maintain the vertical motion of the tool during light well intervention using monohull vessel.

3.2.1 Heave Response in Regular Waves

Heave motion of a structure in waves can be modeled as a cylinder oscillating in water which is given by equation of motion as follows (Journée & Massie, 2001):

$$(m+a)\ddot{z}+b\dot{z}+cz=a\ddot{\zeta}^{*}+b\dot{\zeta}^{*}+c\zeta^{*} \tag{3.23}$$

Where:

m = mass of a oscillating structure (kg)
a = hydrodynamic mass coefficient (Ns^2/m)
b = hydrodynamic damping coefficient (Ns/m)
c = spring coefficient (N/m)
z = vertical displacement (m)
$\dot{z}$ = vertical velocity (m/s)
$\ddot{z}$ = vertical acceleration (m/s^2)

The value of z , $\dot{z}$, $\ddot{z}$ can be obtained by using below formula:

$$z = z_a \cos(\omega t + \varepsilon_{z\zeta})$$
$$\dot{z} = -z_a \omega \sin(\omega t + \varepsilon_{z\zeta})$$
$$\ddot{z} = -z_a \omega^2 \cos(\omega t + \varepsilon_{z\zeta}) \quad (3.24)$$

The terms $a\ddot{z}$ and $b\dot{z}$ in equation 3.23 represent hydrodynamic reaction due to movement of the cylinder in water. The above equations z , $\dot{z}$ and $\ddot{z}$ describe heave response with respect to regular wave. The vertical wave forces acting on cylinder can be calculated using Froude-Krilov formula, but in reality it needs to be corrected since some parts of the wave are diffracted (Journée & Massie, 2001). The correction for Froude-Krilov formula can be given in $a\ddot{\zeta}^*$ and $b\dot{\zeta}^*$. The terms ζ^* are used to calculate a reduced wave elevation as shown in below formulas:

$$\zeta^* = \zeta_a e^{-kT} \cos(\omega t)$$
$$\dot{\zeta}^* = -\zeta_a e^{-kT} \omega \sin(\omega t)$$
$$\ddot{\zeta}^* = -\zeta_a e^{-kT} \omega^2 \cos(\omega t) \quad (3.25)$$

T is draft of the submerged body at rest in meter unit. By substituting the equation 3.24 and 3.25 into equation of heave motion as written in 3.23 will give a following equation:

$$z_a \{c - (m+a)\omega^2\} \cos(\omega t + \varepsilon_{z\zeta}) - z_a \{b\omega\} \sin(\omega t + \varepsilon_{z\zeta}) =$$
$$= \zeta_a e^{-kT} \{c - a\omega^2\} \cos(\omega t) - \zeta_a e^{-kT} \{b\omega\} \sin(\omega t) \quad (3.27)$$

This equation 3.27 can be expressed in other way as:

$$z_a \{\{c - (m+a)\omega^2\} \cos(\varepsilon_{z\zeta}) - \{b\omega\} \sin(\varepsilon_{z\zeta})\} \cos(\omega t)$$
$$- z_a \{\{c - (m+a)\omega^2\} \sin(\varepsilon_{z\zeta}) + \{b\omega\} \cos(\varepsilon_{z\zeta})\} \sin(\omega t) =$$
$$= \zeta_a e^{-kT} \{c - a\omega^2\} \cos(\omega t) - \zeta_a e^{-kT} \{b\omega\} \sin(\omega t) \quad (3.28)$$

From above equation, by eliminating $\cos(\omega t)$ and $\sin(\omega t)$ terms, two new equations consisting of 2 unknowns can be obtained as below:

$$z_a \{\{c - (m+a)\omega^2\} \cos(\varepsilon_{z\zeta}) - \{b\omega\} \sin(\varepsilon_{z\zeta})\} = \zeta_a e^{-kT} \{c - a\omega^2\} \quad (3.29)$$

$$z_a \{\{c - (m+a)\omega^2\} \sin(\varepsilon_{z\zeta}) + \{b\omega\} \cos(\varepsilon_{z\zeta})\} = \zeta_a e^{-kT} \{b\omega\} \quad (3.30)$$

The heave amplitude is a sum of squares from above equations 3.29 and 3.30. It can be written in the following equation:

$$\frac{z_a}{\zeta_a} =_a e^{-kT} \sqrt{\frac{\{c - a\omega^2\}^2 + \{b\omega\}^2}{\{c - (m+a)\omega^2\}^2 + \{b\omega\}^2}} \quad (3.31)$$

3.2.2 Heave Response in Irregular Waves

The irregular wave represented by $\zeta(t)$ can be decomposed into many regular waves with different characteristics using Fourier series. The wave energy $S_\zeta(\omega)$ can be obtained by squaring up the value of ζ_a from each regular wave as shown in the following equation:

$$S_\zeta(\omega)\cdot d\omega = \frac{1}{2}\zeta_a^2(\omega) \tag{3.32}$$

The heave response spectrum equation has a same form as wave energy spectrum $S_\zeta(\omega)$, so the heave response spectrum can be described as a function of:

$$S_z(\omega)\cdot d\omega = \frac{1}{2}z_a^2(\omega) \tag{3.33}$$

Then, the above equation can be written as follows:

$$S_z(\omega)\cdot d\omega = \left|\frac{z_a}{\zeta_a}(\omega)\right|^2 \cdot \underbrace{\frac{1}{2}\zeta_a^2(\omega)}_{S_\zeta(\omega)\cdot d\omega}$$

Thus,

$$S_z(\omega)\cdot d\omega = \left|\frac{z_a}{\zeta_a}(\omega)\right|^2 \cdot S_\zeta(\omega)\cdot d\omega \tag{3.34}$$

By canceling $d\omega$, one can get below formula to transform the energy from wave energy into response energy.

$$S_z(\omega) = \left|\frac{z_a}{\zeta_a}(\omega)\right|^2 \cdot S_\zeta(\omega) \tag{3.35}$$

The heave response spectrum $S_z(\omega)$ can be calculated by multiplying the wave energy spectrum $S_\zeta(\omega)$ with a $|z_a/\zeta_a(\omega)|^2$ function. This function can be called as a transfer function. The heave response spectrum consists of many regular heave responses. By summing up all the different regular heave responses using Fourier series, one can obtain the irregular heave response. A calculated heave response spectrum can be used to obtain characteristic of heave motions, such as significant heave amplitude, mean heave period, and zero-crossing period.

The vessel heave natural period is very important factor in determining the operability of the vessel in certain area or condition. This heave natural period can be used to analyze the amplitude of the heave motion of a vessel. The heave natural period of a vessel should not be the same as the wave period where the vessel is going to operate. Heave natural period of the vessel can be calculated by using given equation (Faltinsen, 1993):

$$T_{n3} = 2\pi\left(\frac{M + A_{33}}{\rho g A_w}\right)^{\frac{1}{2}} \tag{3.36}$$

Where M is the mass, A_{33} is added mass for heave, and A_w is water plane area. The heave motion of the vessel will be in resonant with wave motion by wavelength of:

$$\lambda = \frac{g}{2\pi}T_{n3}^2 \tag{3.37}$$

Where λ is wavelength, g is gravity acceleration, and T_{n3} is heave period of the vessel.

3.3 Currents Loads

Sea currents need to be taken into consideration for designing marine operations. They are causing the drift of vessels or floating structures. The submerged parts of offshore structure will get exposed to the different current forces at different level of water depths. The magnitude of the current forces will vary depends on current speed and direction. In deep sea, currents speed can be found up to 1.3 m/s (Gerwick, 2000). Currents with strong magnitude can result in vortex shedding on marine structures, such as risers, sea cables, and pipelines. The interaction of strong currents and waves can change the wave height and wave period. As seen in **Figure 18**, the current that flows in the same direction as the wave (following current) will extend the wave length and reduce the wave height. Whereas, the current that flows in opposite direction to the wave (opposing current) will shorten the wave length and increase the wave height.

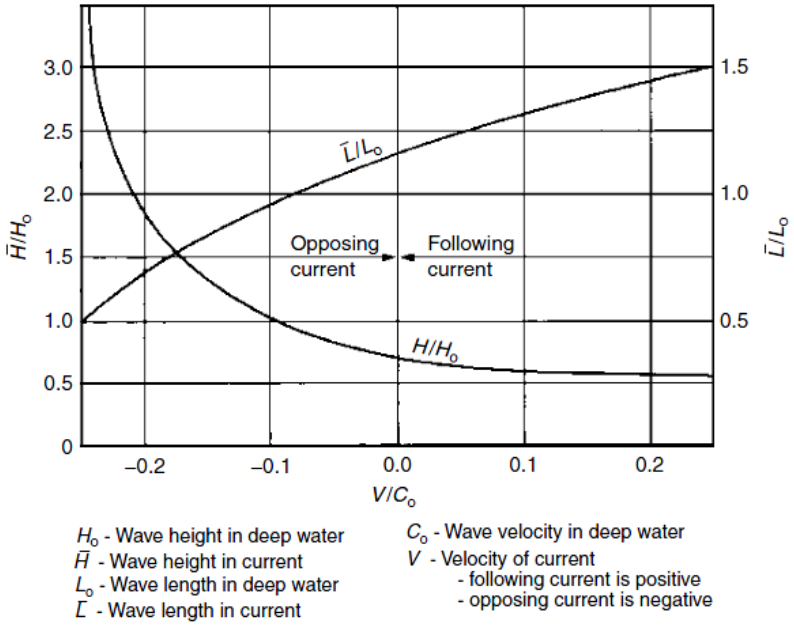

Figure 18. Effect of current in wave height and length (Gerwick, 2000)

The current forces components that act horizontally on the surface of submerged body can be categorized as a drag force which is acting on same direction as current or a lift force which is acting perpendicular to the current direction. These forces are caused by friction and difference in pressure between upstream and downstream side. The current force experienced by the submerged body will depend on density of the flowing fluid, the flow velocity, the surface area of the submerged body that encounters the flow, and the roughness of the submerged body's surface. The friction between fluid and the submerged body will create eddy currents. The water particle in the eddy currents will have higher velocity on downstream side; this high velocity creates lower pressure due to Bernoulli theorem (Gudmestad, 2010). This difference in pressure will cause a force in current direction. General equation for calculating the drag force due to current is:

$$f = \frac{1}{2} \cdot \rho \cdot C_D \cdot A \cdot U^2 \tag{3.38}$$

Where:

ρ = fluid density (kg/m^3)
C_D = drag coefficient from the experiments
A = projected surface area normal to the flow (m^2)
U = flow velocity (m/s)

The drag coefficient C_D is dimensionless and a function of Reynolds number. Reynolds number for current passing through a cylinder can be expressed as:

$$R_e = \frac{u \cdot D}{v} \tag{3.39}$$

Where:

u = the mean velocity of sea water particle (m/s)
D = the diameter of the cylinder (m)
V = the kinematic viscosity of the sea water (m²/s)

The drag coefficient C_D can be related to Reynolds number as shown in below picture for cylindrical structure:

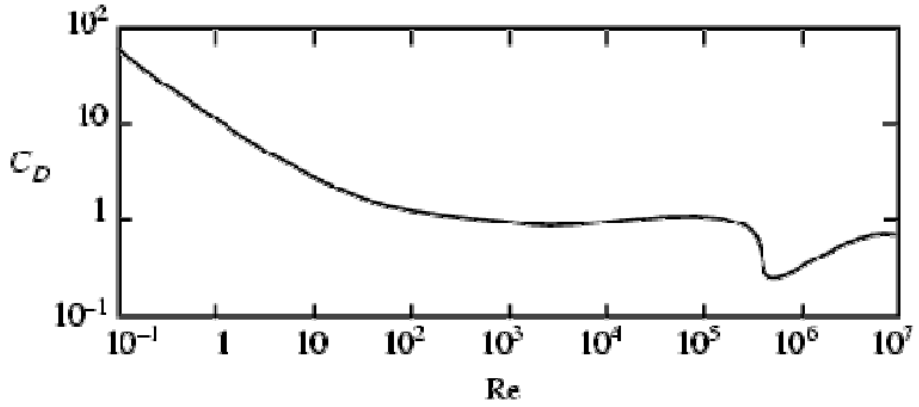

Figure 19. Drag coefficients (Gudmestad, 2010)

The relation between the drag coefficient and Reynolds number for a smooth cylindrical structure has been observed through laboratory experiments. For the value of Reynolds number under 50, the flow is laminar and steady. In this range, the drag coefficient decreases as the Reynolds number increases. The flow will keep laminar up to the Reynolds number of 200. The flow becomes turbulent when the Reynolds number is more than 5000. The value of Reynolds number between $2x10^5$ and $5x10^5$ is considered as the transition. This transition process causes the drag coefficient value to drop significantly. After the significant drop, the drag coefficient increases slowly as the Reynolds number increases. In practice, the surface of the submerged body is not real smooth. A rough surface will get higher forces due to larger eddy current compared to a very smooth surface. Commonly, C_D for rough surface will have value between 1.0 and 1.1, whereas the drag coefficient (C_D) for smooth surface will have value between 0.7 and 0.9 (Gudmestad, 2010).

3.4 Large Displacement Theory

The deflection of the wireline can be explained by using large displacement theory adopted from *Newman, Overstreet, & Beynet (2006)*. This theory can be used to help in analyzing the wireline behavior under strong sea current when it is suspended from intervention vessel to the subsea well.

The suspended wireline will experience a large displacement in horizontal direction during the operation. A wireline model can be discretized by dividing the wireline into N-number of simple beam elements. The global displacement due to load from sea current can be represented by matrix U. The matrix U_g is the matrix showing the global displacement for all steps. The matrix U_t shows the difference in global system coordinate system between current position and its previous position one time step.

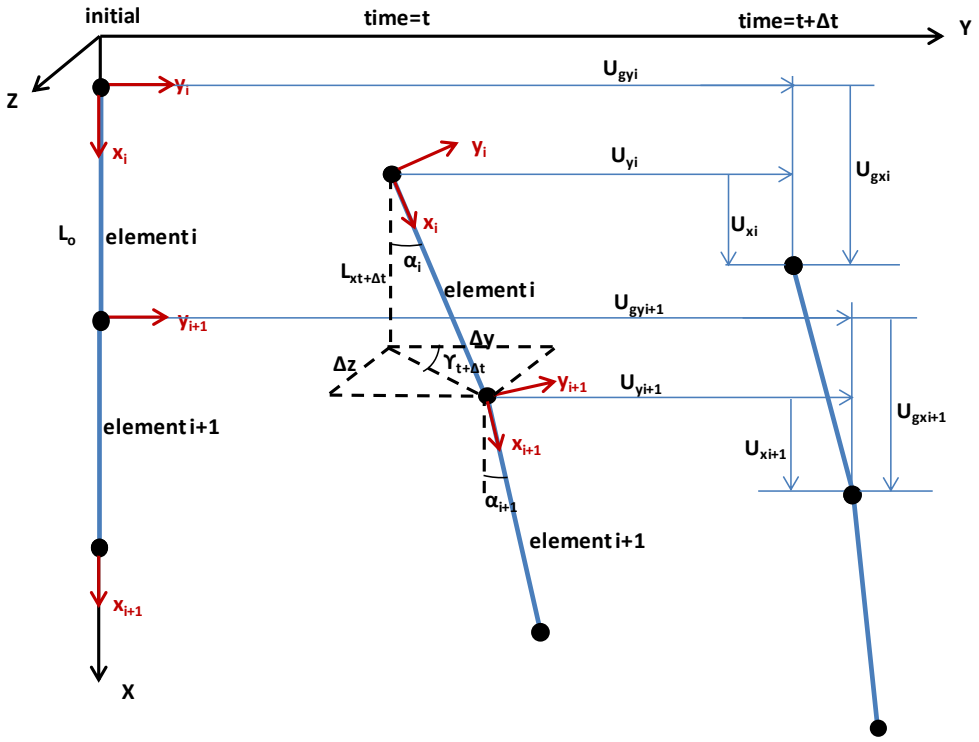

Figure 20. Wireline deformation modeled as a beam element with large displacement (Newman, Overstreet, & Beynet, 2006)

Figure 20 shows the wireline at one position with time t and changing to different position at time t+Δt, where Δt is a time step. In dynamic analysis, the new global coordinate for displacement can be simulated for every time step and it is an iterative process. For initial modeling, wireline is assumed vertical in global coordinate as described in the figure. Due to sea current, the wireline will move horizontally and cause the local coordinate system of each element to change and get rotated. This displacement will be stored and used in the next step. This stored displacement, U_g can be expressed as follows:

$$\overline{U}_{g(t+\Delta t)} = \overline{U}_{g(t)} + \overline{U}_t \tag{3.40}$$

Where Ut is the global displacement from time (t) to (t+Δt)

The local coordinate system will change due to rotation at angle of inclination α from time to time as shown at time=t in the figure. To get appropriate modeling of wireline's deflections, the local coordinate of each node needs to be rotated into new local coordinate system. The degree of rotation can be calculated using following formula:

$$\alpha_{t+\Delta t} = \tan^{-1}\left[\frac{\sqrt{\Delta y^2 + \Delta z^2}}{L_{x_{t+\Delta t}}}\right] \tag{3.41}$$

Where:

$$L_{x_{t+\Delta t}} = L_o + U_{gx_{i+1}} - U_{gx_i};\ \Delta y = U_{gy_{i+1}} - U_{gy_i};\ \Delta z = U_{gz_{i+1}} - U_{gz_i}$$

Azimuth angle, denoted by γ, can be calculated as follow:

$$\gamma_{t+\Delta t} = \tan^{-1}\left[\frac{\Delta z}{\Delta y}\right] \tag{3.42}$$

After inclination angle (α) and azimuth angle (γ) are obtained, the new matrix can be calculated using transformation matrix T as shown in equation 3.50. And the new length of the element in new coordinate system with given time (t+Δt) is calculated by:

$$L_{t+\Delta t} = \sqrt{L^2_{x_{t+\Delta t}} + \Delta y^2 + \Delta z^2} \tag{3.43}$$

This new element's length will be different from its previous length and its new element's length needs to be restored to its original length using some force applied to the element:

$$N_x = \frac{(L_o - L_{t+\Delta t})}{L_0} AE \tag{3.44}$$

This process is an iterative; after one step completed the finite element method will proceed to the next step continuously until the model gets converged.

A finite element method can be utilized to model the deflection of each beam element. A beam element is formed by connecting 2 nodes in each end. The first node is named with node n and the second at the other end is named with node n+1. Each element's node has 3 translational degree of freedom and 3 rotational degrees of freedom. **Figure 21** describes the beam element-i with its longitudinal axis is located along local x- axis. The transitional degrees of freedom are represented by u_x for x displacement, u_y for y displacement, and u_z for z displacement; whereas rotational degrees of freedom are described by u_{rx}, u_{ry}, and u_{rz} which mean rotation about x-axis, y-axis, and z-axis respectively. The small letters of x, y, and z show local coordinate system, whereas the capital letters of X, Y, and Z are used for global coordinate system.

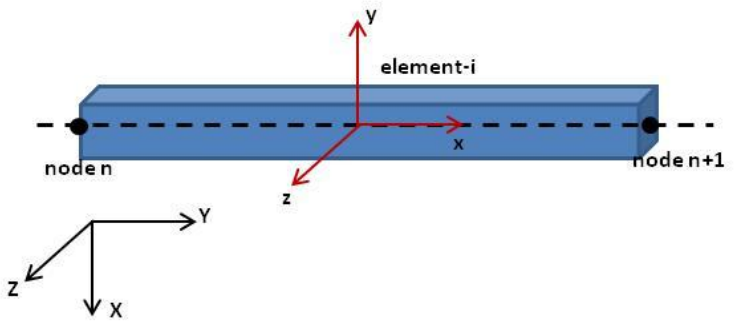

Figure 21. Six degrees of freedom at each node of a beam element in global coordinate system

The finite element method to define the deformation due to certain loads can be expressed by using following basic equation:

$$u_{Li} = k_{Li}^{-1} r_{Li} \tag{3.45}$$

Where k is the matrix of stiffness, u is the matrix of displacement, r is the reaction matrix, L describes the location in the local coordinate system, and i shows the element number. The stiffness matrix for beam element (k_{Li}) that consists of a 12x12 matrix can be formed using basic formula as written in equation 3.46 (Pilkey, 2005):

$$k_{Li} = \begin{bmatrix}
\frac{12EI}{L^3} & 0 & 0 & 0 & \frac{6EI}{L^2} & 0 & -\frac{12EI}{L^3} & 0 & 0 & 0 & \frac{6EI}{L^2} & 0 \\
0 & \frac{12EI}{L^3} & 0 & -\frac{6EI}{L^2} & 0 & 0 & 0 & -\frac{12EI}{L^3} & 0 & -\frac{6EI}{L^2} & 0 & 0 \\
0 & 0 & \frac{AE}{L} & 0 & 0 & 0 & 0 & 0 & -\frac{AE}{L} & 0 & 0 & 0 \\
0 & \frac{6EI}{L^2} & 0 & \frac{4EI}{L} & 0 & 0 & 0 & \frac{6EI}{L^2} & 0 & \frac{2EI}{L} & 0 & 0 \\
\frac{6EI}{L^2} & 0 & 0 & 0 & \frac{4EI}{L} & 0 & -\frac{6EI}{L^2} & 0 & 0 & 0 & \frac{2EI}{L} & 0 \\
0 & 0 & 0 & 0 & 0 & \frac{GJ}{L} & 0 & 0 & 0 & 0 & 0 & \frac{GJ}{L} \\
-\frac{12EI}{L^3} & 0 & 0 & 0 & -\frac{6EI}{L^2} & 0 & \frac{12EI}{L^3} & 0 & 0 & 0 & -\frac{6EI}{L^2} & 0 \\
0 & -\frac{12EI}{L^3} & 0 & \frac{6EI}{L^2} & 0 & 0 & 0 & \frac{12EI}{L^3} & 0 & \frac{6EI}{L^2} & 0 & 0 \\
0 & 0 & -\frac{AE}{L} & 0 & 0 & 0 & 0 & 0 & \frac{AE}{L} & 0 & 0 & 0 \\
0 & -\frac{6EI}{L^2} & 0 & \frac{2EI}{L} & 0 & 0 & 0 & \frac{6EI}{L^2} & 0 & \frac{4EI}{L} & 0 & 0 \\
\frac{6EI}{L^2} & 0 & 0 & 0 & \frac{2EI}{L} & 0 & -\frac{6EI}{L^2} & 0 & 0 & 0 & \frac{4EI}{L} & 0 \\
0 & 0 & 0 & 0 & 0 & \frac{GJ}{L} & 0 & 0 & 0 & 0 & 0 & \frac{GJ}{L}
\end{bmatrix} \tag{3.46}$$

Where:

E = Young's modulus (N/m^2)
I = moments of inertia (m^4)
L = length of element (m)
A = area of cross section (m^2)
G = shear modulus (N/m^2)
J = constant for torsion (Nm^2)

The displacement matrix (u_{Li}) describes degree of freedoms (DOF) for each node in one beam element, where each node consists of 6 DOF (3 translational and 3 rotational movements). The matrix r_{Li} consists of forces that act on each node due to sea current. The matrix for displacement and force can be arranged as follows:

$$u_{Li} = \begin{bmatrix} u_{x1} \\ u_{y1} \\ u_{z1} \\ u_{rx1} \\ u_{ry1} \\ u_{rz1} \\ u_{x2} \\ u_{y2} \\ u_{z2} \\ u_{rx2} \\ u_{ry2} \\ u_{rz2} \end{bmatrix} \qquad r_{Li} = \begin{bmatrix} N_{x1} \\ V_{y1} \\ V_{z1} \\ T_{rx1} \\ M_{ry1} \\ M_{rz1} \\ N_{x2} \\ V_{y2} \\ V_{z2} \\ T_{rx2} \\ M_{ry2} \\ M_{rz2} \end{bmatrix} \tag{3.47}$$

Then for each beam element, the stiffness matrix and the force matrix built in local coordinate system must be transformed into global coordinate system by using the following transformation matrix formula:

$$K_{Gi} = Tk_{Li}T^{T} \tag{3.48}$$

$$R_{Gi} = Tr_{Li} \tag{3.49}$$

Where the transformation matrix T is given by:

$$T = \begin{bmatrix} \cos\alpha & -\sin\alpha\cos\phi & \sin\alpha\sin\phi \\ \sin\alpha\cos\gamma & -\sin\gamma\sin\phi+\cos\alpha\cos\gamma\cos\phi & -\sin\gamma\cos\phi-\cos\alpha\cos\gamma\sin\phi \\ \sin\alpha\sin\gamma & \cos\gamma\sin\phi+\cos\alpha\sin\gamma\cos\phi & \cos\gamma\cos\phi-\cos\alpha\sin\gamma\sin\phi \end{bmatrix} \tag{3.50}$$

and: ϕ = twisting angle if applicable

Then each element of matrix K_{Gi} needs to be summed up to assemble global matrix K_G and the matrix R_{Gi} follows same procedure. After the global matrices for beam stiffness and forces are built, then the global matrix for displacement can be calculated using following formula:

$$U_G = K_G^{-1}R_G \tag{3.51}$$

Once the global matrix for displacement is solved, it can be transferred into local coordinate system for each element by using below formula:

$$u_{Li} = T^{T}U_{Gi} \tag{3.52}$$

Where T^T is a transpose of the transformation matrix T

3.5 Hydrostatic Pressure and Buoyancy

External pressure that acts on the submerged structure is proportional to the water depth. It means as the water depth goes deeper, the external pressure is getting higher. Hydrostatic pressure can be given as:

$$P_H = \rho \cdot g \cdot h \tag{3.53}$$

Where:

ρ = fluid density (kg/m^3)

g = gravity acceleration (m/s^2)

h = water depth (m)

Hydrostatic pressure will be distributed uniformly in all directions. In ocean, the wave also influences the sea water pressure due to different elevation between crest and trough. At the same depth from still water level, the hydrostatic pressure below the crest will be higher than the trough. But this wave effect will be considerably negligible at very deep water. Hydrostatic pressure is related to the buoyancy concept that's explained by Archimedes' principle. The law of Archimedes

states that the hydrostatic pressure acting on a submerged body generates force in upward direction which equals to the weight of displaced water.

Archimedes law assumed that pressure only acts on a completely closed body. In greater depth, the hydrostatic pressure will create significant compression force to its material. This significant force effect can change the material's volume. The change of volume will influence the density of the material, such as fluids or gases. This is the reason why the density of sea water increases with sea depth, the sea water located near sea bed will tend to have higher density. But for simplifying the calculation, the average density of sea water can be assumed as 1025 kg/m^3.

3.5.1 Effective Tension

Figure 22 as shown in next page illustrates a cable that is partly immersed in the fluid in a static condition. In this case, cable is considered as a cylinder body. The distributed self weight from the cylinder cause a tension force that is accumulated on the top end of the cylinder. The common method to calculate the total top tension force is total self weight of the cylinder in air (dry weight) subtracted by buoyancy force that acts on submerged part of cylinder, this total top tension is often called as effective tension. According to Archimedes law, this buoyancy force is equal to the weight of displaced fluid where the cylinder is immersed into it. Based on this concept, the force that acts on the bottom of the cylinder will be close to zero and almost negligible since there will be only very small volume of horizontal thin layer displaced by the fluid. The tension stress yielded along the cylinder is a function of depth; the tension stress is linearly increasing from the bottom of submerged part of the cylinder all the way up to the top section. The effective tension along the cylinder body can be calculated using thr following formula:

$$T_e = (\rho_c - \rho_f) \cdot g \cdot A \cdot (L - D) \tag{3.54}$$

Where:

L = Length of the submerged cylinder (m)
g = Gravity acceleration (m/s^2)
A = Cross sectional area of the cylinder (m^2)
D = Depth coordinate from top to bottom (m)
ρ_c = Mass density of the cylinder material (kg/m^3)
ρ_f = Mass density of the fluid where the cylinder is immersed (kg/m^3)

From the equation 3.54, one can find the tension stress distribution as shown with the dash line a-b in **Figure 22**. Another method to analyze the stress distribution due to buoyancy force is by assuming that the buoyancy force is the total pressure acting on the surface of the submerged body. This method is referred to as pressure-on-flat method (Nergaard, 2012). Based on this method, the horizontal forces that act on the cylinder due to hydrostatic pressures will eliminate each other. So that, only the vertical forces from hydrostatic pressure that act on the lower end area of cylinder will contribute to the tension stress in the cylinder. This vertical force can be calculated as follows:

$$F_f = \rho_f \cdot g \cdot A \cdot L \tag{3.55}$$

Where:

L = Length of the submerged cylinder (m)
g = Gravity acceleration (m/s^2)

A = Cross sectional area of the cylinder (m^2)

ρ_f = Mass density of the fluid where the cylinder is immersed (kg/m^3)

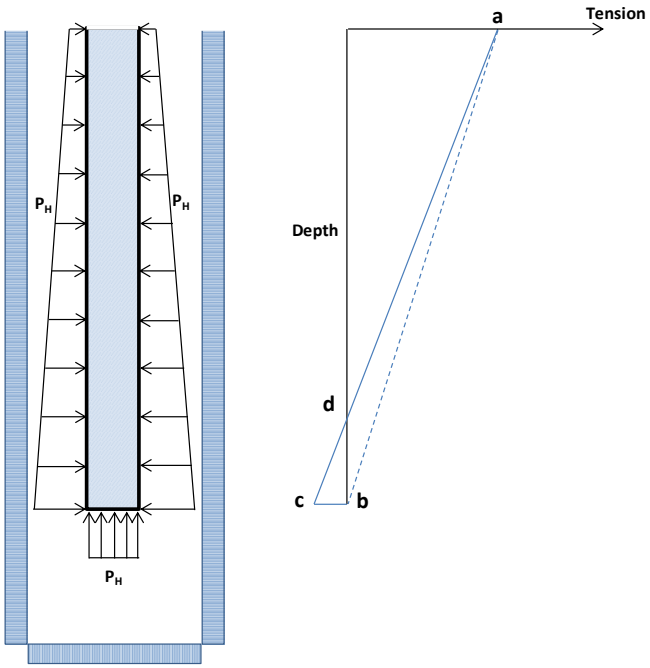

Figure 22. Effective tension force distribution on a submerged cylinder

Then, F_f is the force resulted by hydrostatic pressure from the fluid as shown by line b-c in **Figure 22**. This force creates a compression load that works along the lower parts of cylinder length. The line a-d-c as shown in the figure represents the resultant of axial forces that varies linearly as a function of depth due to the cylinder weight distribution in the fluid and the axial force F_f acting on the bottom section. This compression force will decrease linearly from the bottom to a neutral point with no axial force as shown by point d in the figure. From that neutral point d, the rest of the submerged body will be in tension up to the top section.

CHAPTER 4

ANALYSIS METHODOLOGY

4.1 General

This chapter will describe the methodology used for establishing the analysis model. There will be 180 simulation cases to be run in this project to obtain desired data results. Two types of wireline with six different types of downhole tool weight will be analyzed; those are Sandvik Slickline with 0.125" diameter and Camesa Monoconductor with 7/16" diameter. The different types of downhole tool weight used, as listed in below table, are 150 lbs, 600 lbs, 1000 lbs for Slickline and 500 lbs, 1200 lbs, 2000 lbs for Monoconductor. The simulation model will be established for well depth from 1400 up to 4250 meters for each case.

Table 5. Scheme of different simulation cases

	Wireline Operations				Well Depths (m)
Cases	1	Slickline ∅0.125"	Case 1A	150lbs Downhole Tool	1400-4250
			Case 1B	600lbs Downhole Tool	1400-4250
			Case 1C	1000lbs Downhole Tool	1400-4250
	2	Monoconductor ∅7/16"	Case 2A	500lbs Downhole Tool	1400-4250
			Case 2B	1200lbs Downhole Tool	1400-4250
			Case 2C	2000lbs Downhole Tool	1400-4250

4.2 Methodology

The analysis work flow needs to be developed to minimize the risk of human error. This analysis work flow will be used as a framework to ensure that the analysis process is carried out systematically. The method of analyzing the wireline for wireline operation can be illustrated by following flow chart:

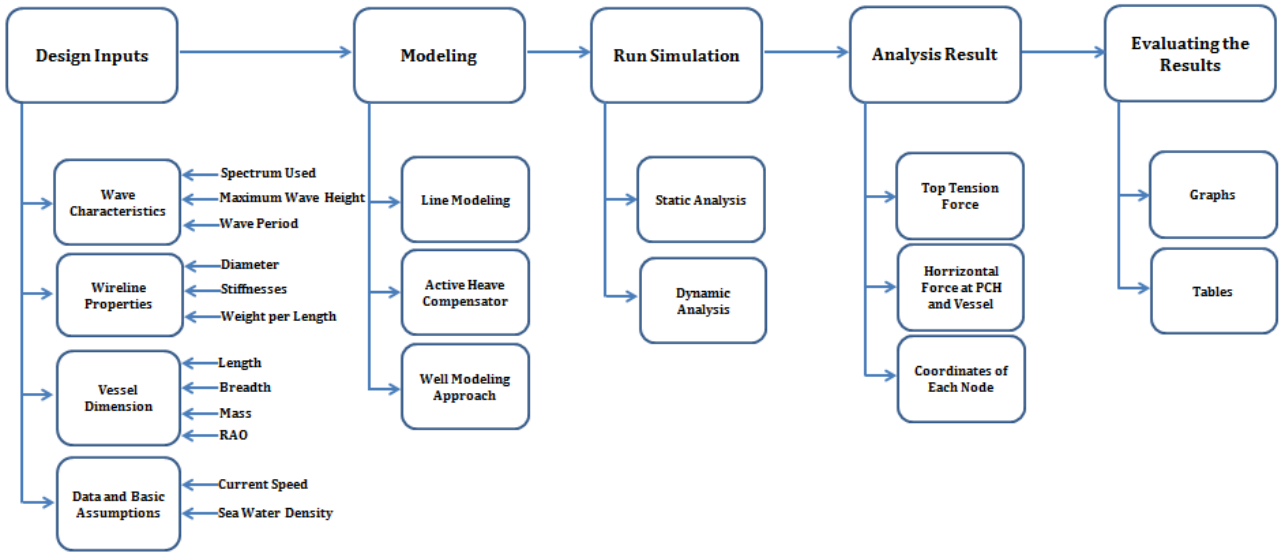

Figure 23. Analysis work flow

Before starting the modeling in OrcaFlex, the correct approximation and assumptions need to be chosen first; otherwise it will lead to unproper modeling. Important parameters that are required to be defined for analysis are environmental conditions that apply on the site, wireline properties, vessel data, and well data. In this project, all the data are provided by Island Offshore Company. Modeling and simulation will be performed in OrcaFlex software built by Orcina to obtain the analysis result. The modeling and simulation will be run in iterative stages based on finite element method. After the simulations are finished, the analysis results will be extracted from the OrcaFlex then be documented and presented into tables and graphs. Tables and graphs are used to visualize the analysis result trends and help in making comparisons. The work procedures need to be carried out in compliance with relevant design requirement, standards, and regulations such as DNV, NORSOK, and ISO.

As shown in **Figure 24**, a simple mechanical model is presented to get better understanding of basic concept in determining downhole tool depth inside the well bore. The system consists of a vessel, sea currents with different velocity, wave height, a wireline, RLWI stack components, and a downhole tool.

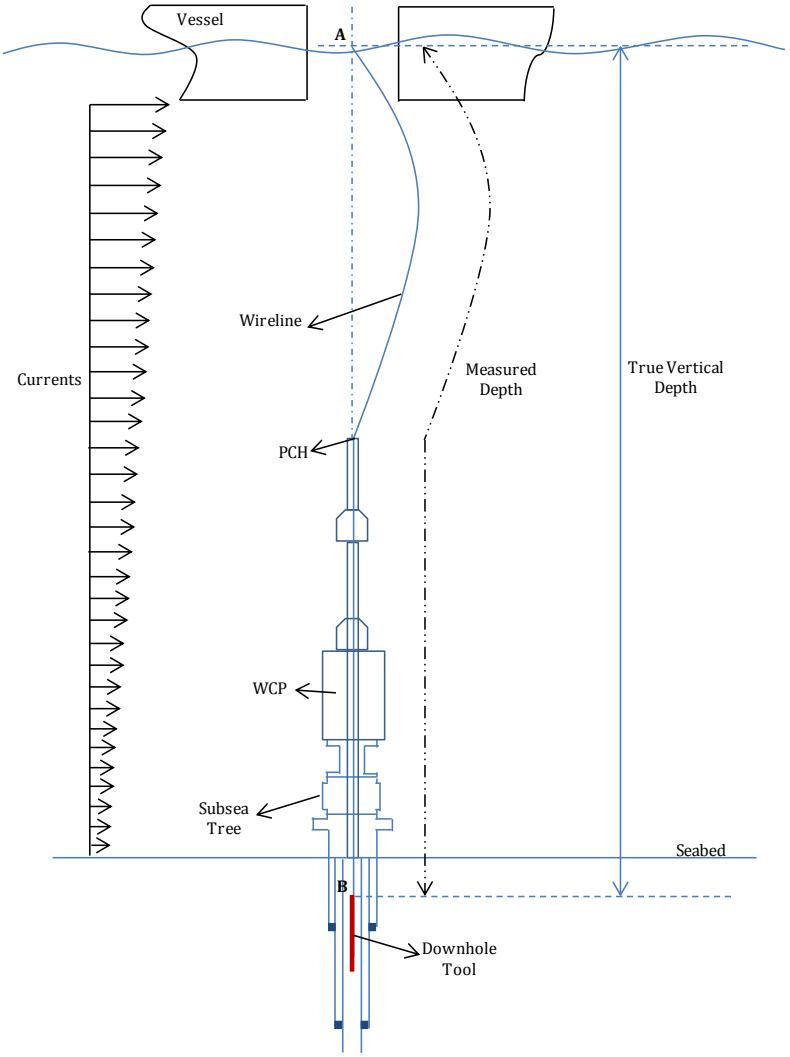

Figure 24. A schematic model for a downhole tool being launched using a wireline

When the downhole tool is being launched, there are two definitions of depth. First, the measured depth which means the depth (distance between mean sea level and downhole tool location) is

measured based on the total length of the cable that has been spooled out from the vessel's winch. Second, the true vertical depth is the perpendicular distance between mean sea level and right location of the downhole tool. Thus, the actual depth of the downhole tool can be simply expressed by following equation:

$$TVD = MD + \Delta Y_{elongation} - \Delta Y_{current} \tag{3.56}$$

Where:

TVD	= True Vertical Depth (m)
MD	= Measured Depth (m)
$\Delta Y_{elongation}$	= vertical displacement due to stretched cable (m)
$\Delta Y_{current}$	= vertical displacement due to sea current (m)

The discrepancy between the value of TVD and MD is called as vertical displacement; it can be either in upward or downward direction. Upward direction means that the true vertical depth is less than the measured depth. While downward direction means that the true vertical depth is more than the measured depth.

4.3 OrcaFlex Software

Some computer softwares are available in the market to simulate marine or offshore operations. There are OrcaFlex, Deeplines, Flexcom, Riflex, and Simo. In this project, OrcaFlex software was used to examine the behavior of the wireline or cable under sea current for different depth cases during light well intervention activities. The OrcaFlex software has capability to model a wide range of marine systems, such as riser, mooring, pipeline installation, and many other systems that are related to offshore dynamics. This section will describe information about OrcaFlex software. The explanations about OrcaFlex mostly will refer to OrcaFlex Manual.

4.3.1 Structural Modeling in OrcaFlex

OrcaFlex uses 3-dimensional coordinates system as shown in below picture. There are two commons coordinate systems in OrcaFlex, those are global coordinate system defined as GXYZ for the entire model and local coordinate system Lxyz for each of component modeled in OrcaFlex. A line can be modeled as a finite element in OrcaFlex. During the analysis, OrcaFlex will discretize the line model into several segments as shown in **Figure 26**. Each of segments will connect the nodes and carry no mass. The mass, weight, and buoyancy will be assigned directly to the nodes, whereas the line segments are used only to model the axial and torsional properties.

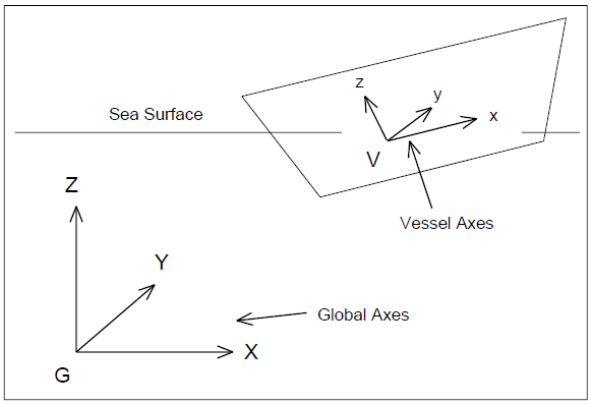

Figure 25. Coordinate systems used in OrcaFlex (Orcina Ltd, 2010)

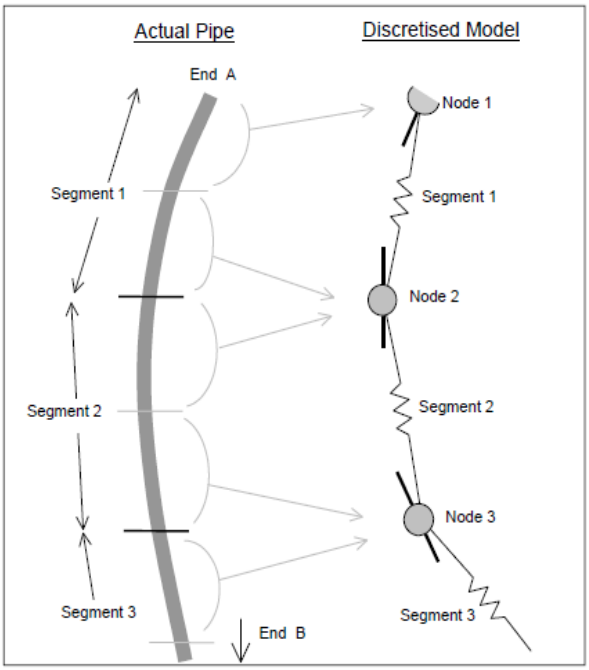

Figure 26. General line model in OrcaFlex (Orcina Ltd, 2010)

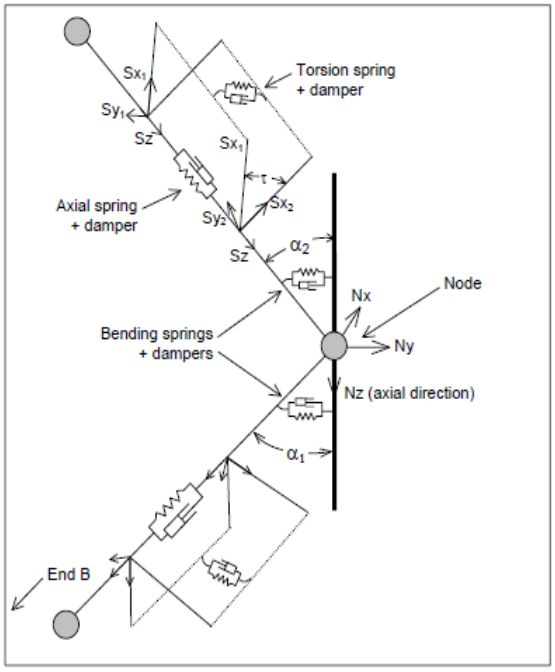

Figure 27. Structural details of OrcaFlex line model (Orcina Ltd, 2010)

Figure 27 shows the detail of structural modeling in each segment and node. As shown in the figure, there are 3 types of spring and dampers. The axial properties will be modeled as spring+dampers in the middle of each segment, which transfers an equal force in opposite direction to each associated node. The bending properties will be modeled as rotational spring+dampers located at the each side of the node, where α represents the degree of the rotation. The torsional properties are modeled as spring+dampers in the middle of each segment, which transfers an equal torque moment to each node at both ends of the segment. The simulation in OrcaFlex can be devided into two states, static analysis and dynamic simulation. The static analysis is a prerequisite before running the dynamic analysis. During the simulation, OrcaFlex will establish a mathematical model from the entire system by considering the interconnection between each system component, such as lines, vessels, and buoys through work sequences as described in **Figure 28**.

4.3.2 Static Analysis

A static analysis is used to obtain the static equilibrium of the system prior to running the dynamic analysis. This static analysis solves the system balance under applied loads using iterative process. This static analysis only takes into account self weight of the structural model, buoyancy, and hydrodynamic drag from current and wind. Once the equilibrium has been calculated, the configuration of the line model can be computed.

4.3.3 Dynamic Analysis

The dynamic analysis is carried out to determine the motion responses of the model due to combination between wave loads, current, wind, and other design parameters over a period of time based on the initial condition as obtained in static analysis.

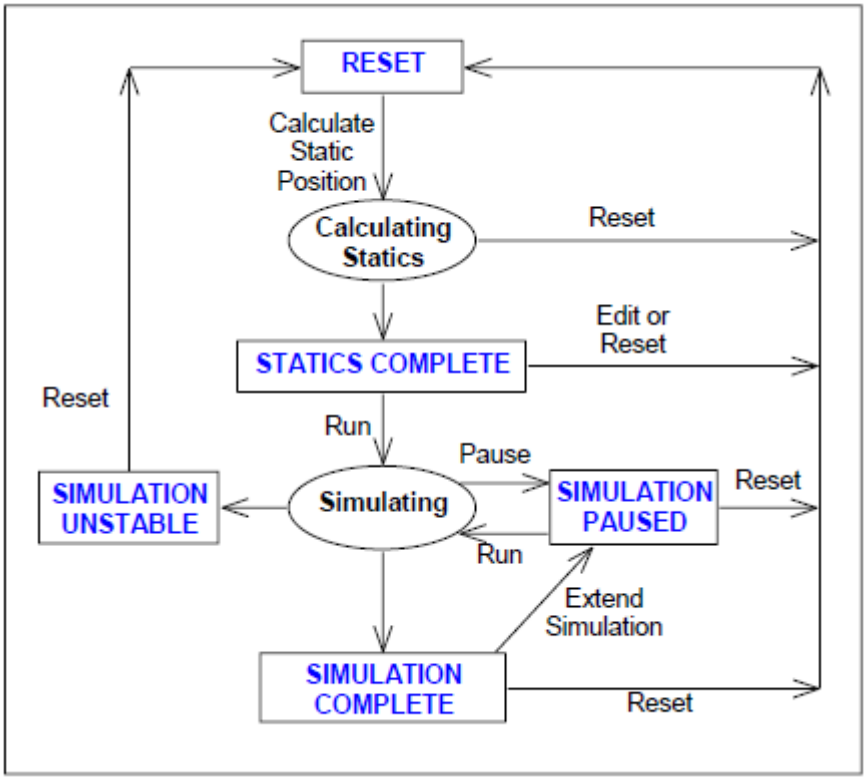

Figure 28. Analysis sequence in OrcaFlex (Orcina Ltd, 2010)

CHAPTER 5

DESIGN CASE

5.1 General

This chapter will describe the general information about case study taken, such as environmental data, wireline properties, vessel data, and key assumptions used for the design. The data will be used for inputs in modeling. The environmental data, vessel data, and wireline properties are based on available data from Island Offshore Subsea and "Design Basis of Luva Field Development-Book 050" by Statoil.

5.2 Design Parameters

The Aasta Hansteen field is located at the Vøringplatå west of Bodø, 300 km from shore at 1300 meters water depth. The Aasta Hansteen field consists of 3 discoveries: Luva that was found in 1997, Snefrid, and Haklang that were found in 2008. The three reservoirs will be developed with two of 4 slots template and a satellite, with a total 7 subsea wells tied back to the Aasta Hansteen platform using infield flowlines.

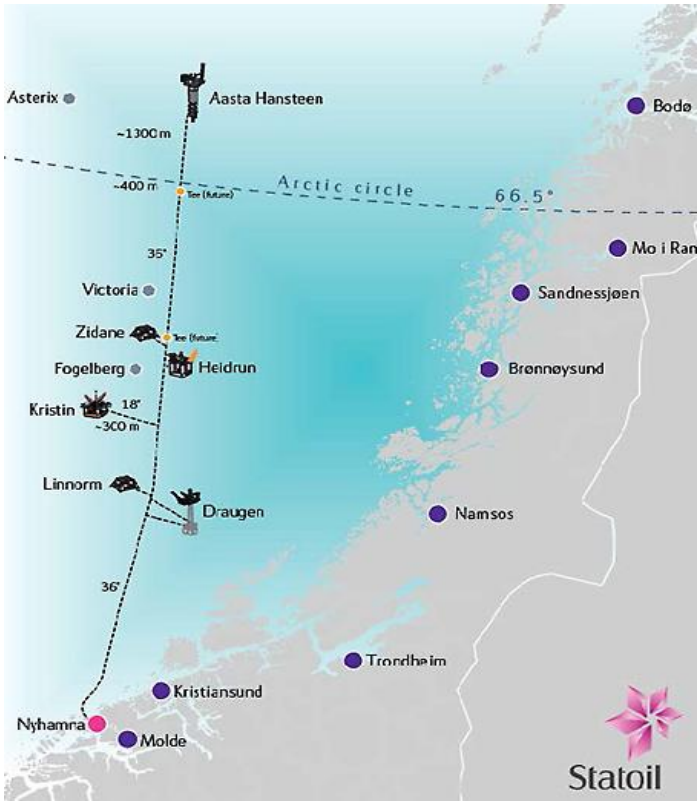

Figure 29. Location of Aasta Hansteen field (Statoil, 2013)

The Aasta Hansteen key operating conditions are :

- Water depth : 1300 meters
- Sea Water Density: 1025 kg/m^3
- Seafloor temperature: approximately -1.5^o C

- Maximum Working Pressure for Well Control System: 690 Bar
- Subsea Xmas Tree type: HXT 7-1/16" system
- H2S concentration: less than 0.5 ppm (estimation)
- Well type: Gas
- Reservoir gas density: 0.7 kg/m^3
- Well pressure: 284-338 bar
- Well depth: 2697-4289 meters
- Vessel for well intervention: Island Wellserver
- RLWI stack: FMC RLWI Mark II

Table 6. Weight of RLWI Mk II components (Seaflex Riser Technologies, 2012)

Unit Name	RLWI Mk II Components	Component Length	Unit Length	Dry weight
		m	m	kg
Pressure Control Head (PCH)	PCH internals	3.824	3.824	750
Upper Lubricator Package (ULP)	10" compact connector	0.7		419
	Lubricator valve	1.18	1.18	706
LUB Tubular	Upper riser joint	8.374		5011
	Mid riser joint	7.95		4757
	Lower riser joint	0.55	16.874	329
Lower Lubricator Package (LLP)	Safety joint (pipe)	3.5		11120
	KC 6-17 connector	0.479	3.979	1522
Well Control Package (WCP)	Upper valve block	1.877		18795
	SSR block	1.105		11065
	Lower valve block	1.524	4.506	15260
WCP running tool				5700
Adapter				8310
Total Length and Weight, excluding adapter and running tools			31.063	69734

5.3 Environmental Data

5.3.1 Wave

The wave data applied for wireline operations are stated in below table. These parameters are obtained based on the maximum design wave condition for RLWI normal operations as specified by FMC (Island Offshore, 2012).

Table 7. Wave data for design

Wave Parameter	Unit	Limit
Maximum Wave Height (H_{max})	m	6.5
Associate Time Period (T_{ass})	sec	9.5

5.3.2 Current

The combined effects between water depth and sea currents need to be considered during the deployment of intervention tools. The Aasta Hansteen current profile as shown in **Table 8** was taken from Statoil metaocean design basis based on 1-year current speed profile.

Table 8. Current velocity at each water depth

Depth (m)	Current m/s
0	1.38
-50	1.06
-100	1.02
-200	0.9
-300	0.77
-400	0.76
-500	0.63
-600	0.51
-800	0.54
-1000	0.53
-1200	0.53
-1300	0.47

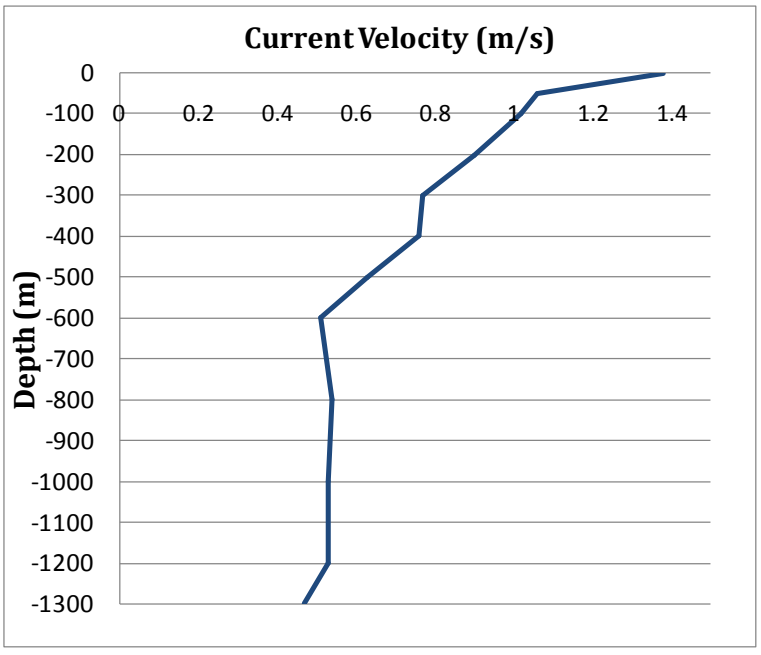

Figure 30. Current speed profile at Aasta Hansteen field

5.4 Island Wellserver

All information related to Island Wellserver vessel was collected from *Island Offshore (2012).* The vessel is built to fulfill the requirement for executing well intervention services in efficient manner compared to conventional drilling unit. The deck area can accommodate effectively the handling for RLWI intervention tools and provide sufficient area for equipment storage. The moonpool dimension is designed to provide enough space for safely deploying the subsea structures and

RLWI Stack for intervention. The vessel is also equipped with cranes and skidding system to support equipment mobilization.

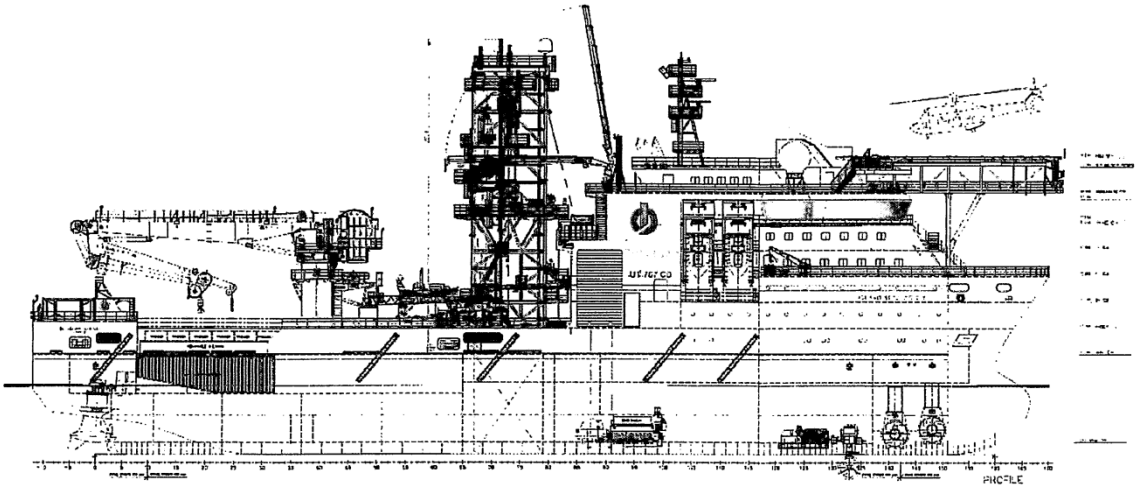

Figure 31. Side view of Island Wellserver (Island Offshore, 2012)

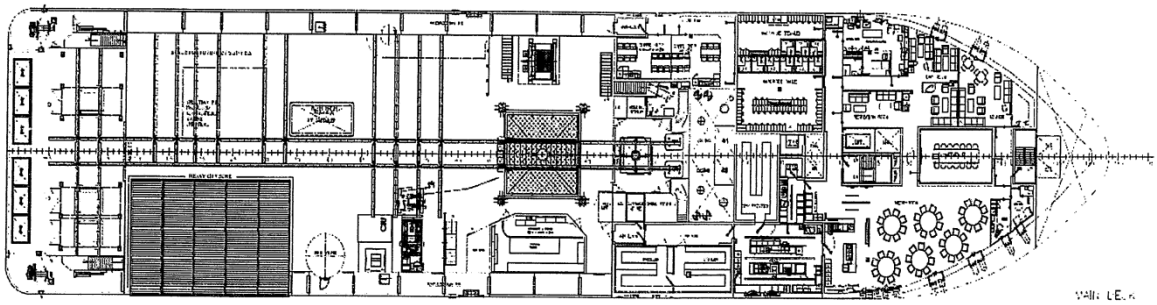

Figure 32. Top view of Island Wellserver (Island Offshore, 2012)

The main characteristics of the Island Wellserver vessel are:

- Deadweight at draught 7.7 m : 5800 tones
- Overall length : 116 m
- Breadth moulded : 25 m
- Deck area : 1150 m^2
- Depth to main deck : 11.2 m
- Max speed : 14 knots
- Moon pool size : 7.8 x 7.8 m
- Design draught : 7.7 m
- Dynamic Positioning system : Rolls Royce, UT 767 CD, DP Class 3.

A well intervention vessel should have DP-3 Dynamic Positioning System. The Island Wellserver utilizes a diesel-electric power plant to provide power for two main Azipull thrusters, one retractable Azimuth thruster, and two Tunnel thrusters. The dynamic positioning system for the Island Wellserver vessel was certified according to IMO Class III to fulfill station keeping requirement for light well intervention.

5.4.1 Island Wellserver Operability

The operational criteria for Island Wellserver were established based on vessel motion due to 30 wave heading. All the motion responses are defined with reference to center of the moon pool. The maximum displacement for translational and rotational motions can be tabulated as follows:

Table 9. Operational criteria of Island Wellserver (Island Offshore, 2012)

Design Mode	Wave Heading	Allowable Displacements, Single Amplitudes				
		Surge	Sway	Heave	Roll	Surge
	deg	m	m	m	deg	deg
Well intervention operations Hs=6.0m; Tp=12.4 s	30	3.4	1.8	4.2	4.6	7.9
Module deployment Hs=4.0m; Tp=10.1 s	30	1.6	0.9	2.1	2.9	5.7
Horizontal skidding modules Hs=4.0m; Tp=8.5 s	30	1.6	0.9	2.1	2.9	5.7
Sub sea support and construction Hs=7.0m; Tp=13.4 s	30	2.5	1.4	3.1	3.6	6.9
Max. umbilical disconnect Hs=7.0m; Tp=13.4	30	4.4	2.4	5.2	5.5	8.7

5.5 Wireline Properties

In this project, the simulation is limited to only for two different types of wireline. The wireline data used for simulation is taken from the Seaflex report (Seaflex Riser Technologies, 2012). The table below shows wirelines properties of Sandvik 5R60 with 0.125" diameter and Camesa Monoconductor with 7/16" diameter that are going to be used in the simulation.

Table 10. Wireline properties for Slickline and Monoconductor (Seaflex Riser Technologies, 2012)

Tool Wire Properties	Unit	Sandvik 5R60 0.125"	Camesa Mono 7/16"
External Diameter	mm	3.175	10.8
Bending Stiffness, EI	Nm^2	0	0
Axial Stiffness, EA	N	1.64E+06	1.90E+07
Torsional Stiffness, GJ	Nm^2	6.31E+05	7.30E+06
Unit Weight in Air	kg/m	0.064	0.499
Unit Weight in Water, filled	kg/m	0.056	0.413
Tension Capacity	kN	11.131	86.8
Drag coefficient, Cd		1	1
Added mass coefficient, Cm		1	1

Excessive horizontal deflection on the wireline during operation will increase the friction on top of PCH and may disrupt the cable to go further down. The BHA weight needs to be increased to keep the wireline deflection as minimum as possible within the recommendations as shown in **Table 11.** These recommendations for deflections are mainly based on the field experience of RLWI operation (Island Offshore, 2012). During the lowering down operations, the tension occurring in the wireline should be less than the working load limit (WLL) of the wireline cable as stated in **Table 12.**

Table 11. Criteria for cable deflection during wireline operations (Island Offshore, 2012)

Operation	Cable	Acceptable	Challenging	Not Recommended
Logging	All sizes	< 7.5% of depth	7.5-10% of MSL	> 10% of MSL
Perforation	All sizes	< 7.5% of depth	7.5-10% of MSL	> 10% of MSL
Plug Setting	All sizes	< 7.5% of depth	7.5-10% of MSL	> 10% of MSL
SPM devices	All sizes	< 5% of depth	5-7.5% of MSL	> 7.5% of MSL
Mech. Ops. Deep in well	0.125" to 7/16"DF	< 5% of depth	5-7.5% of MSL	> 7.5% of MSL

Table 12. Safe working limit for wireline operations (Island Offshore, 2012)

TYPE	Size	WLL	Breaking Strength
Slickline	0.125"	1515 lbs - 687 kg	3030 lbs - 1374 kg
Dyform	7/32"	4200 lbs - 1905 kg	8400 lbs - 3810 kg
Monoconductor	5/16"	5500 lbs - 2496 kg	11000 lbs - 4900 kg
Monoconductor	7/16"	9750 lbs - 4423 kg	19500 lbs - 8845 kg

5.6 Technical Specifications and Standards

All petroleum activities related to planning, design, construction, production and removal in Norwegian Continental Shelf (NCS) should be acknowledged by Petroleum Safety Authority (PSA) Norway. The Norwegian Petroleum Safety Authority is a government organization that has regulatory authority to ensure that the petroleum activities are carried out in accordance with high standards of safety for human and environment. Some standards and recommended practices exist to provide guidelines for well intervention in offshore operation. Some prevailing standards referred by PSA are listed below:

- NORSOK D-002 System Requirements Well Intervention Equipment
  This standard contains the procedures for design, installation, and commissioning of well intervention equipments and their functions. The general requirements for wireline equipment are described in chapter 8 of this standard.
- NORSOK D-010 Well Integrity in Drilling and Well Operations
  This standard provides the guidelines and requirements to ensure well integrity during well operations. The integrity of the well during its life cycle (i.e., drilling, production, and intervention) can be established by using well barriers. The main purpose of well barrier is to prevent the hydrocarbons from flowing unintentionally from the formation, into another formation, or to surface. The requirement for well barriers and well control action procedures in wireline operations are described in chapter 10.
- DNV-OS-E101 Drilling Plant
  This offshore standard provides technical guidelines for design, construction, and commissioning of well intervention facilities and equipments.
- DNV-RP-C205 Environmental Conditions and Environmental Loads
  This latest Recommended Practice (RP) by DNV is used as a practical standard for modeling, analyzing, and predicting the environmental conditions and loads that act on the marine structures or vessels during marine operations. In this case, the loads are wave and current. This Recommended Practice is established based on experience from previous projects.

- DNV-RP-H103 Modeling and Analysis of Marine Operations
  The lifting operations during light well intervention will refer to this Recommended Practice (RP) established by DNV. This Recommended Practice provides simplified formulas in planning and executing marine operations, such as deepwater lowering down operations.

5.7 Analysis Setup

5.7.1 Modeling in OrcaFlex

The global model in OrcaFlex comprises vessel, environmental data, simple active heave compensator, wireline, downhole tool, and artificial well. The PCH, wellhead, and well were modeled as a one artificial well model. The complete model can be described in the following figure.

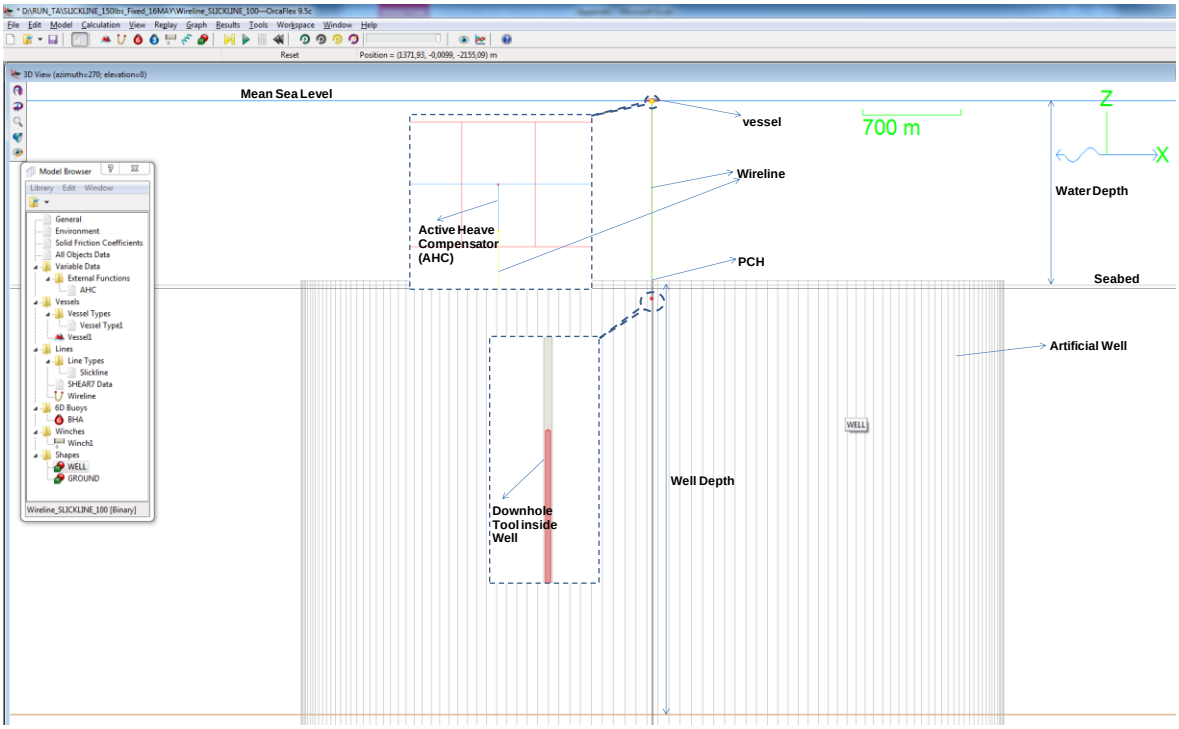

Figure 33. OrcaFlex modeling

The wireline model needs to be discretized with an adequate number of elements to represent correctly the load effects from environmental and other additional loads in critical areas. The wireline is modeled as a line model in the OrcaFlex which is divided into smaller segments. Each segment represents a beam element which connects two nodes. The OrcaFlex will calculate based on this number of segments. To obtain more accuracy in analysis results, finer segmentation is required but it will lead to longer time in OrcaFlex analysis. In this project, the number of segments is chosen and the OrcaFlex will calculate automatically the targeted segment length by dividing the total length by number of segments. In this case the number segments selected is 20.

The top section of the wireline is connected to the heave compensation system and the bottom section is connected directly to downhole tool with different weight cases. Each model will be made separately to analyze different depths and different weights of the downhole tool. The simulation model will be created for every 100 meters case from 1400 meters to 4250 meters well depth (measured from the sea surface). The vessel will be modeled as a standard vessel with RAO

data using default settings from OrcaFlex. The vessel RAO is used to determine the motion of response of the intervention vessel due to wave in dynamic analysis.

For wireline operation, active heave compensator is required to minimize the movement of the downhole tool inside the well during light well intervention. In OrcaFlex this heave compensator can be modeled as a winch. The OrcaFlex can implement the heave compensation system using a generic PID controller through its external function. When modeling the heave compensator, the winch length is controlled for the whole simulation and payout rate of winch wire is controlled by external function embedded in OrcaFlex software. The PID control system can be expressed in following equation (Orcina Ltd, 2010):

$$\text{Winch Payout Rate} = k_0 + k_P + k_I \cdot \int e \cdot dt + k_D \cdot \left(\frac{de}{dt} \right)$$

Where e is the error signal, in this case desired depth control – actual depth and k_0, k_p k_I, and k_D are the constants. During the dynamic simulation, the winch system will try to maintain the downhole tool elevation by paying out or paying in the wire.

The downhole tool is modeled as a 6D buoy in OrcaFlex, in this case the spar buoy type is chosen. The important parameters that need to be inputted are the diameter, length, and mass. This buoy element is selected because it can model the buoyancy force tool and contact force inside the well during well operation. The artificial well is modeled as an elastic solid property. The friction between the well and the wireline and downhole tool will be taken into consideration during simulation.

Stiffness, mass, and hydrodynamics coefficient for the wireline in OrcaFlex need to be determined appropriately to obtain the analysis results as close as possible with the actual conditions of the site. The drag and inertia coefficient can be derived from experiments or Computational Fluid Dynamics (CFD) simulations. These hydrodynamics coefficients depend on parameters, such as shape, roughness, Reynolds number, etc. In this project, the hydrodynamic coefficients will be assigned to OrcaFlex software based on the given data as provided in **Table 10**. These hydrodynamic coefficients then will be used by OrcaFlex for calculating the drag force based on Morison formula. The Morison formulation calculates the drag forces acting on the wireline from the defined velocity and acceleration of sea water particles that are going through the wireline.

5.7.2 Simulations

The static analysis will be performed to determine the initial configuration of the wireline when it gets exposed to the hydrodynamic force from the sea currents. From the static analysis, outputs such as tension force and movement of nodes' coordinate position in static case can be obtained. For dynamic analysis, JONSWAP spectrum is used to represent the sea state in the North Sea area., the wave height and period were chosen based on requirement in **Table 7** of section 5.3, then the peakedness factor (γ) was selected for 3.3 as recommended by DNV-RP-C205. These values will be used as inputs for OrcaFlex in generating the JONSWAP spectrum as shown in **Figure 34**. In dynamic simulation, OrcaFlex can calculate dynamic forces, tensions, and deflection that might occur due to combination of waves, currents, and vessel motion. Then the analysis results obtained from OrcaFlex simulations can be compared for different cases.

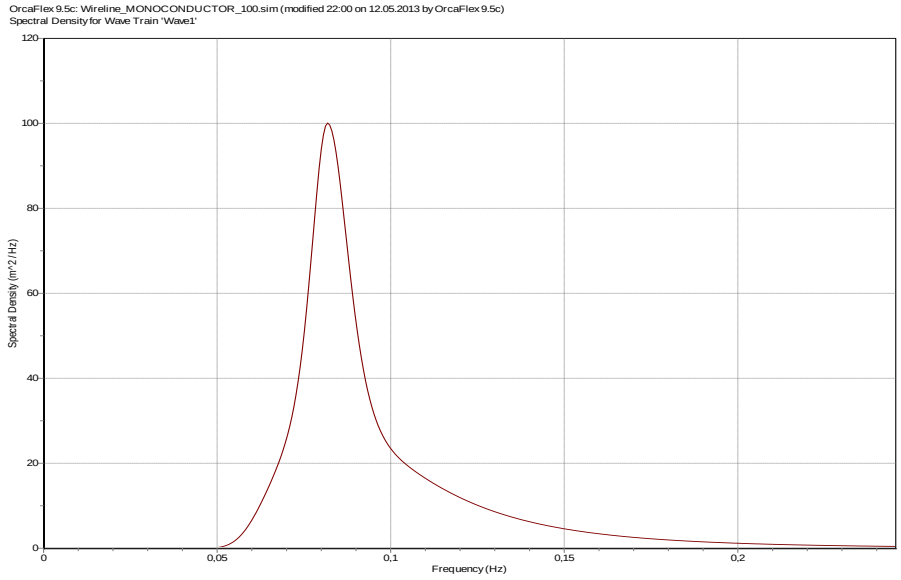

Figure 34. JONSWAP spectral density generated by OrcaFlex software

5.7.3 Wave Search and Time Selection for Dynamic Simulation

DNV recommends to running the simulations for 3 hours in irregular sea states, but it takes enormous amount of time to do so in all the simulations. Since this project is only limited for study case, a simple method to shorten the simulation have been taken to reduce time. For each case, the simulation is run for 180 seconds.

OrcaFlex software can generate wave condition for JONSWAP spectrum for the full 3 hours simulation as shown in **Figure 35**.

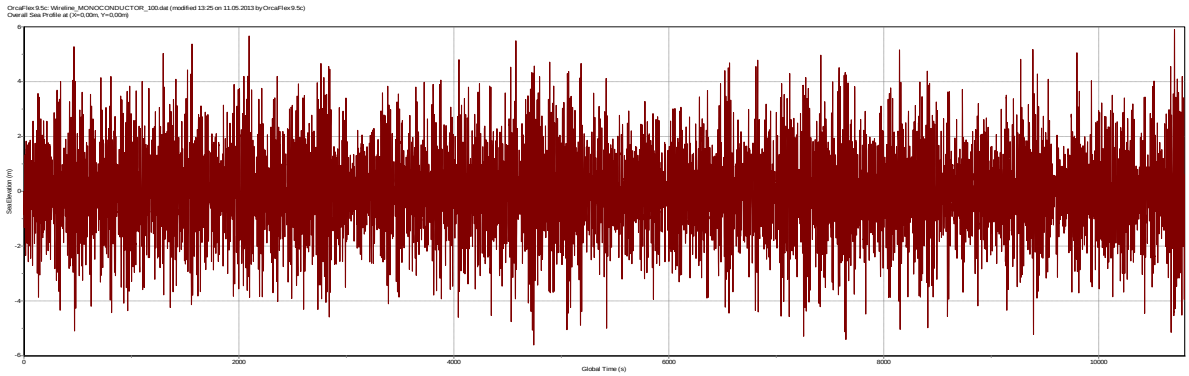

Figure 35. Wave profile generated by OrcaFlex for 3 hours simulation

To ensure that the maximum wave height during 3 hours storm is included in the simplified simulation, a search of wave need to be done. OrcaFlex has capability to list all the events of the wave. A wave search can be performed for the wave height over than 10 meters and steepness more than 0.125 within period of 0 to 10800 seconds (3 hours). From the search, OrcaFlex indicates that the largest rise 10.31 meters with wave crest height 5.90 meters. It occurs at 10700.37th seconds of the total 10800 seconds duration. Hence, the time duration of each simulation is set to include this event, it starts approximately 90 seconds before the largest rise occurs and finishes 90 seconds after the largest rise occurs as shown in **Figure 36**.

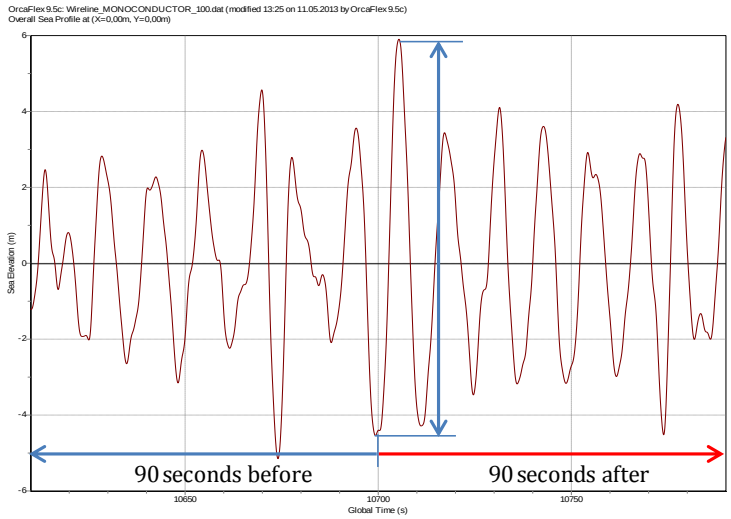

Figure 36. Selection of time duration for the simulation based on maximum wave height location

CHAPTER 6

ANALYSIS RESULTS & DISCUSSIONS

6.1 Analysis Results

This chapter summarizes all the analysis results generated by OrcaFlex for different cases of well depth in wireline operations using Slickline 0.125" diameter and Monoconductor 7/16" diameter. The analysis results are presented in tables and graphs. The analysis results extracted from the OrcaFLex are the coordinates of each wireline segment, the top tension force at the surface vessel, and dynamic forces that acts on wireline at vessel and at PCH.

After OrcaFlex simulations are run, the coordinates of each wireline will move to a new position due to sea current. The new coordinates of each wireline segment for all different well depth cases are plotted in a graph to give a good visualization of how the wireline behave as the function of well depth. This wireline's behavior plays important role in determining the accuracy of downhole tool position since the deflection in free span of the wireline in open water will induce vertical displacement at end point of the wireline that is connected to the downhole tool.

6.1.1 Case 1A

OrcaFlex was used to analyze the wireline behavior during wireline operation for the case of downhole tool having a weight of 150 lbs attached to the 0.125" slickline cable. **Figure 37** shows that the tension increase linearly as the 150 lbs downhole tool goes deeper. The maximum tension is obtained during lowering down the downhole tool into the well at 4250 meters measured depth from sea surface. As the graph shown, the tension will vary from 1.37 kN to 2.91 kN when the 150 lbs downhole tool is being lowered down to a particular depth. During the operation, the wireline will get exposed to the sea currents. **Figure 39** shows the wireline behavior under horizontal forces from varying speed of sea currents. The OrcaFlex software computed that the largest maximum lateral deflection is 122.37 meters at water depth of 592 meters from mean sea level. This largest value of lateral deflection is obtained when the downhole tool is positioned inside the well at 1367.19 meters TVD. As the downhole tool goes deeper, the maximum lateral deflection will decrease and reach its smallest value of 50.10 meters obtained at 542.5 meters water depth from the sea surface. It occurs when the downhole tool is being lowered down for the operation at measured depth of 4250 meters from mean sea level.

These lateral deflections on wireline will induce vertical displacements along the wireline length. There will be an upward displacement at the end point of the wireline. These vertical deflections vary over the depths; with the largest value is 32.81 meters. This largest vertical displacement will occur when the length of wireline is spooled out 1400 meter from winch's vessel (measured depth). The vertical displacement then will decrease as the downhole tool goes deep. From the analysis, the smallest deflection is obtained 1.01 meters in upward direction when the downhole tool is located at measured depth of 4250 meters from the RLWI vessel.

Table 13. Summary of static analysis results from OrcaFlex for case 1A

Measured Depth	True Vertical Depth	Vertical Displacement at Wireline End Point B	Maximum Horizontal Deflection	Top Tension at Wireline End Point A
(m)	(m)	(m)	(m)	(kN)
-1400	-1367.19	32.81	122.37	1.37
-1500	-1470.56	29.44	116.13	1.42
-1600	-1573.22	26.78	111.14	1.48
-1700	-1675.82	24.18	105.88	1.53
-1800	-1777.90	22.10	101.68	1.58
-1900	-1879.76	20.24	97.79	1.64
-2000	-1981.62	18.38	93.61	1.69
-2100	-2083.12	16.88	90.28	1.75
-2200	-2184.48	15.52	87.17	1.80
-2300	-2285.87	14.13	83.76	1.85
-2400	-2387.00	13.00	81.06	1.91
-2500	-2488.04	11.96	78.53	1.96
-2600	-2589.00	11.00	76.15	2.02
-2700	-2689.89	10.11	73.91	2.07
-2800	-2790.73	9.27	71.79	2.12
-2900	-2891.60	8.40	69.38	2.18
-3000	-2992.33	7.67	67.50	2.23
-3100	-3093.01	6.99	65.72	2.29
-3200	-3193.65	6.35	64.03	2.34
-3300	-3294.27	5.73	62.42	2.40
-3400	-3394.85	5.15	60.89	2.45
-3500	-3495.40	4.60	59.44	2.51
-3600	-3595.93	4.07	58.05	2.56
-3700	-3696.44	3.56	56.72	2.61
-3800	-3796.93	3.07	55.46	2.67
-3900	-3897.46	2.54	53.93	2.72
-4000	-3997.91	2.09	52.78	2.78
-4100	-4098.35	1.65	51.67	2.83
-4200	-4197.68	2.32	54.67	2.70
-4250	-4248.99	1.01	50.10	2.91

Table 14. Analysis results of dynamic forces from OrcaFlex for case 1A

Measured Depth	Force At Vessel		Force At Pressure Control Head	
	Horizontal Force Fx	Vertical Force Fz	Horizontal Force Fx	Vertical Force Fz
(m)	(N)	(N)	(N)	(N)
-1400	1003.85	-1334.25	318.27	783.79
-1500	1017.26	-1385.91	339.41	1118.45
-1600	1023.78	-1452.19	323.60	910.62
-1700	1054.48	-1499.64	356.59	1177.66
-1800	1041.29	-1563.73	328.13	1037.71
-1900	1052.61	-1620.84	330.18	1074.65
-2000	1059.90	-1685.37	331.80	1144.89
-2100	1065.57	-1736.40	333.40	1207.46
-2200	1080.94	-1801.38	334.82	1254.84
-2300	1115.09	-1844.79	353.68	1502.39
-2400	1118.08	-1929.57	337.20	1401.15
-2500	1120.61	-1959.20	338.28	1430.79
-2600	1130.50	-2010.82	339.37	1492.14
-2700	1129.77	-2085.03	340.41	1523.35
-2800	1134.68	-2138.83	341.89	1611.38
-2900	1165.69	-2175.35	388.18	1797.83
-3000	1161.43	-2272.74	342.87	1751.39
-3100	1171.37	-2308.50	343.54	1811.81
-3200	1168.63	-2377.50	344.23	1837.68
-3300	1174.32	-2445.72	344.82	1893.24
-3400	1179.78	-2492.43	345.46	1946.45
-3500	1189.37	-2544.71	346.09	2015.99
-3600	1203.96	-2639.58	346.46	2164.97
-3700	1196.70	-2748.88	347.20	2186.33
-3800	1236.44	-2832.64	347.96	2379.39
-3900	1206.48	-2832.48	375.49	2456.28
-4000	1195.54	-2984.32	398.96	2401.00
-4100	1239.86	-3105.26	348.23	2575.49
-4200	1276.87	-2903.06	416.10	2533.98
-4250	1215.82	-3178.41	348.40	2668.19

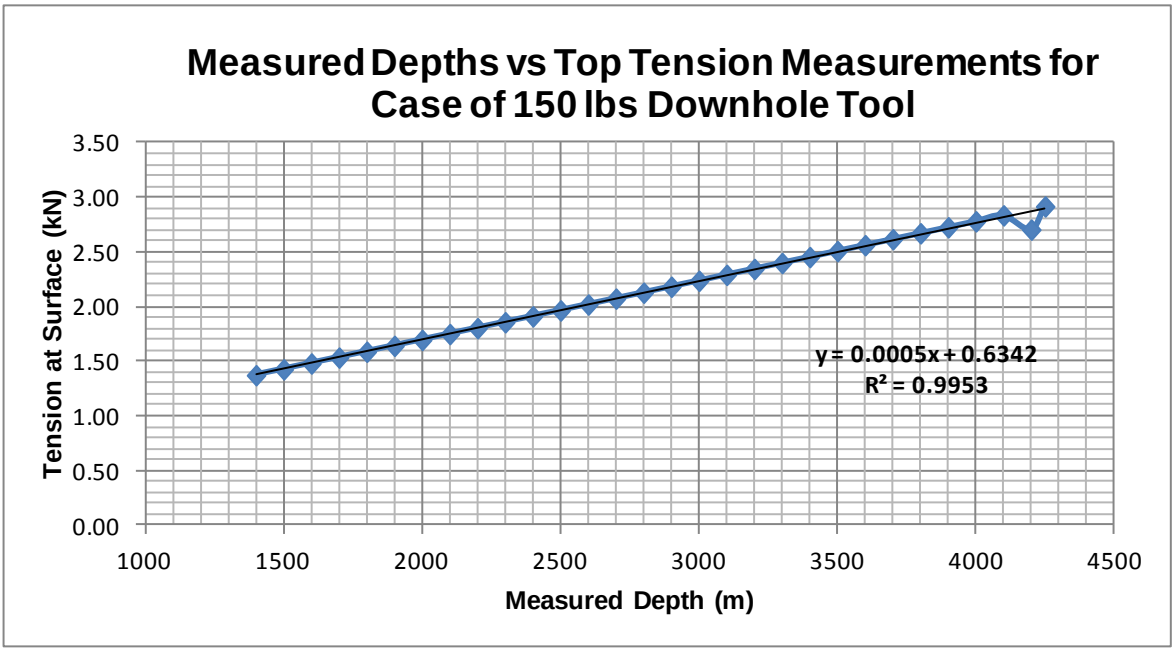

Figure 37. Relation between top tensions and measured depths for case 1A

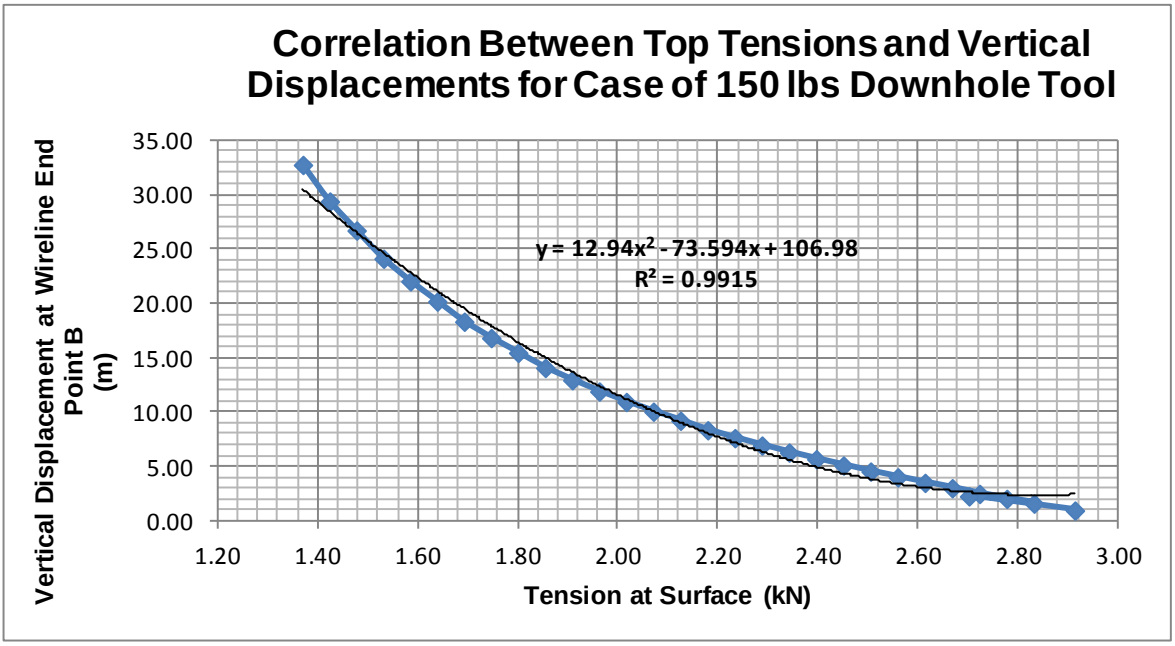

Figure 38. Relation between top tensions and vertical displacements for case 1A

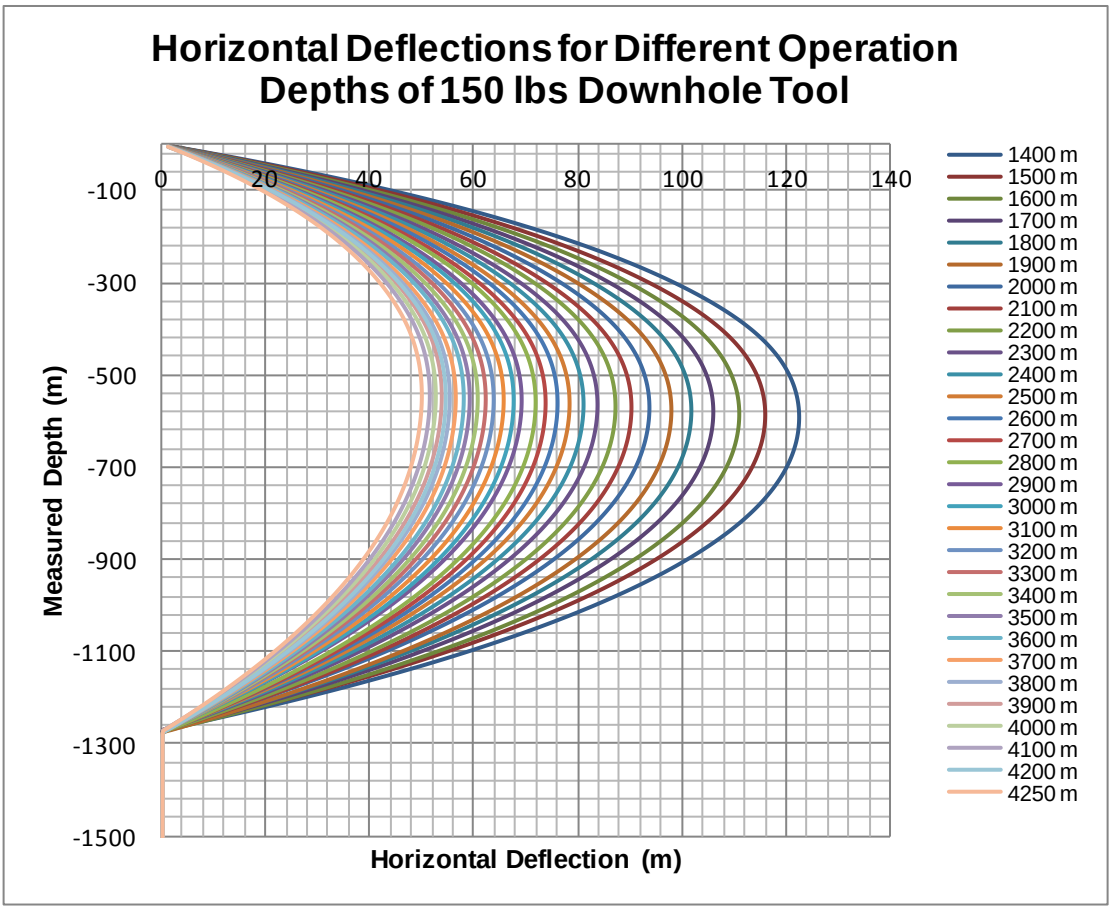

Figure 39. Horizontal deflections for different operation depths of case 1A

6.1.2 Case 1B

The 0.125" Slickline used for wireline operation was simulated for the case of using 600 lbs of downhole tool weight attached. As shown in **Figure 41**, the tension read at surface will have variation from 3.35 kN to 4.21 kN. The vertical displacements occur either in upward or downward direction depending on which depth of the downhole tool is being deployed. The vertical deflection in upward direction means that the true vertical depth is less than the measured depth, while in downward direction means that the true vertical depth is over than the measured depth. From the analysis, the upward deflections are found when the downhole tool is being deployed at measured depth of 1400 meters to 1800 meters from the vessel. The downward deflections are found when the downhole tool is deployed for the operations at measured depth over than 1800 meters.

From the analysis, the largest upward displacement at the end point of wireline connected to the downhole tool is 1.67 meters. It occurs when the downhole tool is being lowered down for the operation at measured depth of 1400 meters from the vessel. It means that the measured depth of the tools needs to be corrected. The downhole tool should be located at 1398.3 meters TVD from the sea surface with reading at vessel's winch showing tension force of 3.35 kN. The largest downward displacement at the end point of the wireline is 6.76 meters for the operation at measured depth of 4250 meters. This analysis result implies that the actual depth of the downhole tool is 4256.76 meters. The lateral deflections of the wireline during deploying the 600 lbs downhole tool into the well are shown in **Figure 42**. The largest value of maximum lateral deflection from simulation is 43.13 meters, it occurs at water depth of 543.5 meters from sea surface for the wireline operation at 1400 meters MD below mean sea level. And the smallest value of maximum lateral deflection is 33.78 meters and located at water depth of 535.4 meters from the sea surface. It occurs for the operation at measured depth of 4250 meters from sea surface.

Table 15. Summary of static analysis results from OrcaFlex for case 1B

Measured Depth	True Vertical Depth	Vertical Displacement at Wireline End Point B	Maximum Horizontal Deflection	Top Tension at Wireline End Point A
(m)	(m)	(m)	(m)	(kN)
-1400	-1398.33	1.67	43.13	3.35
-1500	-1498.68	1.32	42.39	3.40
-1600	-1599.04	0.96	41.67	3.46
-1700	-1699.38	0.62	40.98	3.51
-1800	-1799.73	0.27	40.31	3.57
-1900	-1900.07	-0.07	39.66	3.62
-2000	-2000.41	-0.41	39.03	3.68
-2100	-2100.75	-0.75	38.42	3.73
-2200	-2201.09	-1.09	37.83	3.79
-2300	-2301.43	-1.43	37.26	3.84
-2400	-2401.76	-1.76	36.70	3.89
-2500	-2502.10	-2.10	36.16	3.95
-2600	-2602.43	-2.43	35.64	4.00
-2700	-2702.67	-2.67	35.52	4.02
-2800	-2802.91	-2.91	35.40	4.03
-2900	-2903.15	-3.15	35.29	4.04
-3000	-3003.40	-3.40	35.18	4.05
-3100	-3103.65	-3.65	35.06	4.06
-3200	-3203.90	-3.90	34.95	4.08
-3300	-3304.16	-4.16	34.84	4.09
-3400	-3404.42	-4.42	34.73	4.10
-3500	-3504.68	-4.68	34.61	4.11
-3600	-3604.95	-4.95	34.50	4.13
-3700	-3705.22	-5.22	34.39	4.14
-3800	-3805.49	-5.49	34.28	4.15
-3900	-3905.77	-5.77	34.17	4.16
-4000	-4006.05	-6.05	34.06	4.18
-4100	-4106.33	-6.33	33.95	4.19
-4200	-4206.62	-6.62	33.84	4.20
-4250	-4256.76	-6.76	33.78	4.21

Table 16. Analysis results of dynamic forces from OrcaFlex for case 1B

Measured Depth	Force At Vessel		Force At Pressure Control Head	
	Horizontal Force Fx	Vertical Force Fz	Horizontal Force Fx	Vertical Force Fz
(m)	(N)	(N)	(N)	(N)
-1400	1249.12	-3380.36	351.97	2800.48
-1500	1250.23	-3433.93	352.17	2837.96
-1600	1249.02	-3489.02	352.42	2907.80
-1700	1263.44	-3546.78	352.48	2967.02
-1800	1274.21	-3603.48	352.71	3007.03
-1900	1277.52	-3660.16	352.99	3070.33
-2000	1281.49	-3715.73	353.17	3132.28
-2100	1276.07	-3771.99	353.40	3184.66
-2200	1277.89	-3847.13	353.48	3287.39
-2300	1301.85	-3889.05	353.71	3355.03
-2400	1305.73	-3937.33	353.90	3376.92
-2500	1308.11	-4002.03	354.16	3440.96
-2600	1310.99	-4068.69	357.26	3480.00
-2700	1353.55	-4189.02	364.70	3629.29
-2800	1357.70	-4246.11	374.23	3693.59
-2900	1363.67	-4228.67	385.69	3667.75
-3000	1379.91	-4255.24	398.60	3692.91
-3100	1384.05	-4271.65	414.00	3725.66
-3200	1393.96	-4377.88	432.67	3805.35
-3300	1384.18	-4376.32	453.68	3849.67
-3400	1391.71	-4417.65	477.05	3924.80
-3500	1382.00	-4421.56	503.21	3969.76
-3600	1389.26	-4449.66	531.33	4052.65
-3700	1387.23	-4432.47	561.79	4095.87
-3800	1387.55	-4471.23	593.74	4213.51
-3900	1396.67	-4450.98	627.25	4275.69
-4000	1395.13	-4420.56	661.84	4278.36
-4100	1382.89	-4456.89	696.64	4343.56
-4200	1390.09	-4483.75	732.84	4405.21
-4250	1398.61	-4457.97	751.84	4423.43

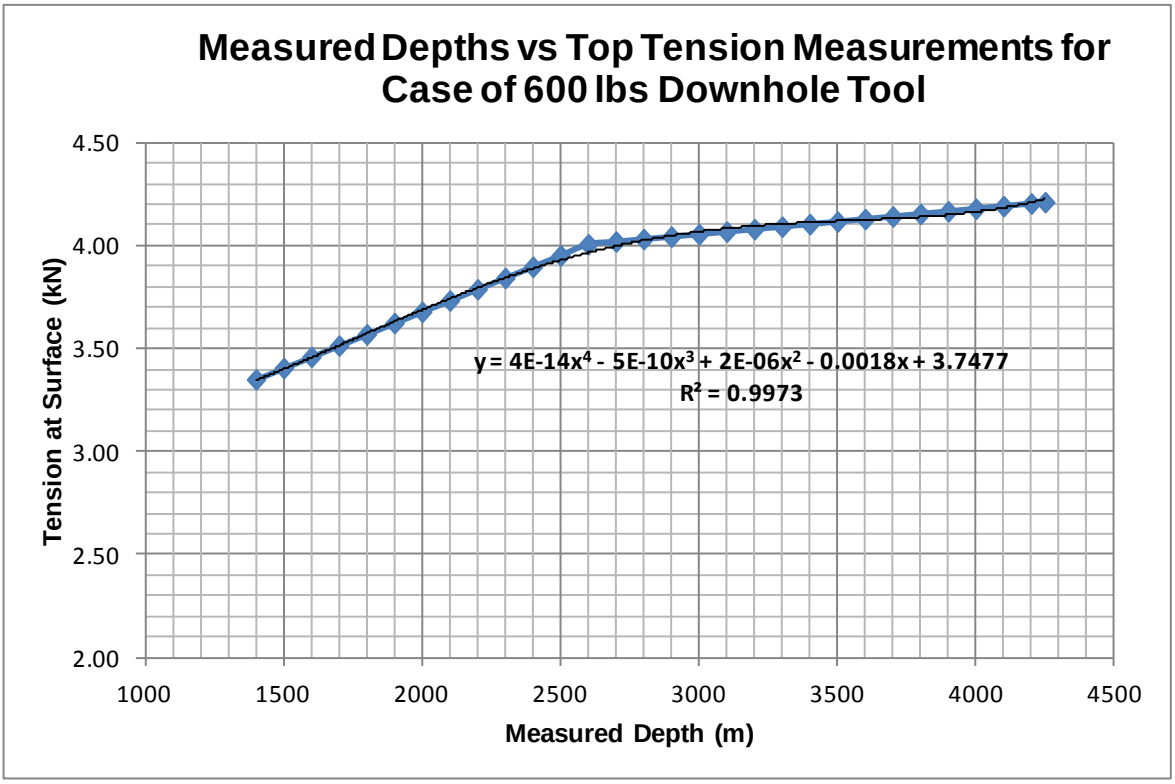

Figure 40. Relation between top tensions and measured depths case 1B

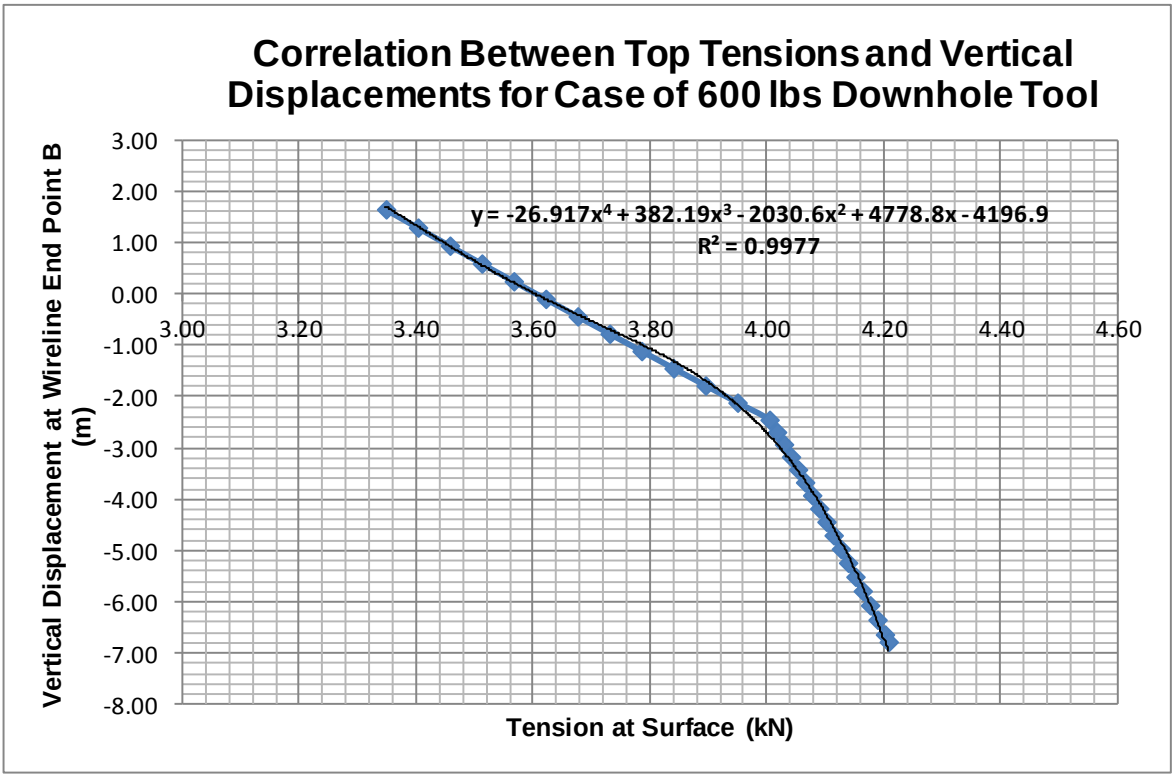

Figure 41. Relation between top tensions and vertical displacements for case 1B

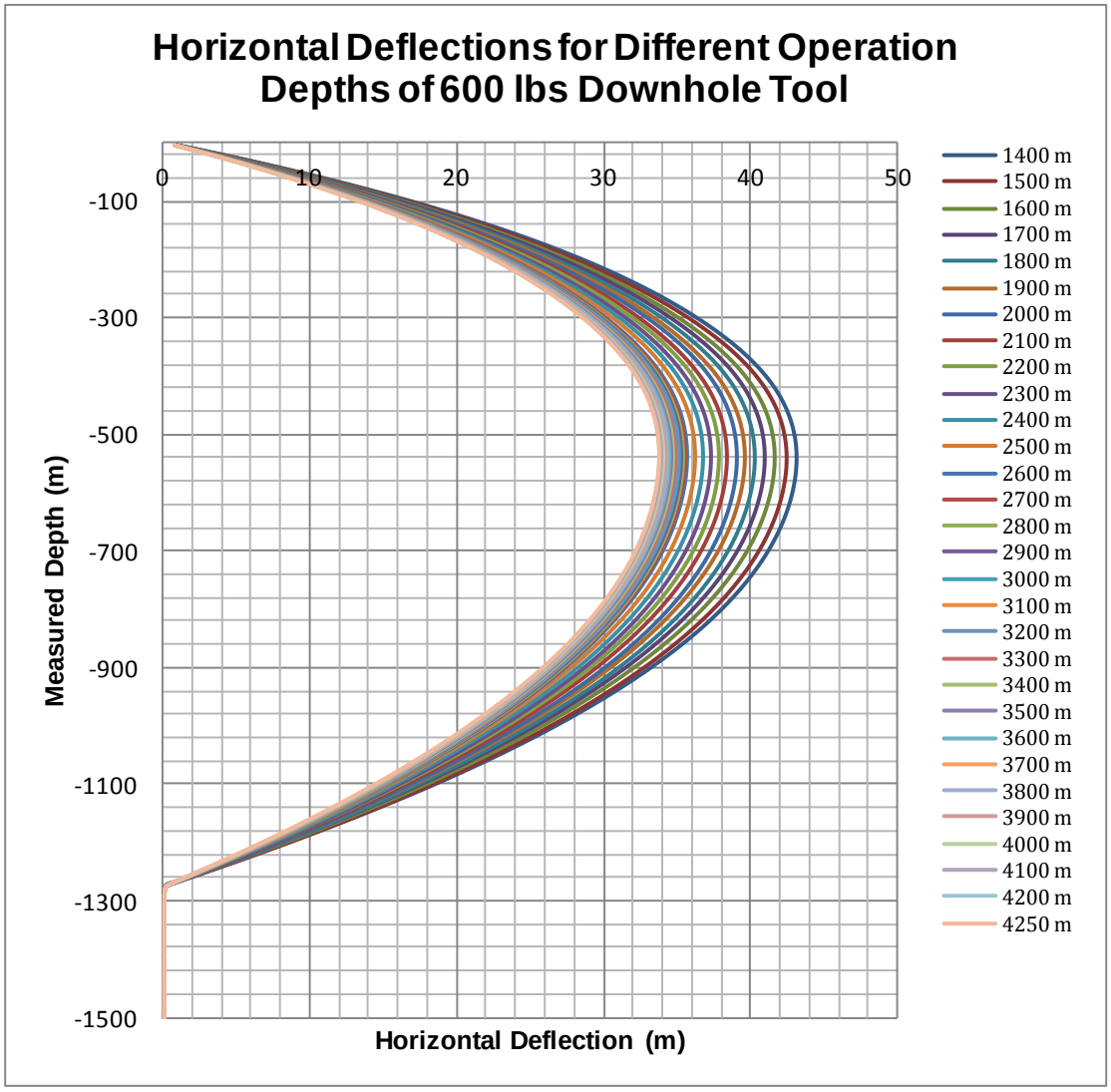

Figure 42. Horizontal deflections for different operation depths of case 1B

6.1.3 Case 1C

Different depth cases for wireline operation using Slickline 0.125" diameter with 1000 lbs downhole tool were evaluated in OrcaFlex software. **Figure 44** shows the correlation between the surface tensions and vertical displacements at end point of the wireline attached to the downhole tool. Based on the OrcaFlex analysis, the vertical displacements of the wireline end point will be in downward direction for every depth case. The largest downward displacement found at wireline end point will be 13.53 meters when the wireline is measured at 4250 meters depth from vessel (measured depth). It indicates that the actual depth of the wireline end point is estimated to be 4263.53 meters TVD. The wireline will experience varying tensions that go linearly from 5.12 kN to 6.68 kN as the downhole tool goes deeper. The maximum tension will occur for the operation at the measured depth of 4250 meters.

As shown in **Figure 45**, during lowering down the downhole tool from the measured depth of 1400 meters to 4250 meters, the part of wireline that is exposed to the open water will be deflected horizontally. Most of the maximum deflection will occur approximately at the mid length of exposed wireline. As presented in the figure, the largest value of maximum horizontal deflection is 27. 36 meters located at 530.6 meters water depth. It will occur when the wireline length is spooled

out 1400 meters of vessel's winch. The smallest value of maximum wireline deflection is 20.76 meters. It will be obtained when the downhole tool is operated in the well at the measured depth of 4250 meters from mean sea level.

Table 17. Summary of static analysis results from OrcaFlex for case 1C

Measured Depth	True Vertical Depth	Vertical Displacement at Wireline End Point B	Maximum Horizontal Deflection	Top Tension at Wireline End Point A
(m)	(m)	(m)	(m)	(kN)
-1400	-1402.38	-2.38	27.36	5.12
-1500	-1502.74	-2.74	27.06	5.18
-1600	-1603.10	-3.10	26.77	5.23
-1700	-1703.46	-3.46	26.48	5.29
-1800	-1803.82	-3.82	26.19	5.34
-1900	-1904.19	-4.19	25.92	5.40
-2000	-2004.56	-4.56	25.65	5.45
-2100	-2104.93	-4.93	25.38	5.50
-2200	-2205.30	-5.30	25.12	5.56
-2300	-2305.68	-5.68	24.87	5.61
-2400	-2406.05	-6.05	24.62	5.67
-2500	-2506.44	-6.44	24.37	5.72
-2600	-2606.82	-6.82	24.13	5.78
-2700	-2707.20	-7.20	23.90	5.83
-2800	-2807.59	-7.59	23.67	5.89
-2900	-2907.98	-7.98	23.44	5.94
-3000	-3008.38	-8.38	23.22	6.00
-3100	-3108.77	-8.77	23.00	6.05
-3200	-3209.17	-9.17	22.79	6.11
-3300	-3309.58	-9.58	22.58	6.16
-3400	-3409.98	-9.98	22.37	6.22
-3500	-3510.39	-10.39	22.17	6.27
-3600	-3610.80	-10.80	21.97	6.33
-3700	-3711.21	-11.21	21.77	6.38
-3800	-3811.63	-11.63	21.58	6.44
-3900	-3912.05	-12.05	21.39	6.49
-4000	-4012.47	-12.47	21.21	6.55
-4100	-4112.89	-12.89	21.03	6.60
-4200	-4213.32	-13.32	20.85	6.66
-4250	-4263.53	-13.53	20.76	6.68

Table 18. Analysis results of dynamic forces from OrcaFlex for case 1C

Measured Depth	Force At Vessel		Force At Pressure Control Head	
	Horizontal Force Fx	Vertical Force Fz	Horizontal Force Fx	Vertical Force Fz
(m)	(N)	(N)	(N)	(N)
-1400	1384.51	-5160.96	356.08	4561.74
-1500	1389.84	-5217.79	356.08	4625.50
-1600	1401.13	-5286.26	356.22	4700.99
-1700	1407.04	-5341.30	356.34	4761.82
-1800	1411.10	-5395.88	356.48	4818.39
-1900	1415.85	-5460.12	356.60	4886.21
-2000	1423.05	-5508.44	356.76	4946.06
-2100	1423.47	-5557.97	356.81	4998.35
-2200	1425.42	-5617.09	356.80	5055.72
-2300	1435.14	-5708.03	356.85	5142.30
-2400	1432.16	-5801.09	357.12	5203.25
-2500	1429.27	-5851.95	357.04	5255.08
-2600	1431.58	-5915.46	357.14	5329.29
-2700	1441.51	-6019.33	357.29	5416.35
-2800	1441.40	-6139.24	357.54	5526.09
-2900	1448.18	-6258.96	357.29	5643.72
-3000	1434.18	-6219.52	357.03	5604.51
-3100	1440.10	-6308.19	357.21	5720.76
-3200	1463.21	-6406.70	356.96	5786.37
-3300	1451.85	-6303.02	357.18	5662.22
-3400	1449.58	-6388.13	357.08	5767.14
-3500	1455.63	-6369.41	357.29	5744.58
-3600	1443.35	-6575.29	357.38	5958.20
-3700	1461.90	-6918.65	357.55	6303.25
-3800	1469.06	-6705.95	357.25	6102.55
-3900	1463.78	-6929.00	357.64	6289.51
-4000	1478.51	-7272.79	358.02	6676.18
-4100	1487.09	-7360.32	358.06	6751.66
-4200	1476.50	-7097.86	357.53	6498.19
-4250	1474.67	-7182.06	357.55	6597.36

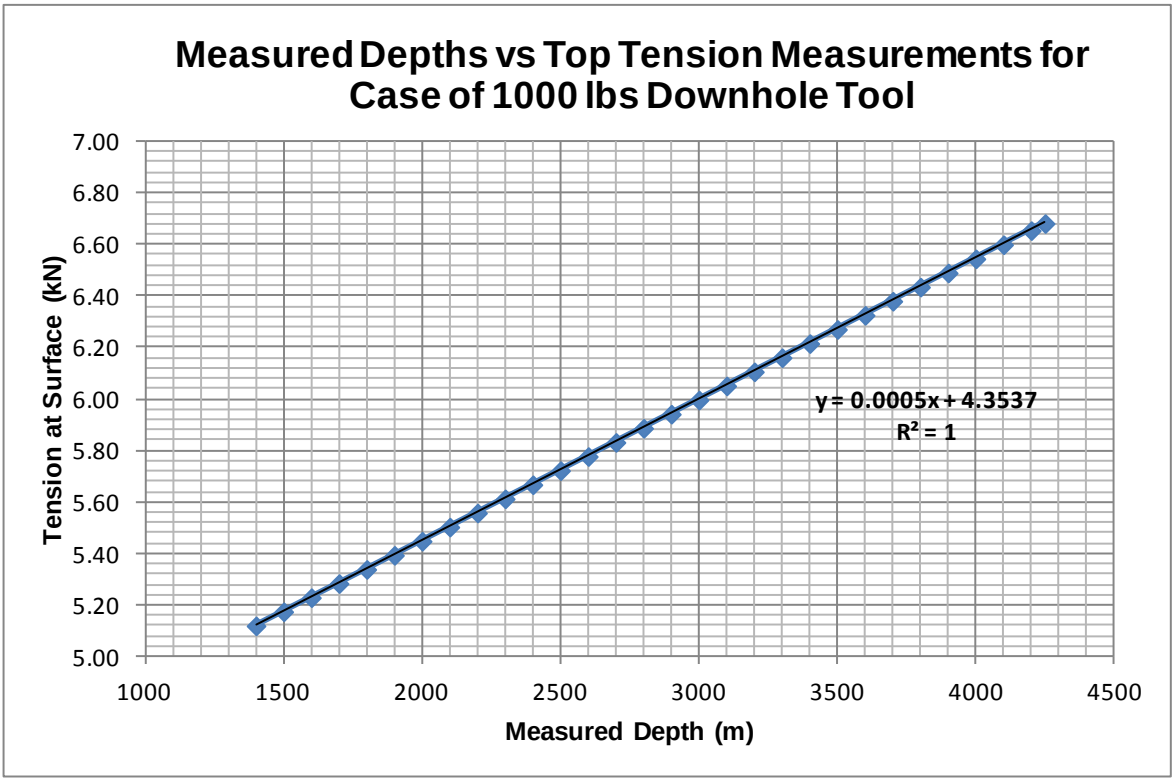

Figure 43. Relation between top tensions and measured depths for case 1C

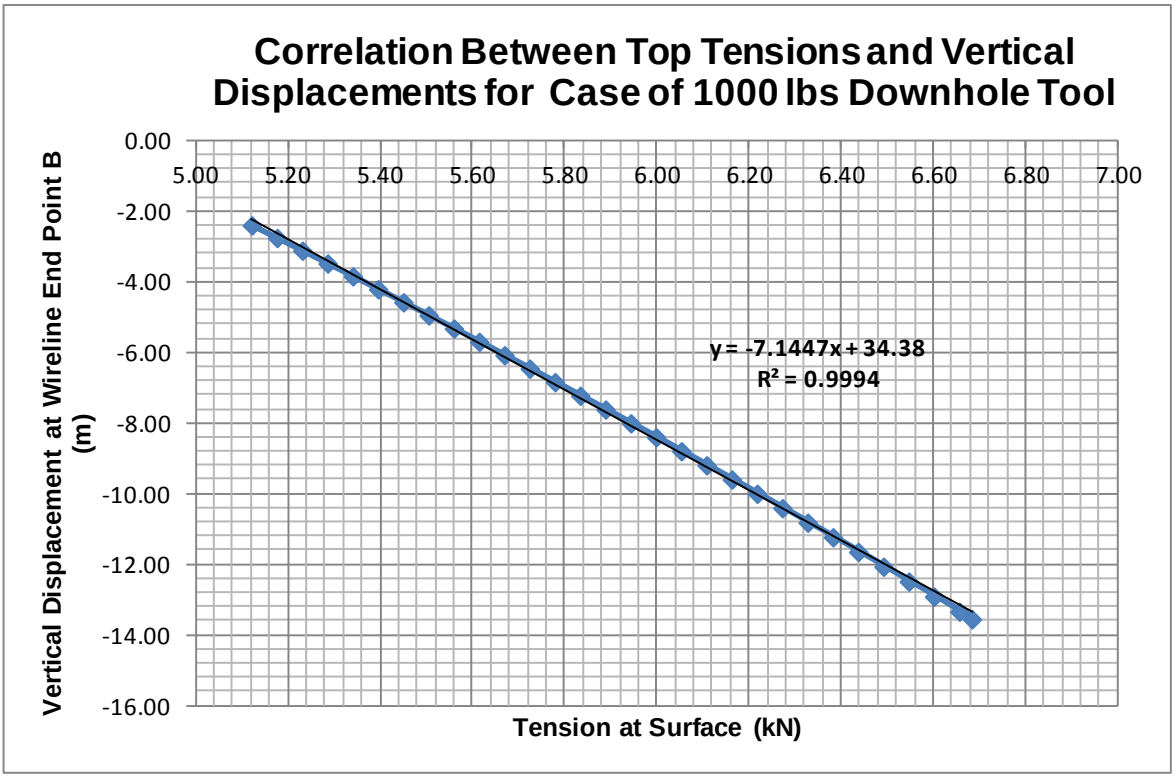

Figure 44. Relation between top tensions and vertical displacements for case 1C

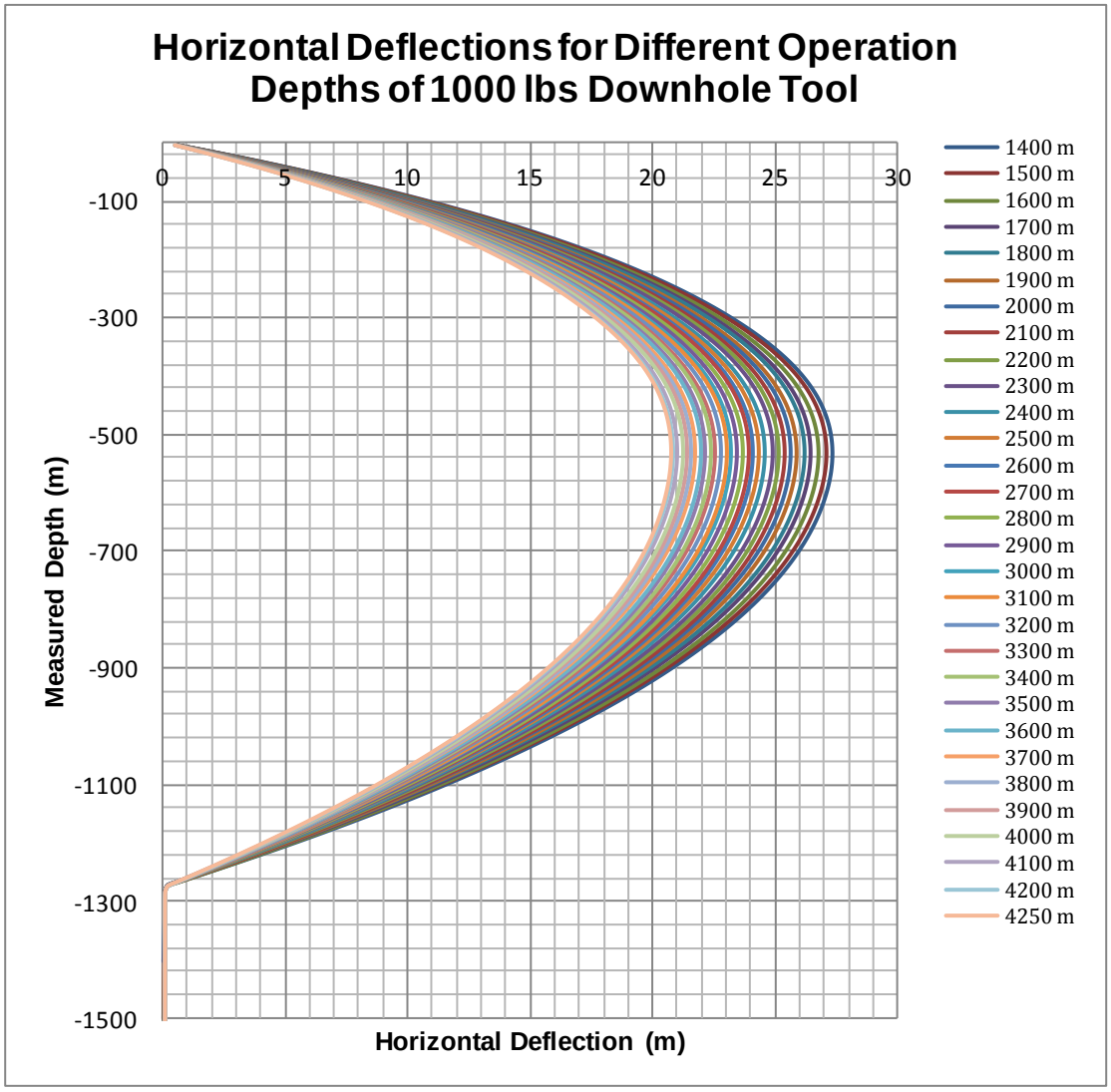

Figure 45. Horizontal deflections for different operation depths of case 1C

6.1.4 Case 2A

The wireline operations were simulated using Camesa Monoconductor cable with diameter 7/16" and 500 lbs of downhole tool installed at the bottom end of the wireline. As shown in **Figure 46**, the top tensions measured in the vessel escalate linearly as the operation depths increase. Based on analysis from OrcaFlex, the tensions measured at the vessel's winch will increase from 6.77 kN to 18.25 kN as the downhole tool is lowered further down into the well. The maximum tension of 18.25 kN will be obtained for the wireline operation at 4250 meters measured depth from the vessel.

The correlation between top tensions and vertical displacements generated by sea currents can be seen in **Figure 47**. The largest value of vertical displacement at wireline end point is 19.44 meters to upward direction. It will occur when the wireline length is reeled out 1400 meters of vessel's winch for lowering the downhole tool down into the well. It means that the true depth of wireline end point is 1380.56 meters for the case of wireline operation at 1400 meters measured depth. For the wireline operations over than 4000 meters, the vertical displacements will be in downward direction and it becomes even higher when the downhole tool goes to greater depth inside the well. The largest downward deflection obtained from the analysis is 0.67 meters when the reading of

wireline length shows 4250 meters. Therefore, the actual depth of the wireline end point is estimated 4250.67 meters TVD from the mean sea level. **Figure 48** shows maximum lateral deflection during wireline operation for each different depth cases. For the first case of wireline operation at 1400 meters measured depth, the wireline will experience the largest maximum lateral deflection due to small tension at wireline end point. This maximum lateral deflection could reach 92.81 meters. The largest value of maximum lateral deflection is found at 640.3 meters from mean sea water level. The smallest value of maximum lateral deflection for exposed wireline is 27.47 meters at estimated water depth of 549.5 meters. It will be obtained for the wireline operation at measured depth of 4250 meters from the vessel. As the downhole operation goes deeper the tension in wireline become higher and creates smaller deflection at mid free span of wireline that is exposed to open water.

Table 19. Summary of static analysis results from OrcaFlex for case 2A

Measured Depth	True Vertical Depth	Vertical Displacement at Wireline End Point B	Maximum Horizontal Deflection	Top Tension at Wireline End Point A
(m)	(m)	(m)	(m)	(kN)
-1400	-1380.56	19.44	92.81	6.77
-1500	-1483.58	16.42	85.71	7.17
-1600	-1586.13	13.87	79.04	7.57
-1700	-1688.03	11.97	73.84	7.97
-1800	-1789.58	10.42	69.29	8.37
-1900	-1890.98	9.02	64.82	8.78
-2000	-1992.06	7.94	61.28	9.18
-2100	-2092.98	7.02	58.12	9.58
-2200	-2193.78	6.22	55.27	9.98
-2300	-2294.47	5.53	52.69	10.38
-2400	-2395.09	4.91	50.34	10.79
-2500	-2495.69	4.31	47.87	11.19
-2600	-2596.17	3.83	45.92	11.60
-2700	-2696.61	3.39	44.12	12.00
-2800	-2797.01	2.99	42.45	12.40
-2900	-2897.38	2.62	40.91	12.80
-3000	-2997.72	2.28	39.48	13.21
-3100	-3098.03	1.97	38.14	13.61
-3200	-3198.32	1.68	36.89	14.01
-3300	-3298.60	1.40	35.73	14.42
-3400	-3398.86	1.14	34.63	14.82
-3500	-3499.10	0.90	33.60	15.23
-3600	-3599.34	0.66	32.63	15.63
-3700	-3699.56	0.44	31.71	16.03
-3800	-3799.78	0.22	30.85	16.44
-3900	-3899.99	0.01	30.03	16.84
-4000	-4000.19	-0.19	29.25	17.24
-4100	-4100.38	-0.38	28.51	17.65
-4200	-4200.57	-0.57	27.81	18.05
-4250	-4250.67	-0.67	27.47	18.25

Table 20. Analysis results of dynamic forces from OrcaFlex for case 2A

Measured Depth	Force At Vessel		Force At Pressure Control Head	
	Horizontal Force Fx	Vertical Force Fz	Horizontal Force Fx	Vertical Force Fz
(m)	(N)	(N)	(N)	(N)
-1400	3901.68	-6756.26	1155.78	3483.00
-1500	3898.68	-7262.17	1045.52	3193.31
-1600	3944.08	-9929.31	1285.36	6480.59
-1700	4004.49	-8056.75	1077.07	4014.25
-1800	4061.21	-8466.88	1089.44	4447.00
-1900	4120.27	-11324.92	1350.73	8876.38
-2000	4157.55	-9300.64	1109.49	5328.25
-2100	4177.39	-9708.99	1117.72	5692.44
-2200	4209.29	-10132.72	1125.13	6119.98
-2300	4242.50	-10543.10	1131.54	6556.71
-2400	4267.07	-10953.79	1142.91	7057.40
-2500	4403.68	-11376.10	1370.61	7750.95
-2600	4361.20	-11769.83	1147.87	7770.14
-2700	4390.81	-12177.03	1151.76	8169.66
-2800	4407.45	-12575.30	1155.85	8551.76
-2900	4446.52	-12986.52	1159.65	8993.87
-3000	4502.67	-13390.13	1163.20	9393.14
-3100	4540.92	-13785.69	1166.33	9798.07
-3200	4559.57	-14205.54	1169.21	10242.47
-3300	4605.98	-14607.11	1171.89	10635.96
-3400	4616.51	-15009.28	1174.44	11056.96
-3500	4625.08	-15392.29	1176.89	11446.64
-3600	4645.22	-15801.09	1179.19	11884.34
-3700	4675.45	-16177.46	1181.42	12257.18
-3800	4714.18	-16650.55	1183.47	12716.01
-3900	4746.39	-17099.59	1185.37	13248.64
-4000	4741.41	-17557.19	1187.11	13735.98
-4100	4745.24	-17839.33	1188.72	14011.13
-4200	4779.20	-18251.83	1190.29	14397.73
-4250	4782.94	-18458.30	1191.03	14579.52

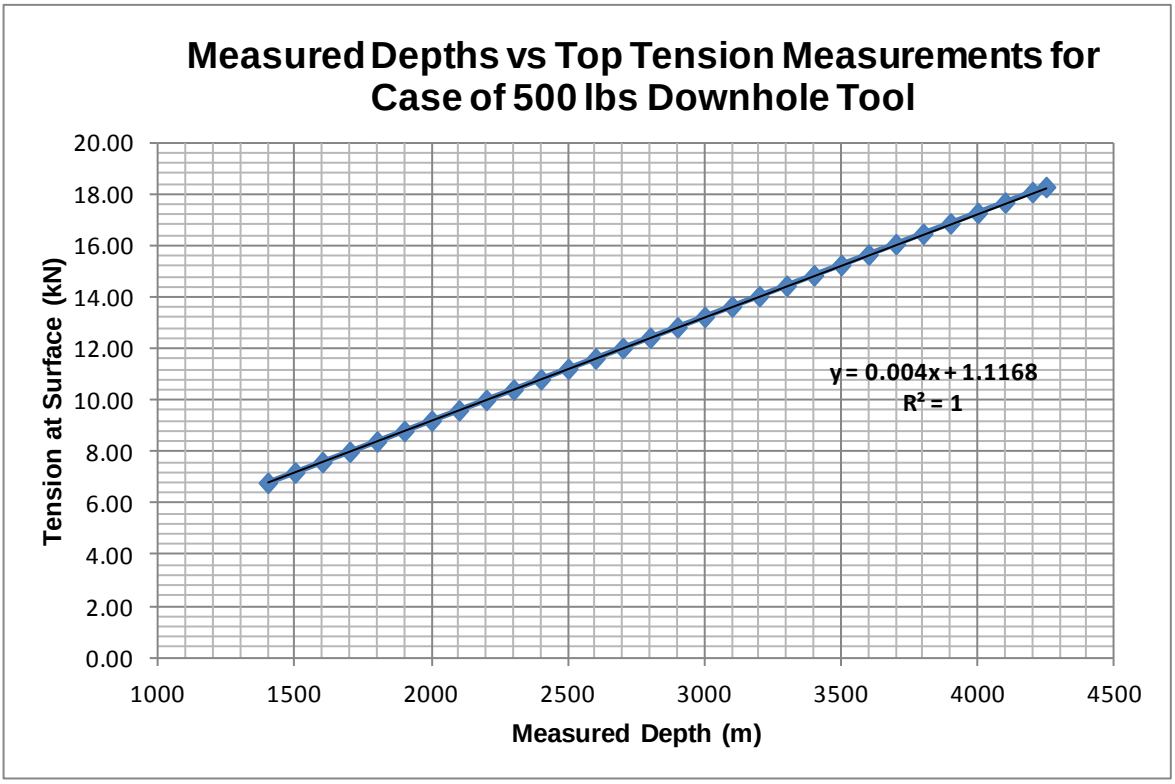

Figure 46. Relation between top tensions and measured depths for case 2A

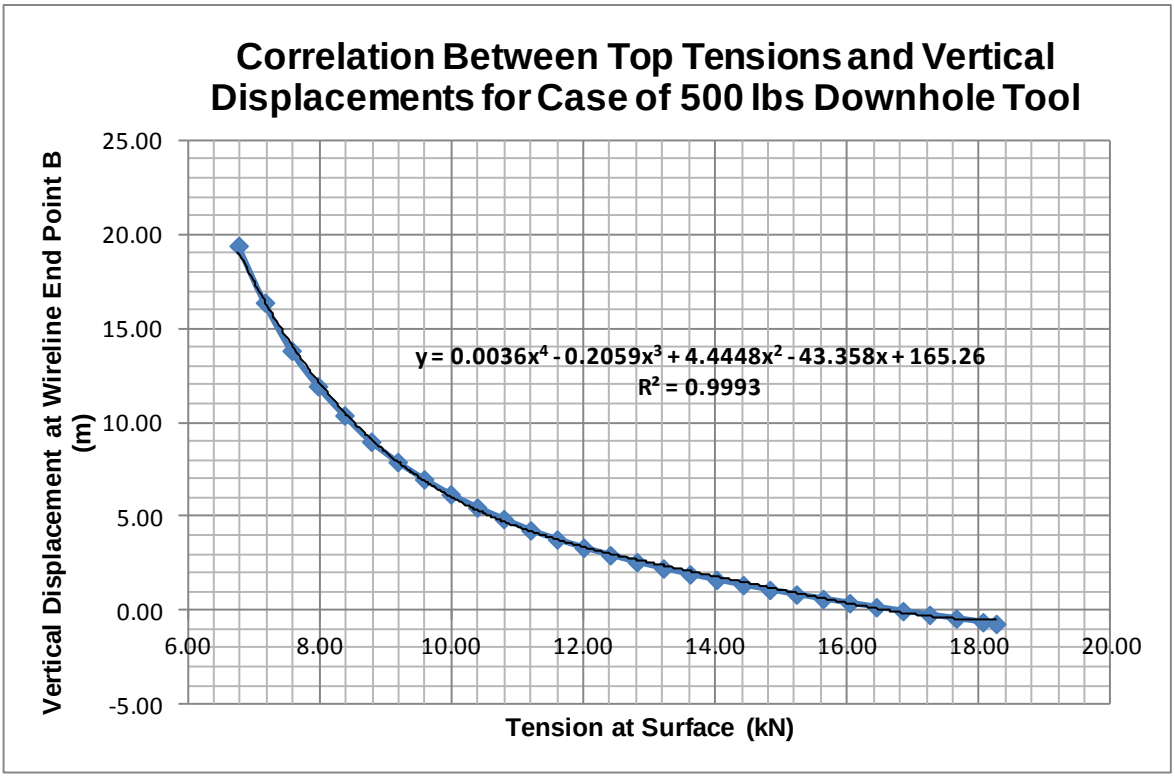

Figure 47. Relation between top tensions and vertical displacements for case 2A

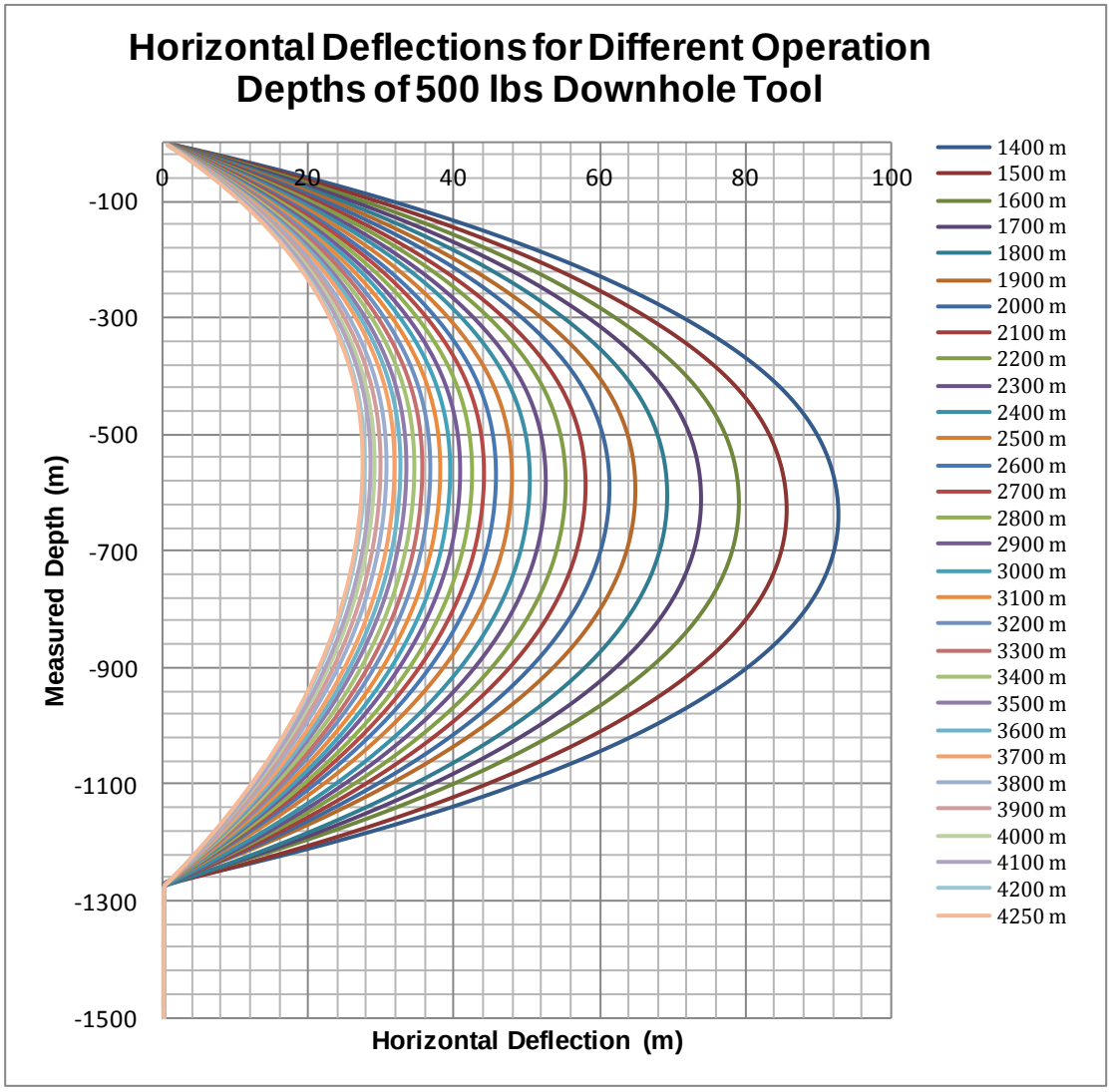

Figure 48. Horizontal deflections for different operation depths of case 2A

6.1.5 Case 2B

The OrcaFlex software was run to simulate how the wireline behave for each different cases of depth in well operation using Monoconductor 7/16" diameter with 1200 lbs downhole tool. As **Table 21** shown, the vertical displacements at the bottom endpoint of the wireline occur either in upward or downward direction. The upward displacements of the wireline will occur during wireline operation for the range of measured depth between 1400 meters to 3300 meters. Based on OrcaFlex analysis, the maximum vertical displacement in upward direction for the wireline end point is 6.61 meters. It indicates that the true vertical depth of wireline end point is located at 1394.80 meters during the wireline operation for the case of 1400 meters measured depth. For the wireline operations that need to be carried out inside the well at depths over than 3300 meters MD from mean sea level, the wireline will experience downward displacement. The maximum value of downward displacement is 1.82 meters for the case of 4250 meters wireline length measured from vessel's winch. It means that the true vertical depth of the wireline end point is 4251.82 meters from the sea surfaces.

Figure 49 shows that the top tension is gradually increasing from 9.86 kN to 21.11 kN as the wireline operation depths increase. **Figure 51** shows when the downhole tool goes to greater depth, the maximum horizontal deflection in the mid span of exposed wireline will become smaller due to larger tension force coming from more suspended length of the wireline inside the well. The largest value of maximum horizontal deflection obtained from the OrcaFlex analysis is 56.12 meters found at the water depth of 586.3 meters from mean sea level. It will occur for the case of wireline operation at 1400 meters measured depth.

Table 21. Summary of static analysis results from OrcaFlex for case 2B

Measured Depth	True Vertical Depth	Vertical Displacement at Wireline End Point B	Maximum Horizontal Deflection	Top Tension at Wireline End Point A
(m)	(m)	(m)	(m)	(kN)
-1400	-1393.39	6.61	56.12	9.86
-1500	-1494.11	5.89	53.46	10.26
-1600	-1594.75	5.25	51.04	10.66
-1700	-1695.37	4.63	48.51	11.07
-1800	-1795.88	4.12	46.51	11.47
-1900	-1896.33	3.67	44.66	11.87
-2000	-1996.74	3.26	42.96	12.28
-2100	-2097.12	2.88	41.38	12.68
-2200	-2197.46	2.54	39.91	13.08
-2300	-2297.78	2.22	38.55	13.49
-2400	-2398.08	1.92	37.27	13.89
-2500	-2498.36	1.64	36.08	14.29
-2600	-2598.63	1.37	34.96	14.70
-2700	-2698.88	1.12	33.91	15.10
-2800	-2799.11	0.89	32.92	15.50
-2900	-2899.34	0.66	31.99	15.91
-3000	-2999.56	0.44	31.11	16.31
-3100	-3099.77	0.23	30.27	16.72
-3200	-3199.97	0.03	29.48	17.12
-3300	-3300.17	-0.17	28.74	17.52
-3400	-3400.36	-0.36	28.02	17.93
-3500	-3500.55	-0.55	27.35	18.33
-3600	-3600.73	-0.73	26.70	18.73
-3700	-3700.91	-0.91	26.08	19.14
-3800	-3801.09	-1.09	25.50	19.54
-3900	-3901.26	-1.26	24.93	19.95
-4000	-4001.44	-1.44	24.40	20.35
-4100	-4101.61	-1.61	23.88	20.76
-4200	-4201.75	-1.75	23.56	21.02
-4250	-4251.82	-1.82	23.44	21.11

Table 22. Analysis results of dynamic forces from OrcaFlex for case 2B

Measured Depth	Force At Vessel		Force At Pressure Control Head	
	Horizontal Force Fx	Vertical Force Fz	Horizontal Force Fx	Vertical Force Fz
(m)	(N)	(N)	(N)	(N)
-1400	4229.81	-9947.54	1121.85	6027.48
-1500	4270.73	-10354.55	1128.81	6508.23
-1600	4292.80	-10799.97	1135.01	6908.44
-1700	4414.72	-11156.01	1276.27	7918.48
-1800	4331.82	-11703.03	1145.88	7679.41
-1900	4354.52	-12118.18	1149.21	8065.99
-2000	4403.30	-12513.43	1153.38	8431.73
-2100	4457.06	-12903.32	1157.33	8861.83
-2200	4493.34	-13294.57	1160.87	9259.66
-2300	4504.20	-13677.63	1164.28	9714.29
-2400	4537.19	-14074.76	1167.32	10119.41
-2500	4566.83	-14465.08	1170.11	10443.20
-2600	4608.21	-14855.05	1172.68	10897.23
-2700	4643.39	-15298.36	1175.08	11351.45
-2800	4653.66	-15656.56	1177.36	11695.31
-2900	4690.27	-16227.61	1179.65	12307.91
-3000	4694.50	-16547.62	1181.61	12650.14
-3100	4722.49	-16950.76	1183.39	12982.46
-3200	4779.29	-17435.49	1185.02	13576.39
-3300	4802.11	-18049.48	1186.37	14314.01
-3400	4798.53	-18408.97	1188.48	14676.44
-3500	4806.97	-18730.78	1189.38	14851.17
-3600	4827.95	-18985.49	1190.94	15035.59
-3700	5335.93	-22287.24	1194.05	19822.12
-3800	5284.84	-22720.35	1194.86	20265.07
-3900	5446.02	-23129.44	1197.46	20752.08
-4000	5437.02	-23693.97	1204.57	20934.08
-4100	5474.04	-23984.20	1220.83	20951.42
-4200	5145.00	-24228.18	1246.32	20935.31
-4250	5045.56	-24149.58	1262.06	20878.78

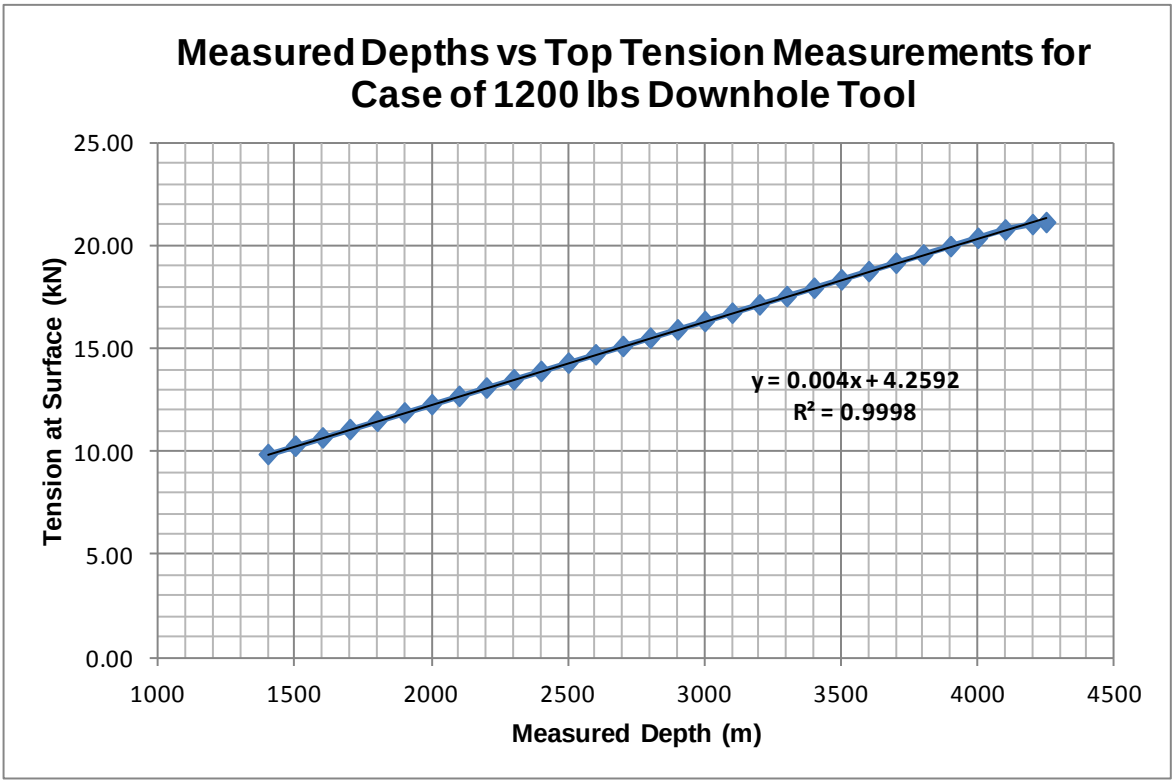

Figure 49. Relation between top tensions and measured depths for case 2B

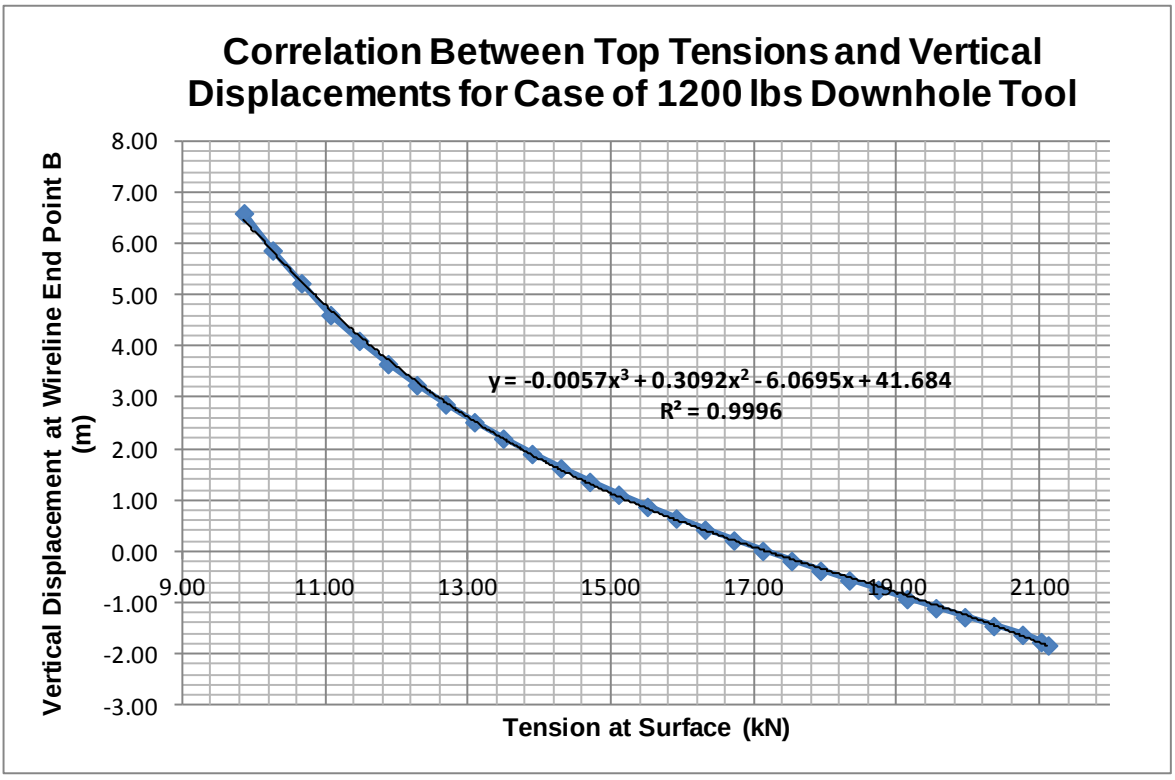

Figure 50. Relation between top tensions and vertical displacements for case 2B

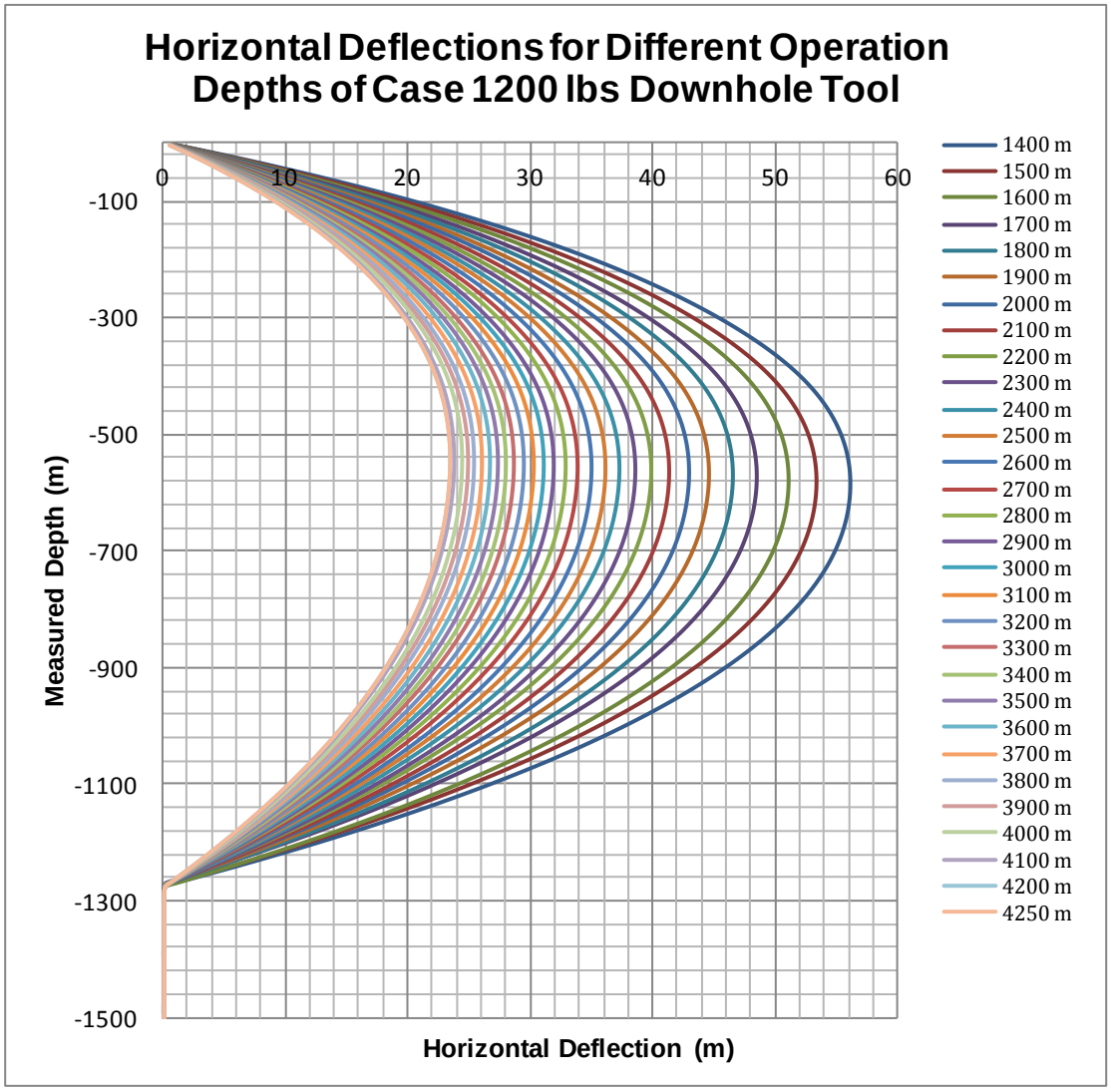

Figure 51. Horizontal deflections for different operation depths of case 2B

6.1.6 Case 2C

The performance of wireline operations using Monoconductor cable 7/16" diameter with 2000 lbs downhole tool were analyzed in OrcaFlex and the analysis results for each depth cases can be tabulated as shown in **Table 23** and **Table 24**. The loads from sea currents create lateral deflections in the mid span of exposed wireline. This lateral deflection will also affect the vertical displacement at the end point of the suspended wireline inside the well. This vertical displacement can be in upward direction or downward direction.

In case of wireline operations from measured depth of 1400 meters to 2500 meters, the wireline vertical displacements will be in upward direction. While the wireline operations from measured depth of 2600 meters to 4250 meters, the vertical displacement will be in downward direction. The largest upward displacement at wireline end point is 2.61 meters; it will be found when the wireline operation is performed for 1400 meters measured depth case. The largest downward displacement is 3.01 meters; it will be found when the wireline operation is performed for 4250 meter measured depth case. **Figure 52** shows the top tension values are plotted versus different cases of well depth during wireline operations. As shown in the graph, the top tension force is almost linearly increasing as the downhole tool goes deeper. At measured depth of 4250 meters, the top tension

force reaches 24.92 kN. The Monoconductor cable performances in terms of horizontal deflections under sea current can be seen in **Figure 54**. The largest value of maximum horizontal deflection computed by OrcaFlex is 38.83 meters for wireline operation at 1400 measured depth case. This maximum horizontal deflection will be located at water depth of 563.39 meters below mean sea level.

Table 23. Summary of static analysis results from OrcaFlex for case 2C

Measured Depth	True Vertical Depth	Vertical Displacement at Wireline End Point B	Maximum Horizontal Deflection	Top Tension at Wireline End Point A
(m)	(m)	(m)	(m)	(kN)
-1400	-1397.39	2.61	38.83	13.40
-1500	-1497.69	2.31	37.53	13.80
-1600	-1597.98	2.02	36.33	14.21
-1700	-1698.24	1.76	35.19	14.61
-1800	-1798.50	1.50	34.13	15.01
-1900	-1898.74	1.26	33.13	15.42
-2000	-1998.96	1.04	32.18	15.82
-2100	-2099.18	0.82	31.29	16.23
-2200	-2199.40	0.60	30.45	16.63
-2300	-2299.60	0.40	29.65	17.03
-2400	-2399.80	0.20	28.89	17.44
-2500	-2499.99	0.01	28.17	17.84
-2600	-2600.18	-0.18	27.49	18.25
-2700	-2700.36	-0.36	26.83	18.65
-2800	-2800.54	-0.54	26.21	19.05
-2900	-2900.72	-0.72	25.62	19.46
-3000	-3000.90	-0.90	25.05	19.86
-3100	-3101.07	-1.07	24.51	20.27
-3200	-3201.24	-1.24	23.99	20.67
-3300	-3301.39	-1.39	23.61	20.97
-3400	-3401.52	-1.52	23.37	21.17
-3500	-3501.66	-1.66	23.13	21.37
-3600	-3601.79	-1.79	22.90	21.57
-3700	-3701.93	-1.93	22.67	21.78
-3800	-3802.26	-2.26	21.16	23.10
-3900	-3902.43	-2.43	20.77	23.50
-4000	-4002.59	-2.59	20.40	23.91
-4100	-4102.76	-2.76	20.03	24.31
-4200	-4202.93	-2.93	19.68	24.72
-4250	-4253.01	-3.01	19.51	24.92

Table 24. Analysis results of dynamic forces from OrcaFlex for case 2C

Measured Depth	Force At Vessel		Force At Pressure Control Head	
	Horizontal Force Fx	Vertical Force Fz	Horizontal Force Fx	Vertical Force Fz
(m)	(N)	(N)	(N)	(N)
-1400	4513.03	-13612.20	1163.20	9490.99
-1500	4551.57	-14022.88	1166.43	9859.47
-1600	4579.40	-14415.08	1169.38	10278.20
-1700	4581.21	-14818.72	1172.07	10782.13
-1800	4624.94	-15215.50	1174.78	11101.23
-1900	4660.14	-15604.45	1176.98	11530.79
-2000	4671.63	-16016.38	1178.95	12029.25
-2100	4691.06	-16423.36	1181.07	12414.00
-2200	4708.63	-16834.48	1182.92	12832.44
-2300	4742.07	-17250.47	1184.88	13214.81
-2400	4748.78	-17671.56	1186.59	13718.00
-2500	4810.60	-18091.06	1188.24	14160.90
-2600	4813.10	-18507.54	1189.79	14500.77
-2700	4826.34	-18930.45	1191.27	14882.88
-2800	4833.61	-19349.88	1192.63	15280.76
-2900	4876.91	-19763.46	1194.01	15803.52
-3000	4898.88	-20166.39	1194.90	16215.88
-3100	4940.60	-20580.14	1196.28	16609.13
-3200	4929.41	-20969.42	1199.96	17000.52
-3300	4948.63	-21447.68	1227.31	17452.75
-3400	5008.87	-21972.68	1270.29	17976.73
-3500	5074.09	-22206.63	1325.21	18161.83
-3600	5105.81	-22449.62	1390.84	18481.84
-3700	5105.74	-22778.22	1475.82	19042.12
-3800	5110.16	-25769.35	1207.48	22688.64
-3900	5116.98	-27183.60	1203.22	24092.89
-4000	5046.11	-27995.33	1206.32	25078.49
-4100	5236.88	-28246.68	1207.63	25296.87
-4200	5098.41	-27205.10	1205.49	23774.79
-4250	5115.92	-26807.06	1205.84	23242.05

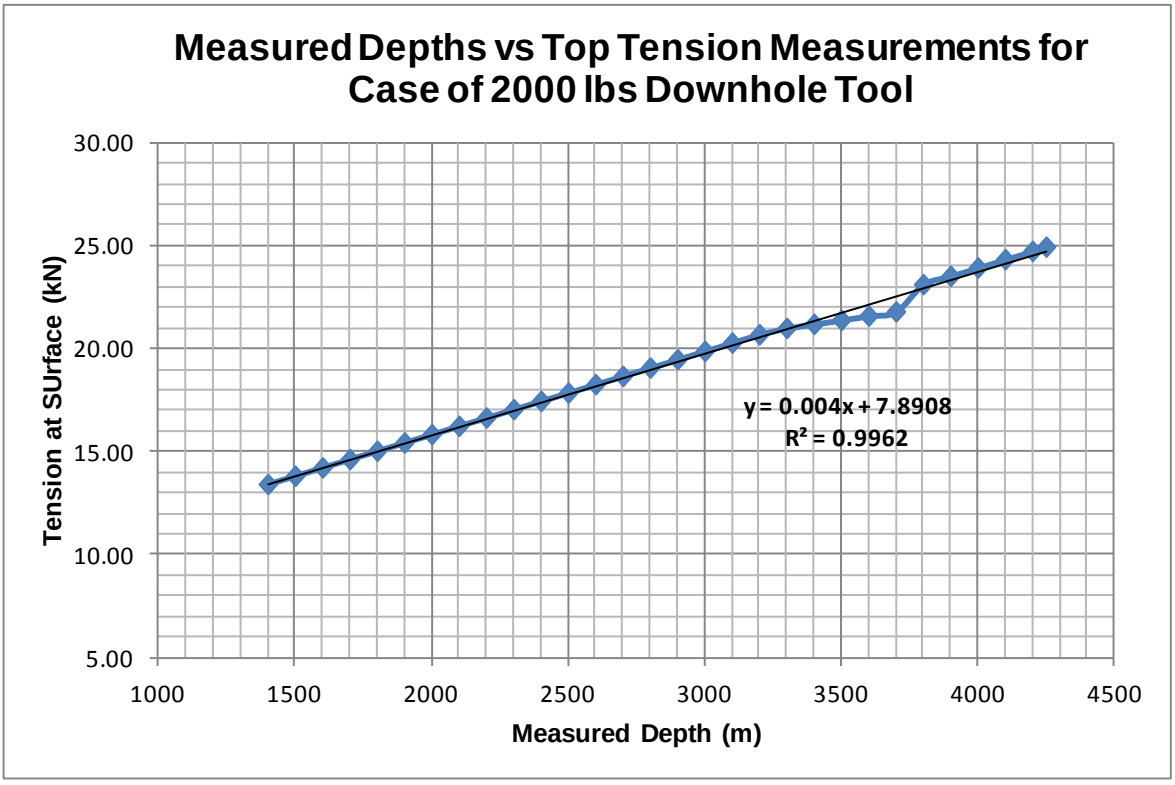

Figure 52 Relation between top tensions and measured depths for case 2C

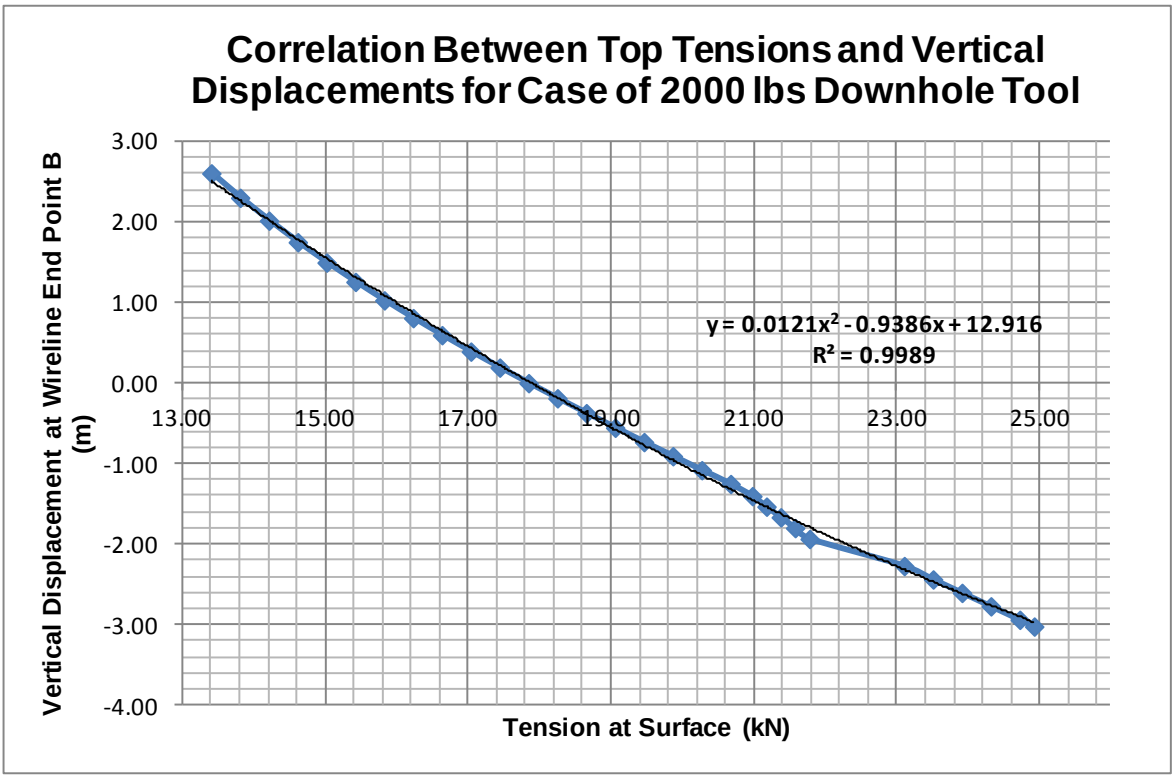

Figure 53. Relation between top tensions and vertical displacements for case 2C

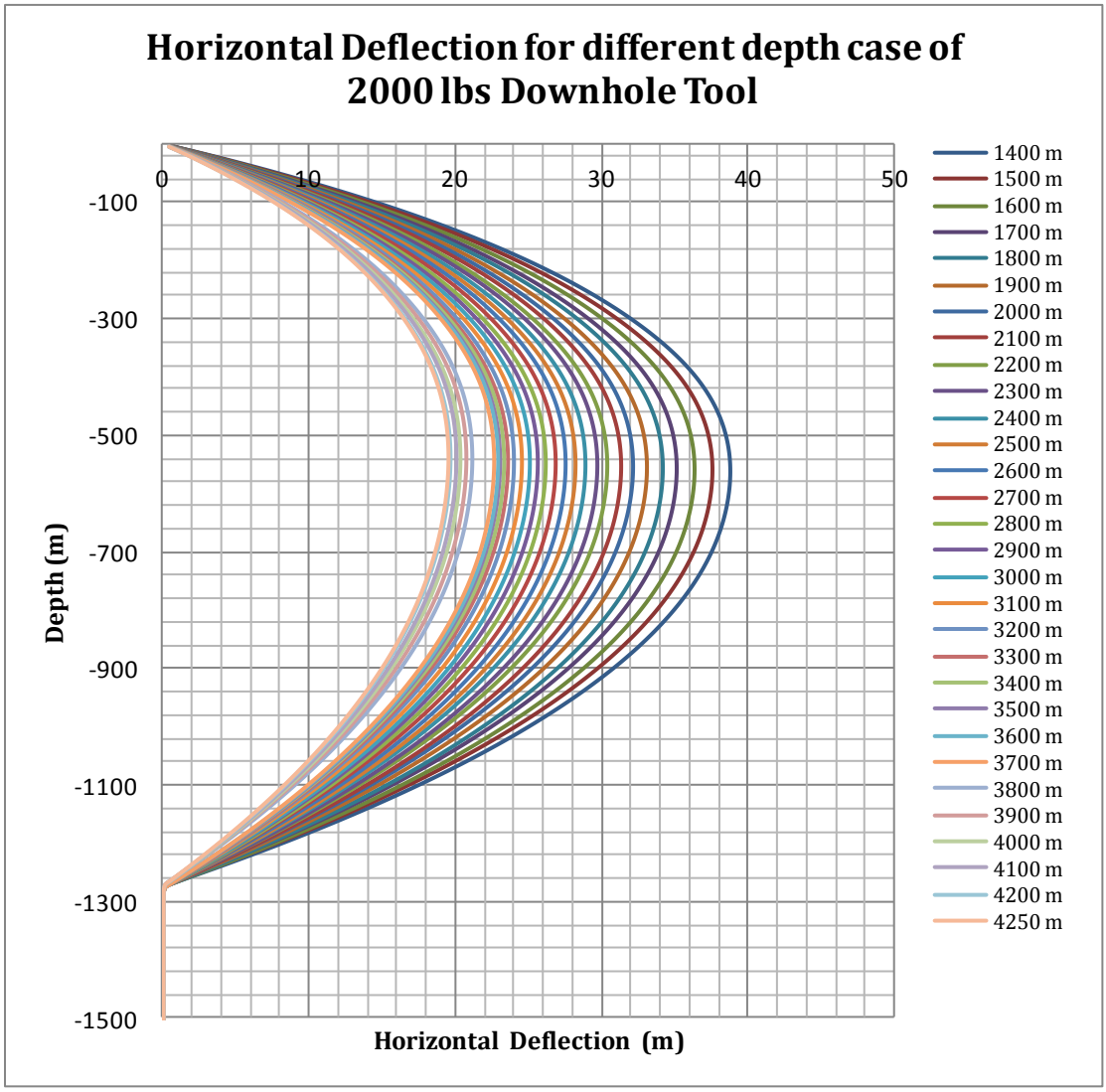

Figure 54. Horizontal deflections for different operation depths of case 2C

6.2 Results Discussion and Comparison

The graphs that are generated based on analysis result from OrcaFlex can be utilized to help the operator monitoring continuously the actual depth of the downhole tool during RLWI operation. There are three graphs presented for each of the case. First graph shows the relation between top tension and vertical displacement; second graph shows the relation between measured depths versus top tensions; and the third graph shows horizontal deflection along the cable length. From each of first and second graph, an equation can be obtained by adding the trendline to the graph in the excel spreadsheet. This equation along with the graph can be used as a tool to correct the depth of downhole tool inside the well. In **Appendix B,** an example for estimating the actual depth of the wireline is shown.

Table 14, 16, and 18 show dynamic forces obtained from running the simulation for 180 seconds. OrcaFlex computes that the maximum dynamic horizontal forces at PCH are 416.10 kN for case 1A, 751.84 kN for case 1B, and 357.55 kN for case 1C. Whereas, from table 20, 22, and 24, OrcaFlex calculates that the maximum dynamic horizontal forces at PCH are 1370.61 kN for case 2A; 1276.27 kN for case 2B; and 1475.82 kN for case 2C. These horizontal forces can be used as inputs for calculating the friction force at PCH. During lowering the downhole tool down into the

well, there will be pressure from the reservoir and friction at top PCH that can restrain the wireline to move down. These friction force and well pressure need to be overcome by sufficient weight from the downhole tool. From the calculation in **Appendix A**, it is concluded that the downhole weight used for operation in each of cases is sufficient enough to overcome the forces.

From OrcaFlex analysis, the largest maximum horizontal deflection of the cable is 122.37 meters found in case 1A. Based on the criteria for cable deflection in **Table 11**, the maximum allowable horizontal deflection is 130 meters (10% of MSL). It means the largest horizontal deflection that occurs is still within the acceptable limit. By increasing the weight of the downhole tool, this deflection can be reduced.

The maximum tensions at surface are taken from table 13, 15, 17, 19, 21, and 23 for each case of wireline operation at measured depth of 4250 m. The percentage of cable utilization is ratio between maximum effective tension at surface and safe working load limit (WLL) as stated in **Table 11.**

Table 25. Slickline capacity utilization during wireline operation for different downhole weight cases

0.125" Slickline	Max. Tension at Vessel	Max. Available Tension at Vessel	Utilization
	Newton	Newton	%
150 lbs Downhole Tool Weight	2910.00	3827.17	43.19%
600 lbs Downhole Tool Weight	4210.00	2527.17	62.49%
1000 lbs Downhole Tool Weight	6680.00	57.17	99.15%

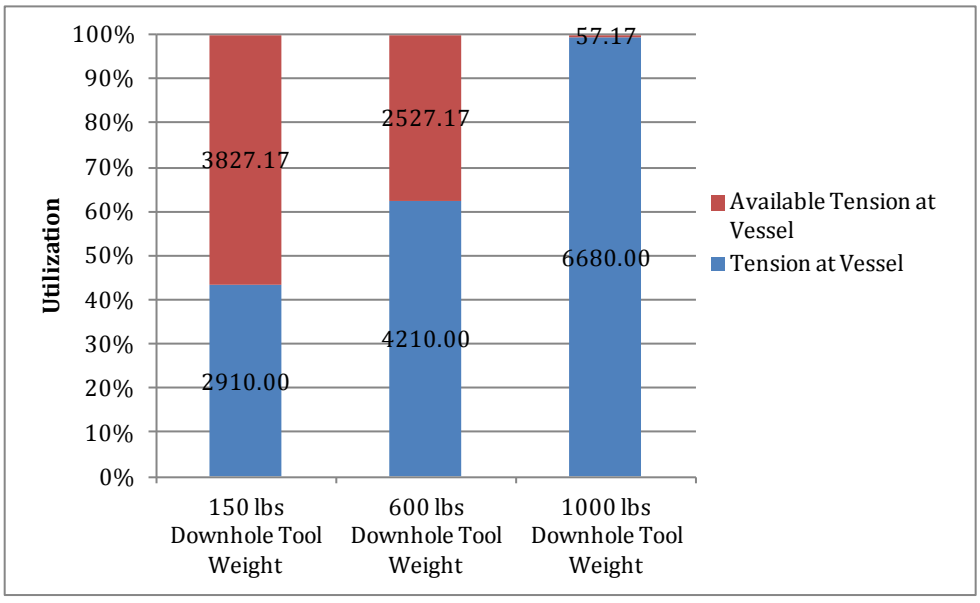

Figure 55. Comparison of slickline capacity utilization

For operation using slickline cable, **Figure 55** shows that it is not feasible for performing the downhole operation using weight of BHA more than 600 lbs. Island offshore states that the cable utilization for safety reason should be less than 80%. The graph also indicates that there is some

remains capacity for increasing the weight of downhole tool to ensure having adequate weight to overcome the forces generated by sea current.

Table 26. Monoconductor capacity utilization during wireline operation for different downhole weight cases

7/16" Monoconductor	Max. Tension at Vessel	Max. Available Tension at Vessel	Utilization
	Newton	Newton	%
500 lbs Downhole Tool Weight	18250.00	25124.81	42.08%
1200 lbs Downhole Tool Weight	21110.00	22264.81	48.67%
2000 lbs Downhole Tool Weight	24920.00	18454.81	57.45%

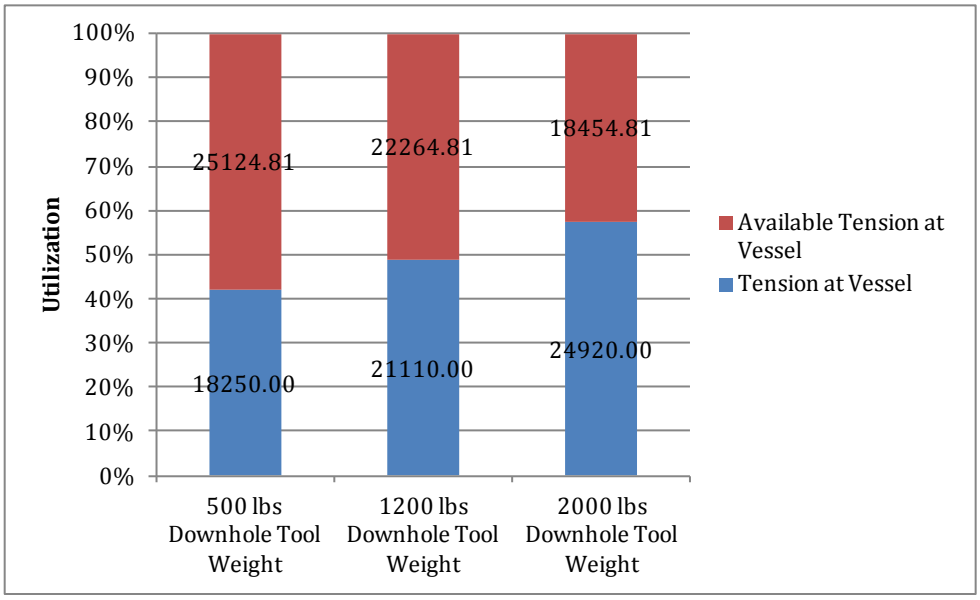

Figure 56. Comparison of monoconductor capacity utilization

For operation using monoconductor cable, **Figure 56** clearly shows that there is some available "rooms" to increase the weight of downhole tool to ensure sufficient weight to overcome the forces induced by sea current for all the cases. The highest percentage of monoconductor cable utilization is 57% for case of 2000 lbs downhole tool, it is still considered within "safe working window".

CHAPTER 7

SUMMARY&CONCLUSION

Nowadays RLWI becomes most preferable method in performing light well intervention, because it offers more efficient, cheaper, and faster way to do well intervention replacing conventional semisubmersible rigs. But the use of wireline in open water will impose some greater challenges on the operations. One of the challenges is the effect of the sea current on cable. Sea currents are considered as the major problem in performing downhole works inside the well. The drag force as a result from sea currents acting along the part of cable submerged in open water will create horizontal deflection. The downhole tool's weight and self weight of the suspended cable will also make the cable stretched. The combination between cable elongation and horizontal deflection of the cable will influence the accuracy of the depth measurement during "in well" work and it is difficult to predict. The vertical displacement that occurs can be either in upward direction or downward direction. It depends on the dimensional properties and the stiffness of the cable used and downhole tool weight.

In this thesis, the analysis was performed in OrcaFlex to study the impact of wireline behavior on depth accuracy of downhole tool in RLWI operation. The case study was based on Aasta Hansteen field with 1300 meters water depth. Different cases of well depth, wireline types, and downhole tool weights were analyzed to investigate the behavior of the cables deflections induced by sea current. In this project, total 180 simulation cases were run to get desired data for creating the correlation between the tension at surface and the depth measurement. From the simulations, analysis results can be arranged and plotted into the graphs to give good visualization and approximation of the cable displacements.

Based on the analysis, the largest downward displacement will occur for case 1C with 13.53 meters deviation from measured depth and the largest upward displacement will occur for case 1A with 32.81 meters inaccuracy from measured depth. For the analysis of a wireline operation using slickline 0.125" with 150 lbs downhole tool (case 1A), the vertical displacements for every depth are in upward direction. The deeper the downhole tool goes into the well, the smaller upward vertical displacement will be. The upward displacement is being reduced because the tension yielded by suspended cable inside the well is increasing. Higher tension will reduce the lifting force as a result of the normal forces from sea current acting on the cable area. For the analysis of a wireline operation using slickline 0.125" with 1000 lbs downhole tool (case 1C), the vertical displacements for every depth are in downward direction. The analysis result for downward displacements from OrcaFlex shows that as the downhole tool goes deeper, the larger downward displacement will be. It means that the vertical displacement is more influenced by the cable elongation rather than horizontal deflection of the cable due to drag forces from sea currents. From the horizontal deflection graphs as presented in chapter 6 analysis results, when using heavier downhole tool weight, it shows that as the downhole tool goes deeper the cable horizontal deflection will slightly change from depth to depth due to higher tension on the cable.

From the analysis results in chapter 6, it can be seen that most of the graphs showing relation between top tension and vertical displacement would follow a certain pattern. It can be polynomial or linear function. These graphs can be used as a mean to estimate the true vertical depth of

downhole tool during the operation. It can also be used to help in choosing the optimal BHA weight for a wireline operation by adjusting the BHA weight to get more reliable relation between top tension and vertical displacement.

The effect of sea current becomes less when performing the wireline operation in the deeper depth of the well. The combined weight of cable self weight and downhole tool weight increases the tension force and decrease the horizontal deflection. But the total weight needs to be kept as low as possible to avoid excessive cable elongation and to keep the maximum tension force below the maximum allowable tension of the wireline cable.

CHAPTER 8

RECOMMENDATION FOR FUTURE WORK

After studying the wireline operation for RLWI, some following measures can be taken into consideration to improve the depth control, such as:

- It is necessary to develop a special simulation tool that can incorporate both conditions in open water and in well. This simulation tool is supposed to be able to model appropriately drag force due to sea current, lifting force due to pressure in well, friction in well and PCH, and simulate downhole tool vertical displacement during performing RLWI operation.
- A new tension measuring device is recommended to be built to reduce uncertainties in reading the wireline tension. This measuring device will be installed on top of the PCH to help the wireline operator in reading the tension force at top of PCH. It will accurately monitor the tension of the suspended cable inside the well without any interference from sea current by transmitting the real-time data about wireline tension at PCH to the surface. These tension data can be used to calculate the length of cable part that is located inside the well and to estimate the actual depth of the downhole tool.

During the simulations, some assumptions were made to fulfill the analysis requirements. These assumptions may lead to inaccuracy in analysis results. Further studies need to be conducted to minimize these uncertainties. There are several things that can be improved for further studies in analyzing wireline behavior during RLWI operation, such as:

- In this project, the well trajectory was assumed as a straight vertical. Further investigations on deviated wells need to be carried out in analyzing the accuracy of downhole tool position.
- There are difficulties in predicting the friction at PCH during running down the wireline into the well. This friction depends on so many factors, such as geometrical or shapes of the wireline, temperature characteristics, viscosity of the grease inside the PCH, and roughness. It is necessary to conduct experiment tests about this friction.
- The analysis of cable behavior in this project is only restricted to the effect of sea currents from one direction. For next study, a sensitivity analysis should be conducted for various sea current directions to analyze how far this issue will influence the behavior of the cable. Detail information about sea current conditions should be provided for further studies. Direct surveys on site need to be conducted to reduce uncertainties and assumption during gathering the data for the model. To analyze how wireline behave under sea current, a scale model for experiment can be built to examine directly the deflection of the wireline under various current speeds. This experiment data then can be compared to the analysis results computed by OrcaFlex software; in this case a calibration factor might be needed to approach the real situation.
- Well work activities, such as jarring will create some impacts that can be recognized by some specific tensions. These tensions are supposed to be different from tensions that are created by the downhole tool weight only. The tension comes from downhole activities should be considered for further studies.

The wireline's types being examined in this project are limited only to 2 different types of diameter which are 0.125 inch and 7/16" diameter. In addition, further analyses for many different types of wireline's size should be performed to give more measurements.

References

Apornsuvan, A. (2009): "Concept Design of Self Contained Remotely Controlled Running Tool", University of Stavanger, Stavanger, Norway.

AT-Marine Oy (2012): "Ship Motion Control" [cited February 2013] <Available at: http://www.atmarine.fi/?id=77>

Birkeland, S. T. (2005): "Well Integrity of Subsea Wells during Light Well", Department of Production and Quality Engineering, Norwegian University of Science and Technology, Trondheim, Norway.

Chakrabarti, S. (2005): "Handbook of Offshore Engineering (2-volume set)", Elsevier Science, Oxford, UK.

Crawford, N. C., & Still, I. R. (2010): "Riserless Subsea Well Intervention: Technology and Practice", OTC 20420 presented at the Offshore Technology Conference, 3-6 May, Houston, Texas, USA.

Det Norske Veritas(2009): "Drilling Plant", Offshore Standard, DNV-OS-E101, October 2009.

Det Norske Veritas(2010): "Environmental Conditions and Environmental Loads", Recommended Practice, DNV-RP-C205, October 2010.

Det Norske Veritas(2011): "Modelling and Analysis of Marine Operations", Recommended Practice, DNV-RP-H103, April 2010.

FMC Technologies (2012): "Riserless Light Well Intervention (RLWI)" [cited February 2013] <Available at: http://www.fmctechnologies.com/~/media/Subsea/Subsea%20Collateral%202012/HOW%20-%20Riserless%20Light%20Well%20Intervention_LOW%20RES.ashx?force=1&track=1>

Faltinsen, O. (1993): "Sea Loads on Ships and Offshore Structures", Cambridge University Press, Melbourne, Australia.

Friedberg, R., Jøssang, S. N., Gramstad, B., & Dalane, S. (2010): "Experiences From Operating New Generation Riserlesss Light Well Intervention Units in the North Sea, Challenges and Future Opportunities", OTC 20418 presented at the Offshore Technology Conference, 3-6 May, Houston, Texas, USA.

Gerwick, B. C. (2000): "Construction of Marine and Offshore Structures", CRC Press, Boca Raton, Florida, USA.

Gudmestad, O. T. (2010): "Marine Technology and Design Compendium", University of Stavanger, Stavanger, Norway.

Harestad, B. (2009): "MPE 190: Well Interevention Operations", University of Stavanger, Stavanger, Norway.

Island Offshore (2012): "Feasibility Study Report: RLWI on Aasta Hansteen development project by using Island Wellserver RLWI Systems", No. Document: 111-IOSS-Z-RA-004.

Island Offshore (2012): "Light Well Intervention" [cited 5 May 2013]<Available at: http://islandoffshore.com/#cid=47&mid=1>

Jensen, Ø. (2008): "Riser less Light Well Intervention (RLWI) - A success for reducing OPEX - cost and increasing oil recovery for subsea completed fields", Underwater Technology Conference, Bergen Norway [cited 8 May 2013] <Available at: http://www.possibility.no/utc2008/ps/A3%20-%20Oyvin%20Jensen.pdf>

Jøssang, S. N., Friedberg, R., Buset, P., & Gramstad, B. (2008): "Present and Future Well Intervention on Subsea Wells", SPE 112661 presented at the SPE Drilling Conference, 4-6 March, Orlando, Florida, USA.

Journée, J. M., & Massie, W. W. (2001): "Offshore Hydromechanics", Delft University of Technology, Delft, Netherlands [cited 7 February 2013] <Available at: http://www.shipmotions.nl/DUT/LectureNotes/index.html>

Khurana, S., DeWalt, B., & Headworth, C. (2003): "Well Intervention Using Rigless Techniques", OTC 15177 presented at the Offshore Technology Conference, 5-8 May, Houston, Texas, USA.

Krogstad, H. E., & Arntsen, Ø. A. (2000): "Linear Wave Theory", Norwegian University of Science and Technology, Trondheim, Norway [cited 17 March 2013] <Available at: http://folk.ntnu.no/oivarn/hercules_ntnu/LWTcourse/>

Larimore, D., Ashwell, C., & Zainal Abidin, A. H. (1999): "First Diverless Subsea Wireline Well Intervention Performed in Offshore Vietnam offers Low-Cost Solution for Light Well Workovers: Case Histories and Future Trends", SPE 54316 presented at the SPE Asia Pacific Oil and Gas Conference,20-22 April, Jakarta, Indonesia.

Lindland, H. J., Inderberg, O., Headworth, C., & Braut, A. (2003): "New Well Intervention Technology That Will Enable Increase In Recovery Rate", OTC 15182 presented at the Offshore Technology Conference, 5-8 May, Houston, Texas, USA.

Mathiassen, E., Munkerud, P. K., & Skeels, H. B. (2008): "Well Intervention in Deep Waters", OTC 19552 presented at the Offshore Technology Conference, 5-8 May, Houston, Texas, USA.

Munkerud, P. K., & Inderberg, O. (2007): "Riserless Light Well Intervention (RLWI)", OTC 18746 presented at the Offshore Technology Conference, 30 April- 3 May, Houston, Texas, USA.

Nergaard, A. (2012): "Subsea Technology Lecture Notes", University of Stavanger, Stavanger, Norway.

Newman, K. R., Overstreet, C. C., & Beynet, P. (2006): "Dynamic FEA Models for Snubbing Buckling and Riserless Subsea Wireline Intervention", SPE 99749 presented at the SPE Coiled Tubing Conference, 4-5 April, Woodlands, Texas, USA.

NORSOK Standard (2000): "System Requirement Well Intervention Equipment", NORSOK Standard D-002, October 2000.

NORSOK Standard (2004): "Well Intergrity in Drilling and Well Operations", NORSOK Standard D-010, August 2004.

Orcina (2011): "OrcaFlex Manual Version 9.5a", Orcina Ltd, Cumbria, UK [cited 2 May 2013] <Available at: http://www.orcina.com/SoftwareProducts/OrcaFlex/Documentation/OrcaFlex.pdf>

Pilkey, W. D.(2005): "Formulas for Stress, Strain, and Structural Matrices", John Wiley & Sons, Inc., Hoboken, New Jersey, USA.

Seaflex Riser Technologies (2012): "Analysis of RLWI Component Installation - 1300m Water Depth", No. Document: P1039808-RPT01-REV01.

Statoil (2013): "Aasta Hansteen and Polarled plans submitted for government approval" [cited 14 April 2013] <Available at: http://www.statoil.com/en/NewsAndMedia/News/2013/Pages/08Jan_AastaHansteen_PDO.aspx>

Statoil (2012): "Riserless light well intervention - a tool for improved recovery" [cited 5 May 2013] <Available at: http://www.statoil.com/en/technologyinnovation/optimizingreservoirrecovery/wellintervention/qualificationcampaignriserlesslightwellintervention/pages/riserless%20light%20well%20intervention.aspx>

Stewart, R. D. (2003): "Well Intervention Vessels for Intervening Subsea Wells", OMC 2003 presented at the Offshore Mediterranean Conference and Exhibition, 26-28 March, Ravenna, Italy.

Stewart, R. H. (2006): "Chapter 16 - Ocean Waves", Department of Oceanography, Texas A&M University, Texas, USA [cited 10 February 2013] <Available at: http://oceanworld.tamu.edu/resources/ocng_textbook/chapter16/chapter16_04.htm>

Wright, J. (2011, January): "An introduction to well intervention", Aberdeen, UK [cited 13 March 2013] <Available at: http://www.spe-uk.org/Downloads/Past%20Presentations%20Aberdeen/JimWright-SPEAberdeenJanuarypresentation.pdf>

Zijderveld, G., Tiebout, J., Hendriks, S., Poldervaart, L., & GustoMSC (2012): "Subsea Well Intervention Vessel and Systems", OTC 23161 presented at the Offshore Technology Conference, 30 April - 3 May, Houston, Texas, USA.

Appendix A – Downhole tools weight required to overcome pressure from the well

MINIMUM DOWNHOLE TOOL WEIGHT REQUIRED (CASE 1A)

INPUTS:

Wireline Type	=	Slickline	
True Vertical Depth (TVD)	=	4289	m
Shut In Well Head Pressure (SIWHP)	=	307.00	bar
Reservoir Fluid Density(ρ_{well})	=	0.700	kg/m^3
Wireline Diameter (OD)	=	0.125	inch
Contact Force at PCH (from OrcaFlex) (N)	=	416.10	Newton
Coefficient of Friction (assumed) (μ)	=	0.30	mm^2
Steel Density =	ρ_{steel} =	7850.00	kg/m^3

OUTPUTS:

Area of the Wireline (A) =	$\pi/4 \times OD^2$ =	7.92	mm^2
Friction (F) =	$\mu \times N$ =	124.83	Newton
Force from Pressure (FP) =	$SIWHP/A$ =	243.06	Newton
The Required Weight of Downhole Tool (W_{req}) =	$FP + F$ =	367.89	Newton
The Required Mass of Downhole Tool (M_{req}) =	$W_{req}/9.81$ =	37.50	kg
The Req. Mass of Downhole Tool in Air =	$\frac{M_{req}}{(\rho_{steel} - \rho_{well})} \times \rho_{steel}$ =	**37.51**	kg
Mass of Downhole Tool Available	=	**68.04**	kg **> Req. Mass, OK!!!**

MINIMUM DOWNHOLE TOOL WEIGHT REQUIRED (CASE 1B)

INPUTS:

Wireline Type	=	Slickline	
True Vertical Depth (TVD)	=	4289	m
Shut In Well Head Pressure (SIWHP)	=	307.00	bar
Reservoir Fluid Density(ρ_{well})	=	0.700	kg/m^3
Wireline Diameter (OD)	=	0.125	inch
Contact Force at PCH (from OrcaFlex) (N)	=	751.84	Newton
Coefficient of Friction (assumed) (μ)	=	0.30	mm^2
Steel Density = ρ_{steel}	=	7850.00	kg/m^3

OUTPUTS:

Area of the Wireline (A) = $\pi/4 \times OD^2$	=	7.92	mm^2
Friction (F) = $\mu \times N$	=	225.55	Newton
Force from Pressure (FP) = $SIWHP/A$	=	243.06	Newton
The Required Weight of Downhole Tool (W_{req}) = $FP + F$	=	468.61	Newton
The Required Mass of Downhole Tool (M_{req}) = $W_{req}/9.81$	=	47.77	kg
The Req. Mass of Downhole Tool in Air = $\frac{M_{req}}{(\rho_{steel} - \rho_{well})} \times \rho_{steel}$	=	**47.77**	kg
Mass of Downhole Tool Available	=	**272.16**	kg **> Req. Mass, OK!!!**

MINIMUM DOWNHOLE TOOL WEIGHT REQUIRED (CASE 1C)

INPUTS:

Wireline Type	=	Slickline	
True Vertical Depth (TVD)	=	4289	m
Shut In Well Head Pressure (SIWHP)	=	307.00	bar
Reservoir Fluid Density(ρ_{well})	=	0.700	kg/m^3
Wireline Diameter (OD)	=	0.125	inch
Contact Force at PCH (from OrcaFlex) (N)	=	357.55	Newton
Coefficient of Friction (assumed) (μ)	=	0.30	mm^2
Steel Density =	ρ_{steel} =	7850.00	kg/m^3

OUTPUTS:

Area of the Wireline (A) =	$\pi/4 \times OD^2$ =	7.92	mm^2
Friction (F) =	$\mu \times N$ =	107.27	Newton
Force from Pressure (FP) =	$SIWHP/A$ =	243.06	Newton
The Required Weight of Downhole Tool (W_{req}) =	$FP + F$ =	350.33	Newton
The Required Mass of Downhole Tool (M_{req}) =	$W_{req}/9.81$ =	35.71	kg
The Req. Mass of Downhole Tool in Air =	$\frac{M_{req}}{(\rho_{steel} - \rho_{well})} \times \rho_{steel}$ =	**35.71**	kg
Mass of Downhole Tool Available	=	**453.59**	kg **> Req. Mass, OK!!!**

MINIMUM DOWNHOLE TOOL WEIGHT REQUIRED (CASE 2A)

INPUTS:

Wireline Type	=	Monoconductor	
True Vertical Depth (TVD)	=	4289	m
Shut In Well Head Pressure (SIWHP)	=	307.00	bar
Reservoir Fluid Density(ρ_{well})	=	0.700	kg/m^3
Wireline Diameter (OD)	=	0.219	inch
Contact Force at PCH (from OrcaFlex) (N)	=	1370.61	Newton
Coefficient of Friction (assumed) (μ)	=	0.30	mm^2
Steel Density = ρ_{steel}	=	7850.00	kg/m^3

OUTPUTS:

Area of the Wireline (A) = $\pi/4 \times OD^2$	=	24.25	mm^2
Friction (F) = $\mu \times N$	=	411.18	Newton
Force from Pressure (FP) = $SIWHP/A$	=	744.38	Newton
The Required Weight of Downhole Tool (W_{req}) = $FP + F$	=	1155.56	Newton
The Required Mass of Downhole Tool (M_{req}) = $W_{req}/9.81$	=	117.79	kg
The Req. Mass of Downhole Tool in Air = $\frac{M_{req}}{(\rho_{steel} - \rho_{well})} \times \rho_{steel}$	=	**117.80**	kg
Mass of Downhole Tool Available	=	**226.80**	kg **> Req. Mass, OK!!!**

MINIMUM DOWNHOLE TOOL WEIGHT REQUIRED (CASE 2B)

INPUTS:

Wireline Type	=	Monoconductor	
True Vertical Depth (TVD)	=	4289	m
Shut In Well Head Pressure (SIWHP)	=	307.00	bar
Reservoir Fluid Density(ρ_{well})	=	0.700	kg/m^3
Wireline Diameter (OD)	=	0.438	inch
Contact Force at PCH (from OrcaFlex) (N)	=	1276.27	Newton
Coefficient of Friction (assumed) (μ)	=	0.30	mm^2
Steel Density = ρ_{steel}	=	7850.00	kg/m^3

OUTPUTS:

Area of the Wireline (A) = $\pi/4 \times OD^2$	=	96.99	mm^2
Friction (F) = $\mu \times N$	=	382.88	Newton
Force from Pressure (FP) = $SIWHP/A$	=	2977.50	Newton
The Required Weight of Downhole Tool (W_{req}) = $FP + F$	=	3360.38	Newton
The Required Mass of Downhole Tool (M_{req}) = $W_{req}/9.81$	=	342.55	kg
The Req. Mass of Downhole Tool in Air = $\frac{M_{req}}{(\rho_{steel} - \rho_{well})} \times \rho_{steel}$	=	**342.58**	kg
Mass of Downhole Tool Available	=	**544.31**	kg **> Req. Mass, OK!!!**

MINIMUM DOWNHOLE TOOL WEIGHT REQUIRED (CASE 2C)

INPUTS:

Wireline Type	=	Monoconductor	
True Vertical Depth (TVD)	=	4289	m
Shut In Well Head Pressure (SIWHP)	=	307.00	bar
Reservoir Fluid Density(ρ_{well})	=	0.700	kg/m^3
Wireline Diameter (OD)	=	0.438	inch
Contact Force at PCH (from OrcaFlex) (N)	=	1475.82	Newton
Coefficient of Friction (assumed) (μ)	=	0.30	mm^2
Steel Density = ρ_{steel}	=	7850.00	kg/m^3

OUTPUTS:

Area of the Wireline (A) = $\pi/4 \times OD^2$	=	96.99	mm^2
Friction (F) = $\mu \times N$	=	442.75	Newton
Force from Pressure (FP) = $SIWHP/A$	=	2977.50	Newton
The Required Weight of Downhole Tool (W_{req}) = $FP + F$	=	3420.25	Newton
The Required Mass of Downhole Tool (M_{req}) = $W_{req}/9.81$	=	348.65	kg
The Req. Mass of Downhole Tool in Air = $\frac{M_{req}}{(\rho_{steel} - \rho_{well})} \times \rho_{steel}$	=	**348.68**	kg
Mass of Downhole Tool Available	=	**907.18**	kg **> Req. Mass, OK!!!**

Appendix B – Example of using the graph

First graph shows the relationship between measured depths versus top tension and second graph shows the vertical displacements for the case of lowering down 1200 lbs downhole tool using monoconductor cable (case 1B). When the vessel winch reading at surface shows the length of the wireline cable that has been spooled out from vessel winch (measured depth) is 2500 meters, the tension will be 14.259 kN according to the first graph. Then from this tension value, the vertical displacement can be determined by directly reading the second graph. For the tension force of 14.259 kN, the vertical displacement will be 1.48 meters in upward direction due to combination of sea current effect and cable elongation. It means that the actual depth for wireline end point is supposed to be 2498.52 meters.

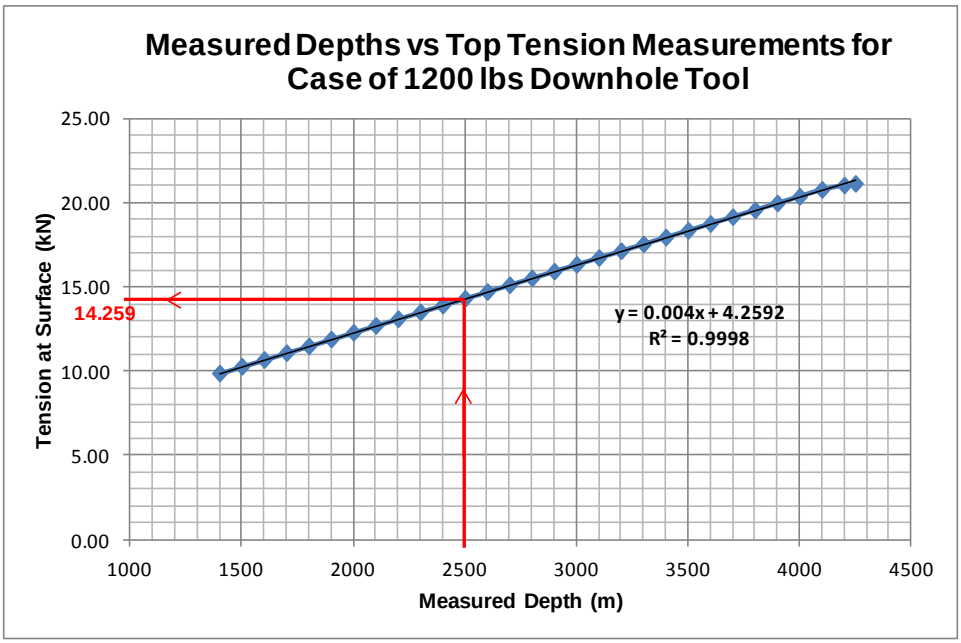

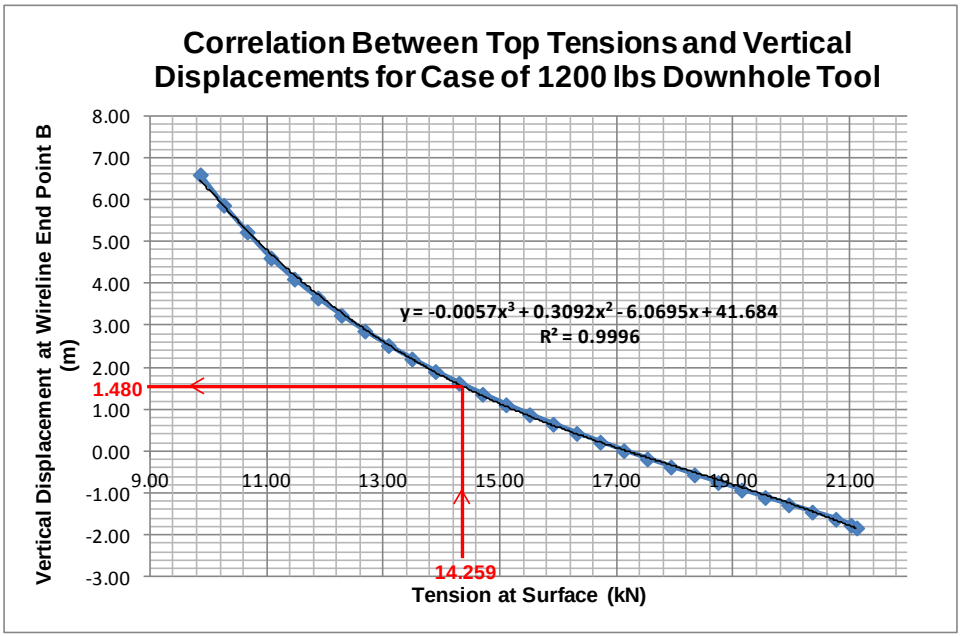

Appendix C – Drag forces on cables

Depth	Current Velocity	Drag Forces	
		Slickline	Monoconductor
(m)	(m/s)	N	N
0	1.38	3.10	10.85
-50	1.06	1.83	6.40
-100	1.02	1.69	5.93
-200	0.9	1.32	4.61
-300	0.77	0.96	3.38
-400	0.76	0.94	3.29
-500	0.63	0.65	2.26
-600	0.51	0.42	1.48
-800	0.54	0.47	1.66
-1000	0.53	0.46	1.60
-1200	0.53	0.46	1.60
-1300	0.47	0.36	1.26

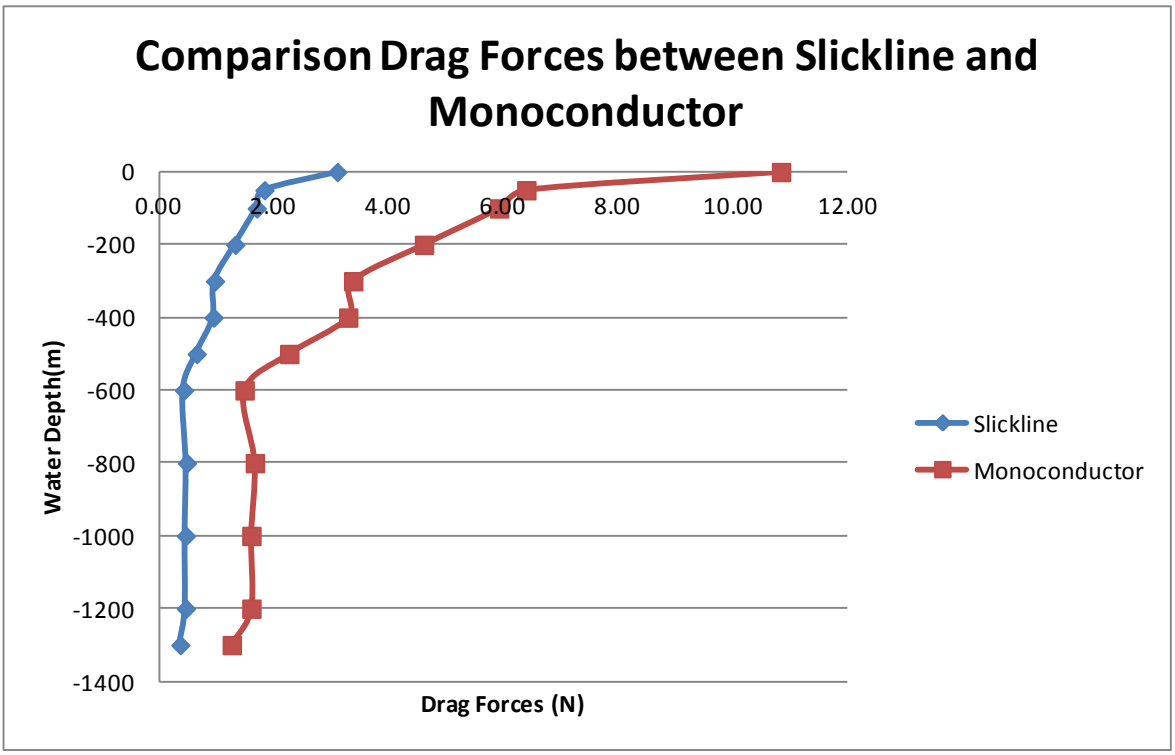

Appendix D – OrcaFlex analysis results

The analysis results presented in this Appendix are for the well depth of 100 meters and 1500 meters below the seabed. The remaining analysis results can be seen in OrcaFlex file included in the DVD. The OrcaFlex files are with extension .dat and .sim extension. The models in OrcaFlex are saved in .dat and the simulation files are saved in .sim. Then the analysis results were extracted and processed using a spreadsheet which is put in the same folder as OrcaFlex files for each of case.

In this project, there are two important analysis results directly generated by OrcaFlex software after running the dynamic simulations for each case:

1. Time history graphs
   The time history graphs plot the relation between time and motion amplitude of the downhole tool over the time period during wireline operation.
2. Range graphs
   Range graphs are used to present the OrcaFlex analysis results for wireline solid contact force, effective tension, and deflection along the wireline arc length.

OrcaFlex Analysis Results of Case 1A for 100 meters Well Depth

Case 1A: Range Graph for Wireline Deflection

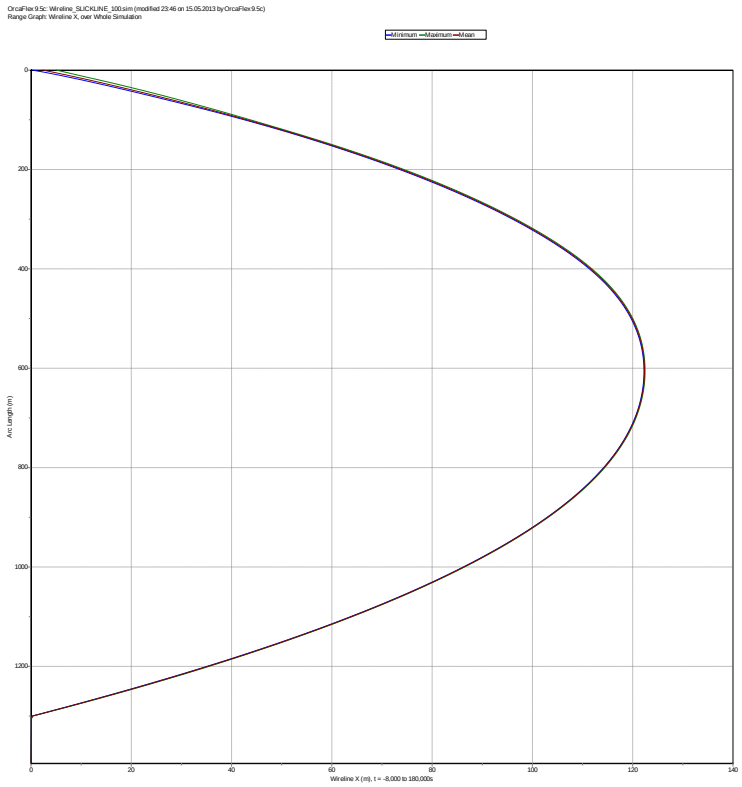

Case 1A: Range Graph for Wireline Effective Tension

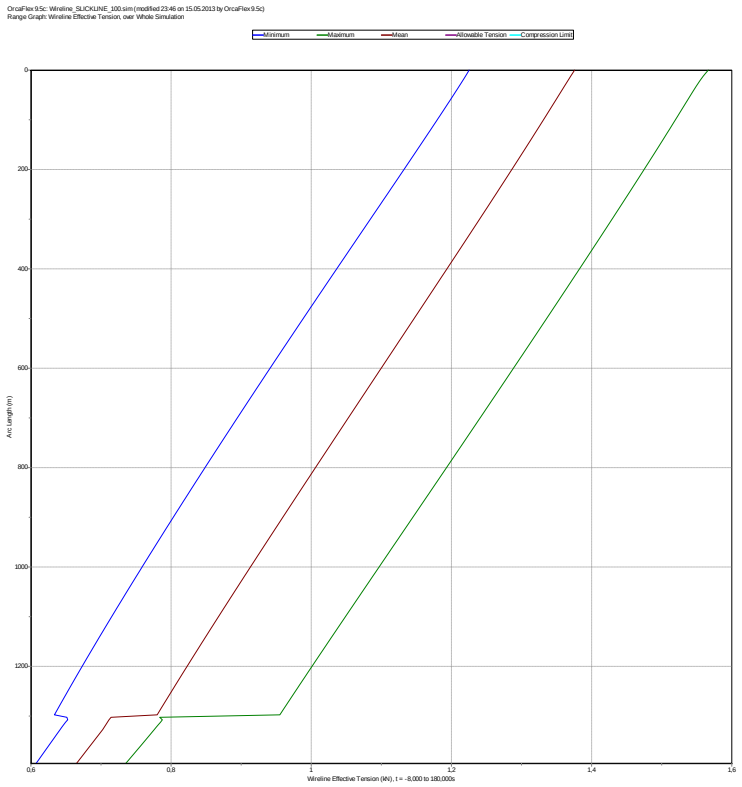

OrcaFlex Analysis Results of Case 1A for 100 meters Well Depth

Case 1A: Time History for Wireline Vertical Displacement at End B

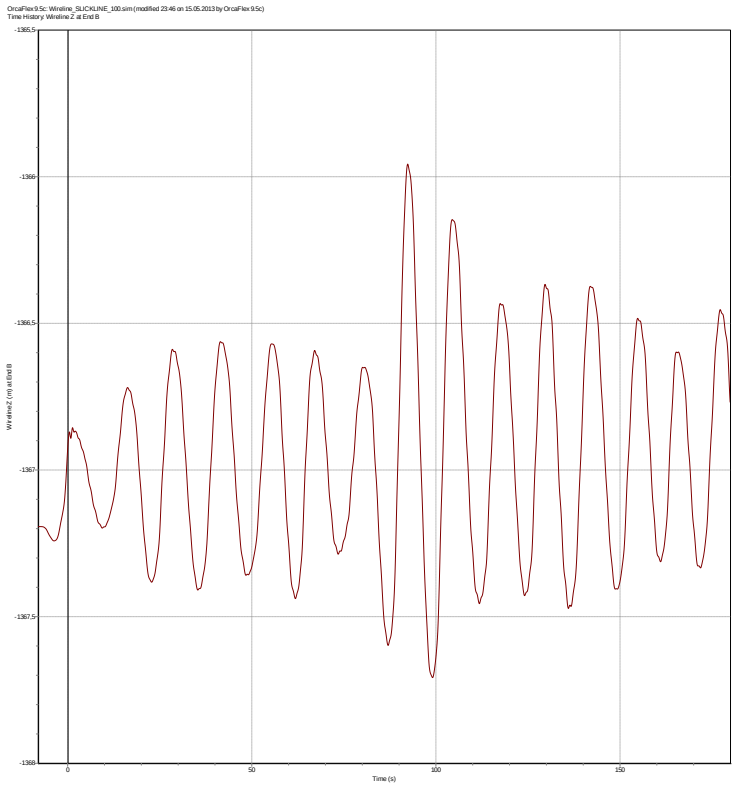

Case 1A: Range Graph for Wireline Solid Contact Force

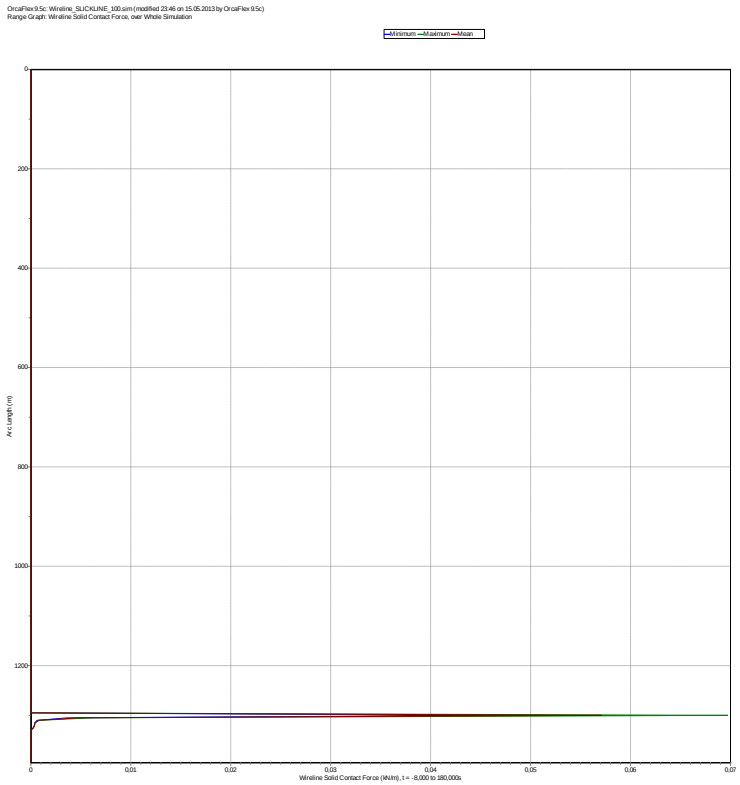

OrcaFlex Analysis Results of Case 1A for 1500 meters Well Depth

Case 1A: Range Graph for Wireline Deflection

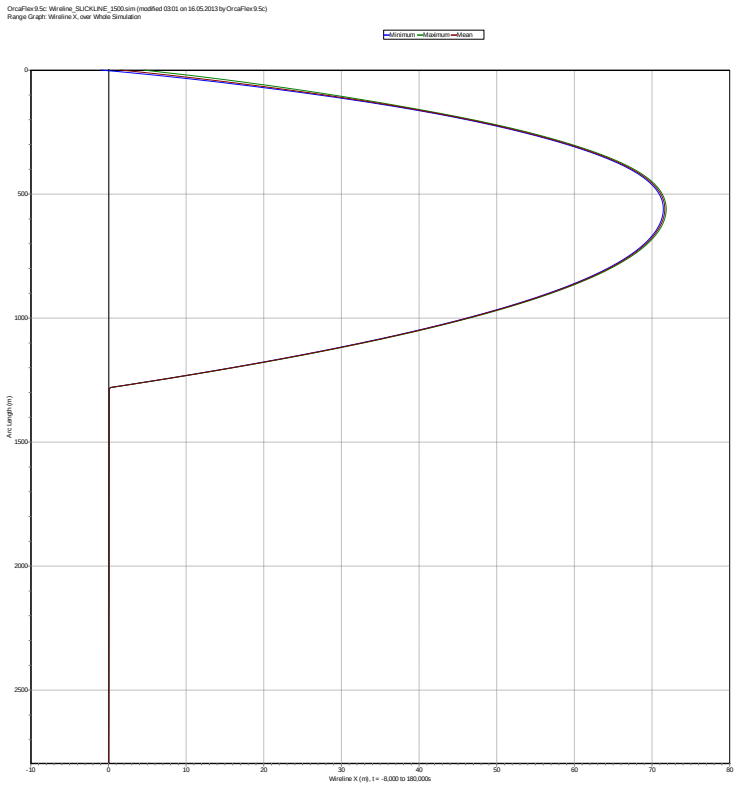

Case 1A: Range Graph for Wireline Effective Tension

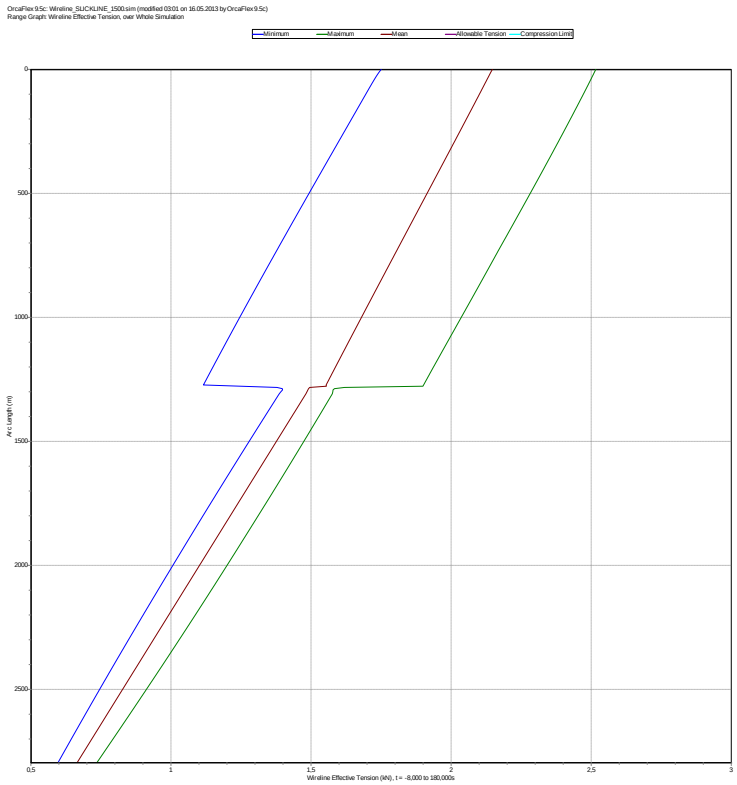

OrcaFlex Analysis Results of Case 1A for 1500 meters Well Depth

Case 1A: Time History for Wireline Vertical Displacement at End B

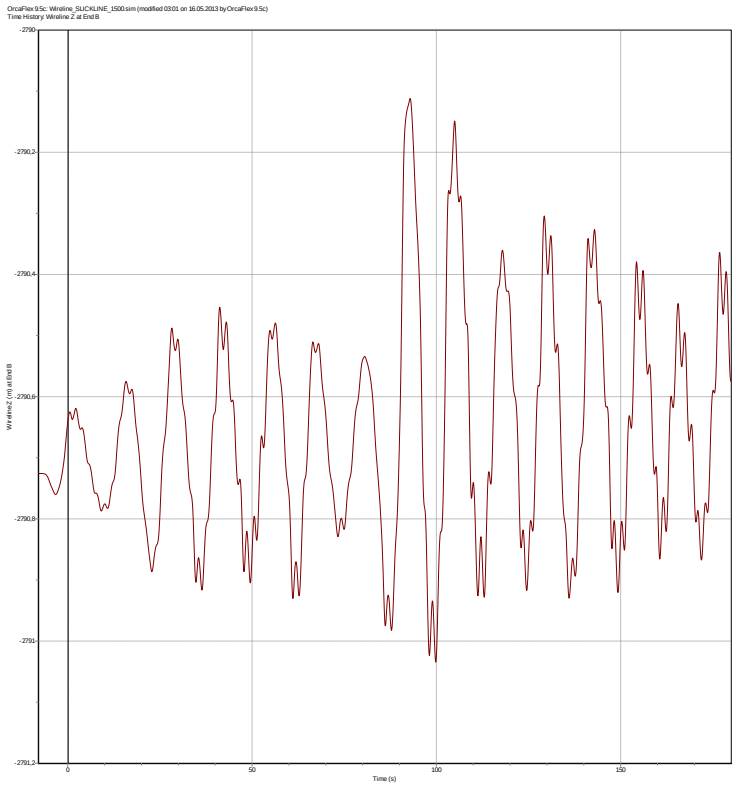

Case 1A: Range Graph for Wireline Solid Contact Force

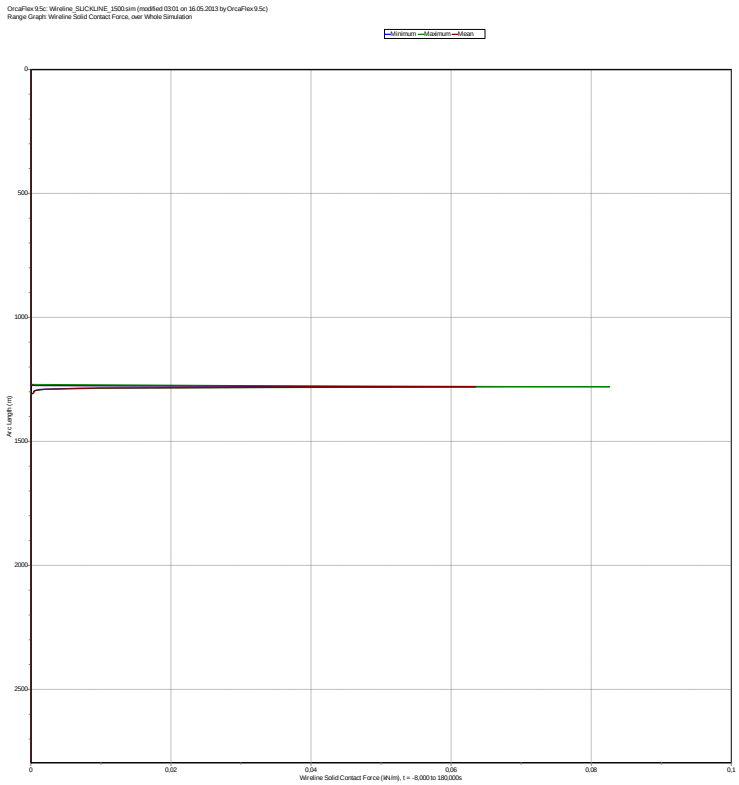

OrcaFlex Analysis Results of Case 1B for 100 meters Well Depth

Case 1B: Range Graph for Wireline Deflection

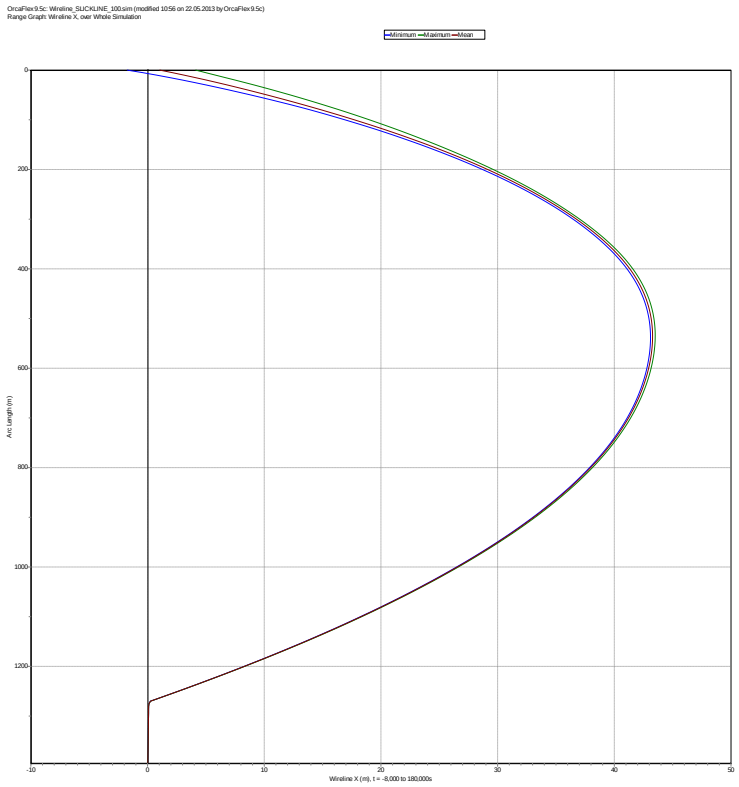

Case 1B: Range Graph for Wireline Effective Tension

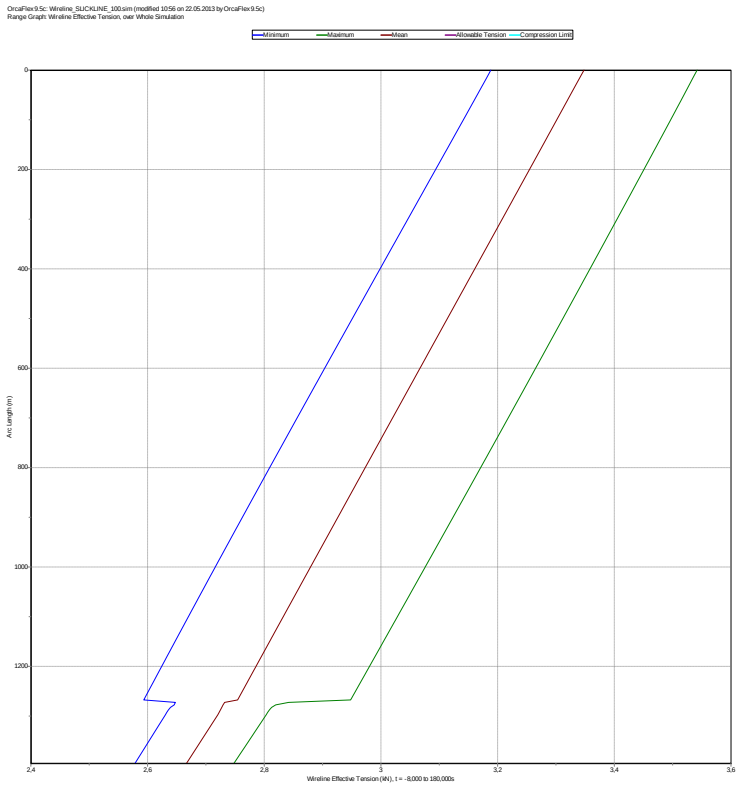

OrcaFlex Analysis Results of Case 1B for 100 meters Well Depth

Case 1B: Time History for Wireline Vertical Displacement at End B

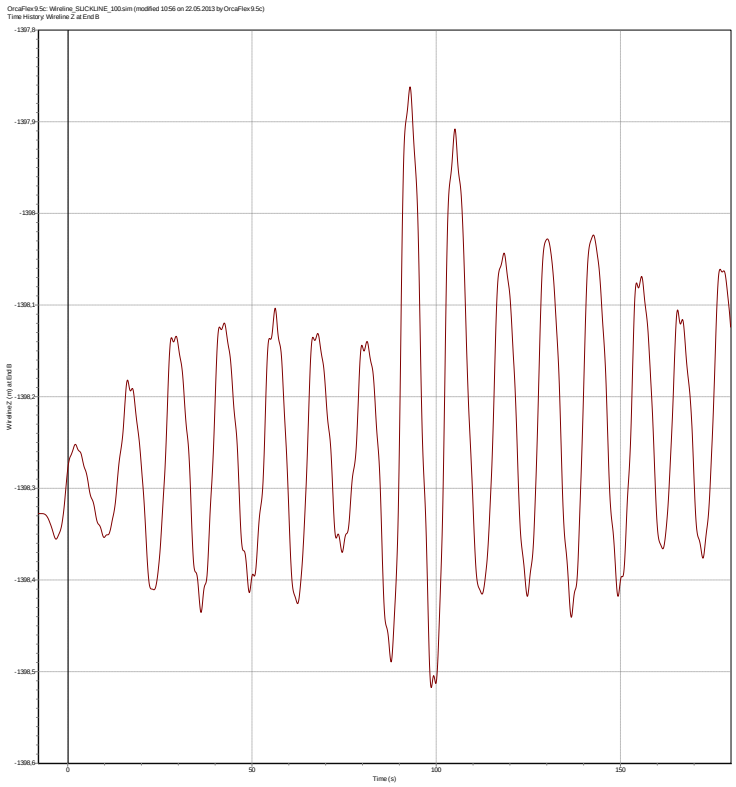

Case 1B: Range Graph for Wireline Solid Contact Force

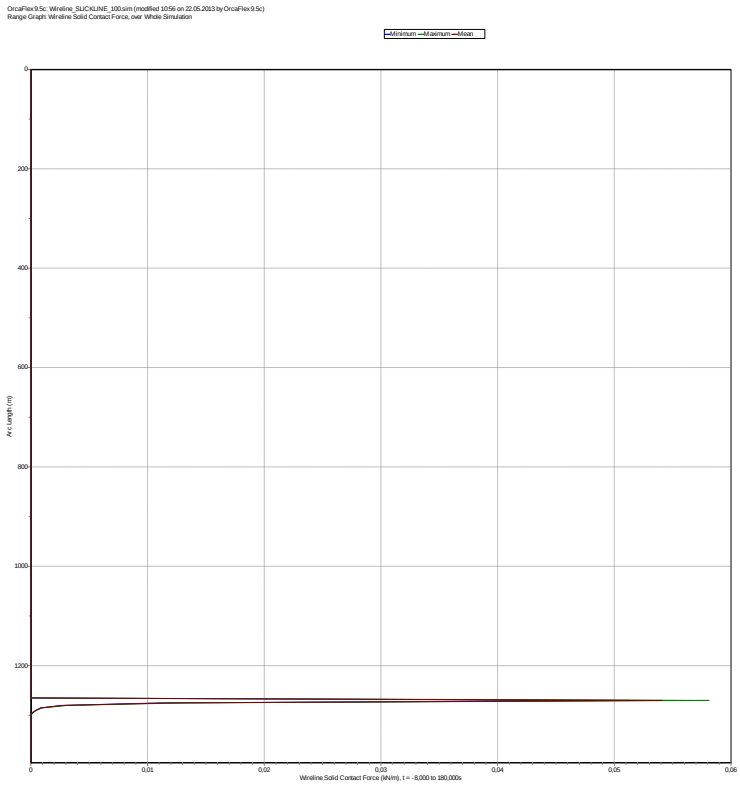

OrcaFlex Analysis Results of Case 1B for 1500 meters Well Depth

Case 1B: Range Graph for Wireline Deflection

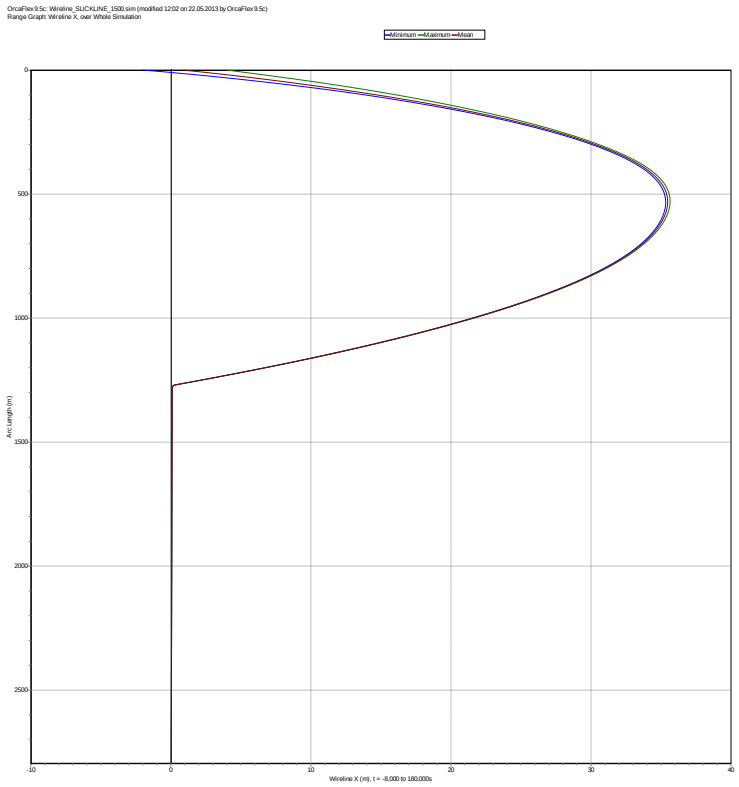

Case 1B: Range Graph for Wireline Effective Tension

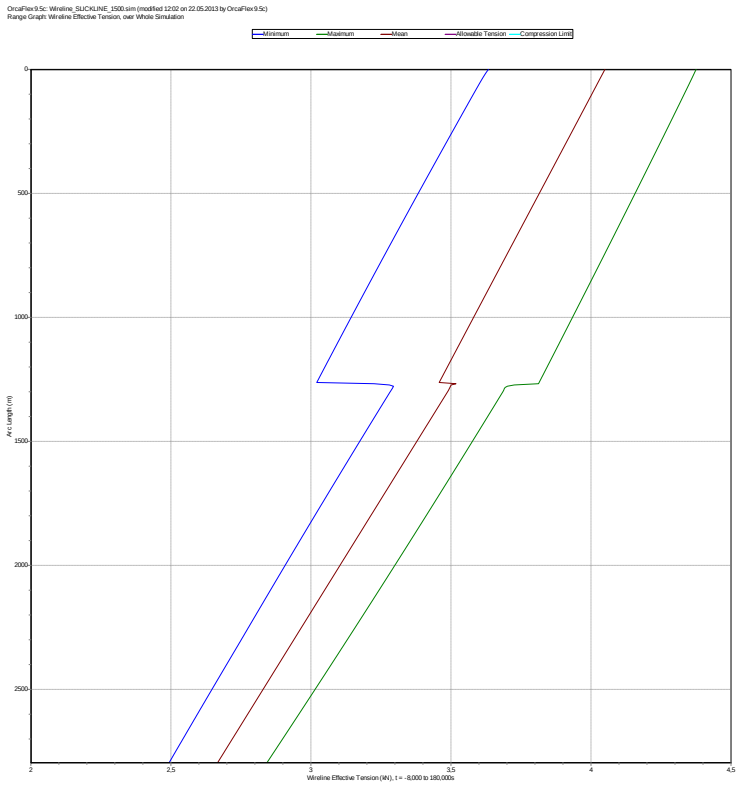

OrcaFlex Analysis Results of Case 1B for 1500 meters Well Depth

Case 1B: Time History for Wireline Vertical Displacement at End B

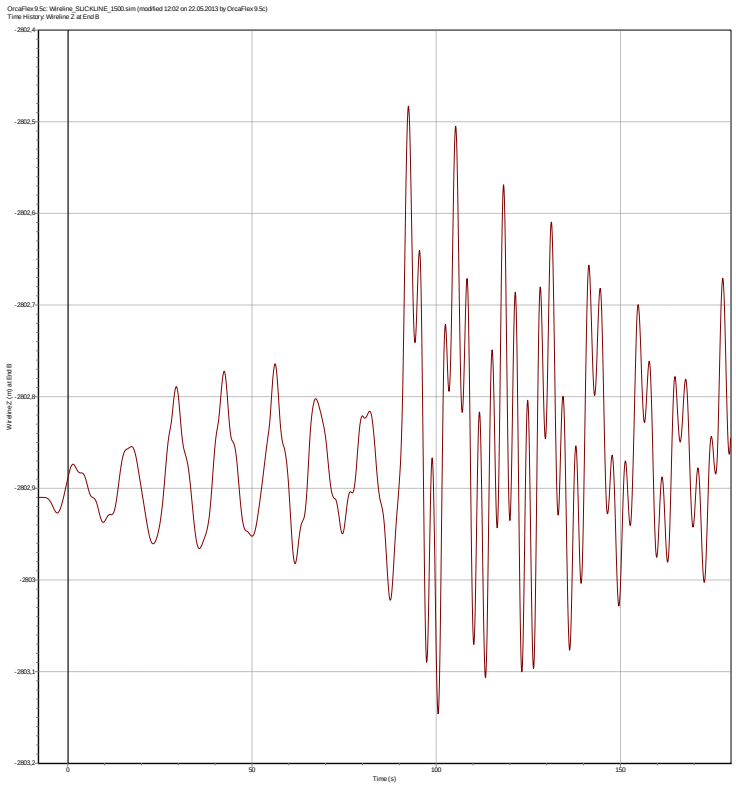

Case 1B: Range Graph for Wireline Solid Contact Force

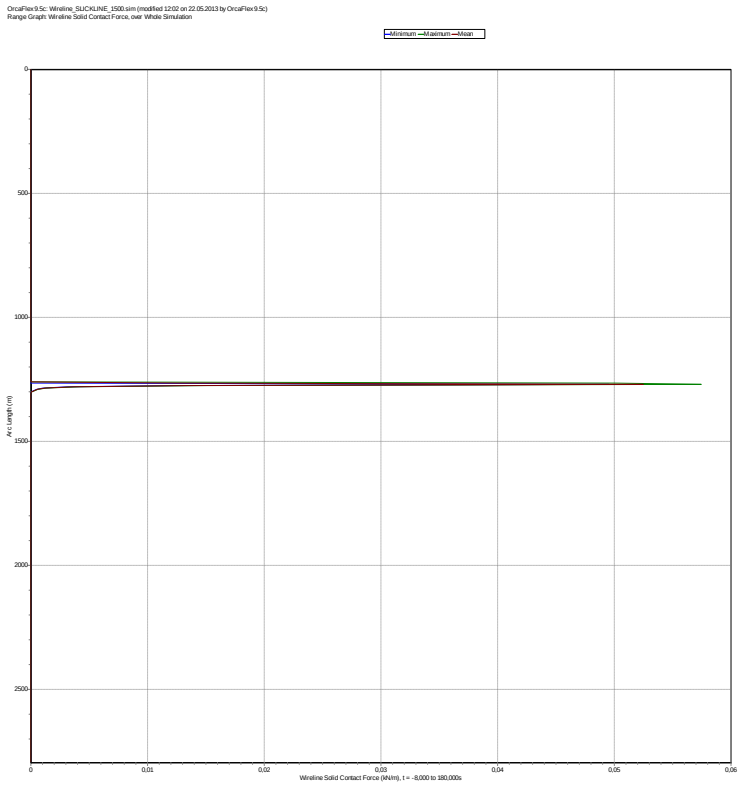

OrcaFlex Analysis Results of Case 1C for 100 meters Well Depth

Case 1C: Range Graph for Wireline Deflection

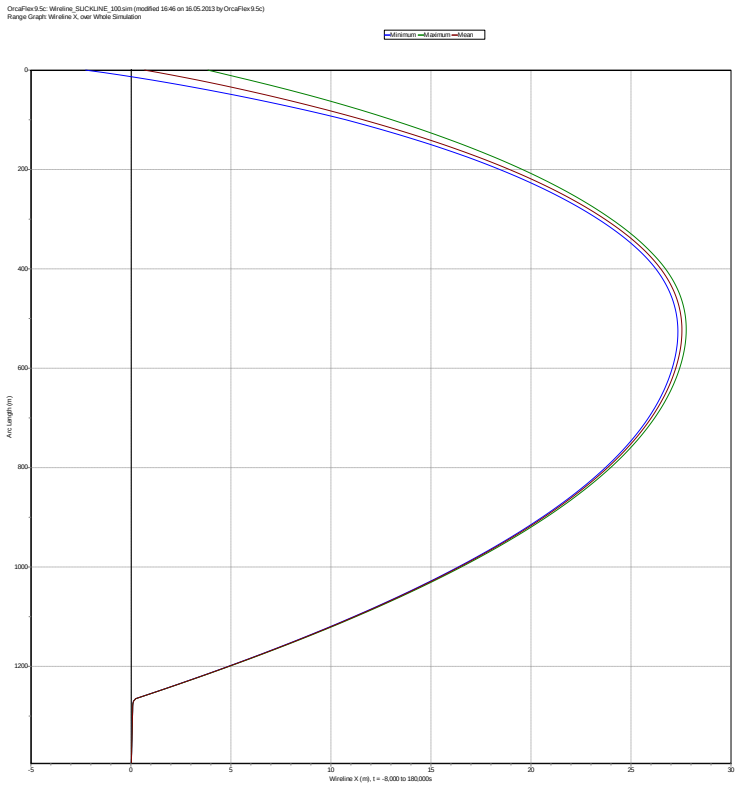

Case 1C: Range Graph for Wireline Effective Tension

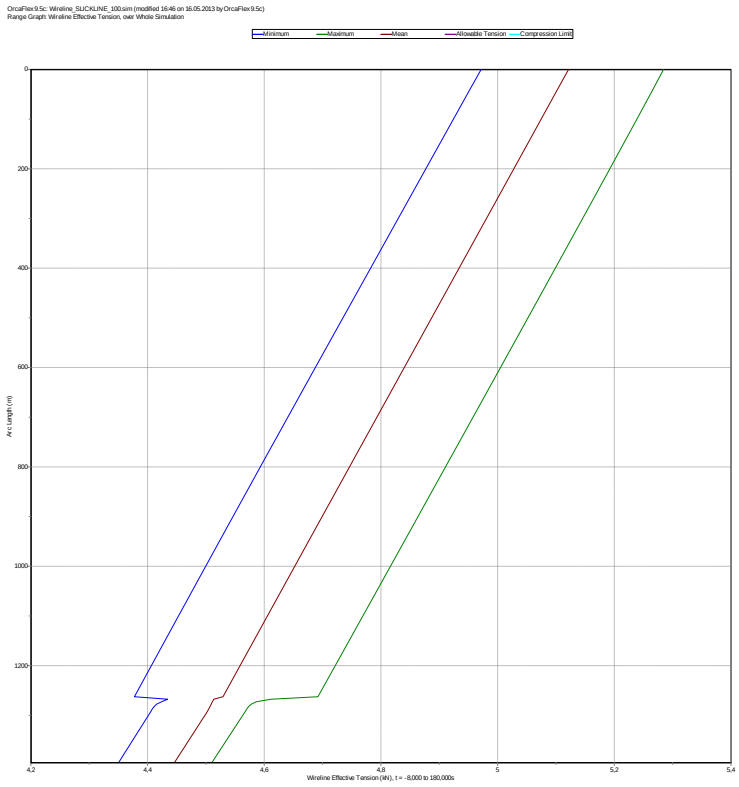

OrcaFlex Analysis Results of Case 1C for 100 meters Well Depth

Case 1C: Time History for Wireline Vertical Displacement at End B

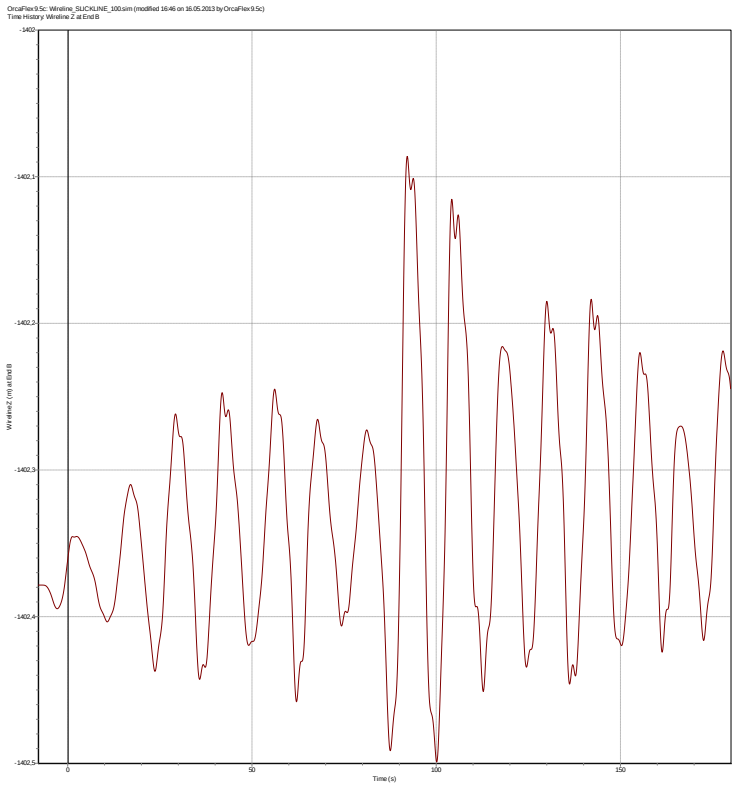

Case 1C: Range Graph for Wireline Solid Contact Force

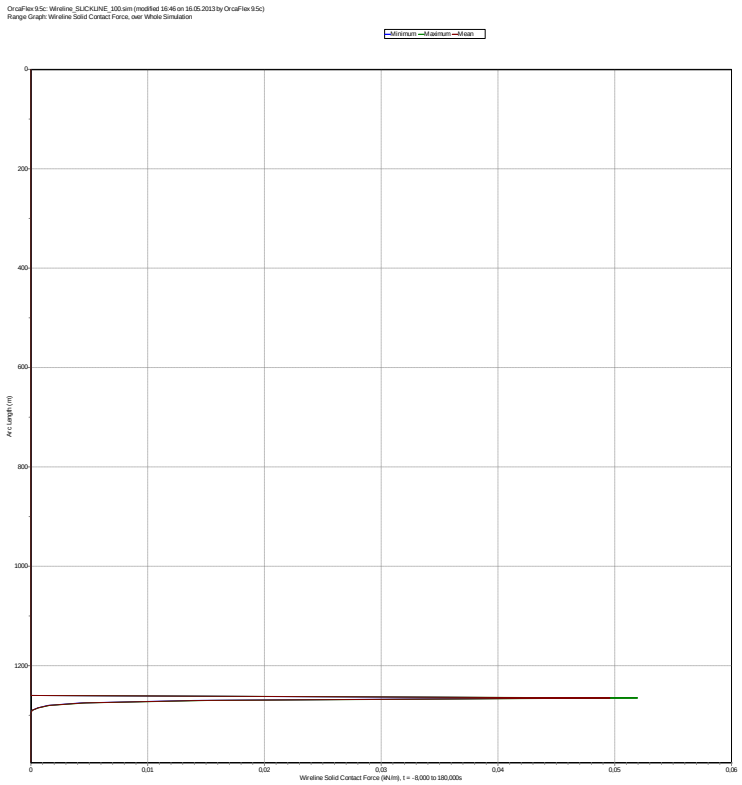

OrcaFlex Analysis Results of Case 1C for 1500 meters Well Depth

Case 1C: Range Graph for Wireline Deflection

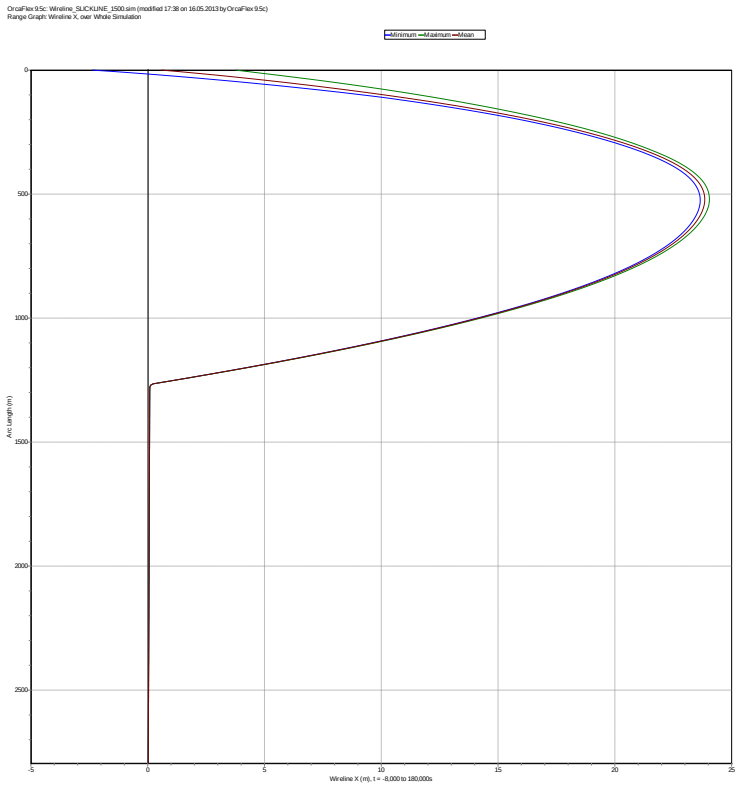

Case 1C: Range Graph for Wireline Effective Tension

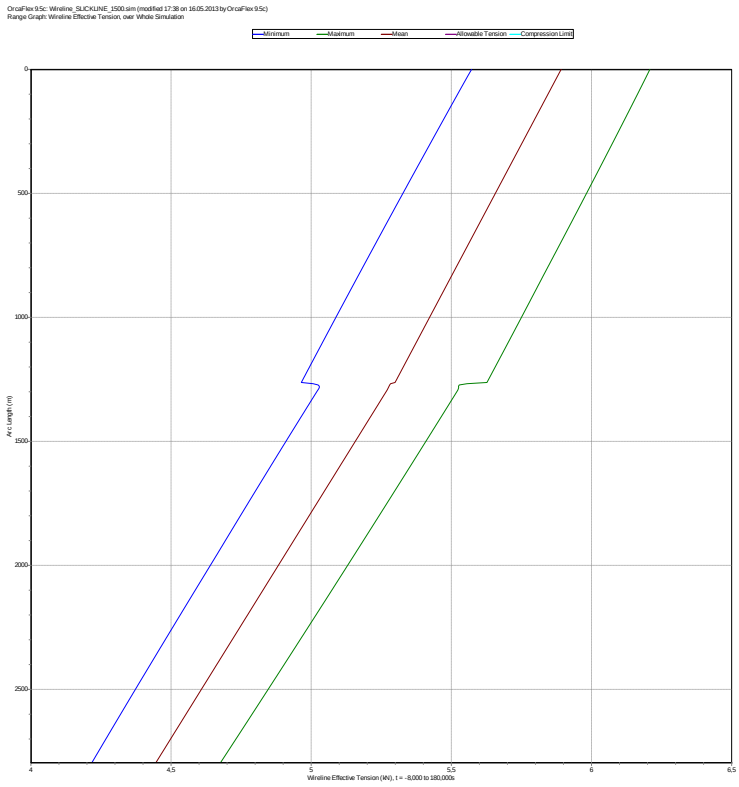

OrcaFlex Analysis Results of Case 1C for 1500 meters Well Depth

Case 1C: Time History for Wireline Vertical Displacement at End B

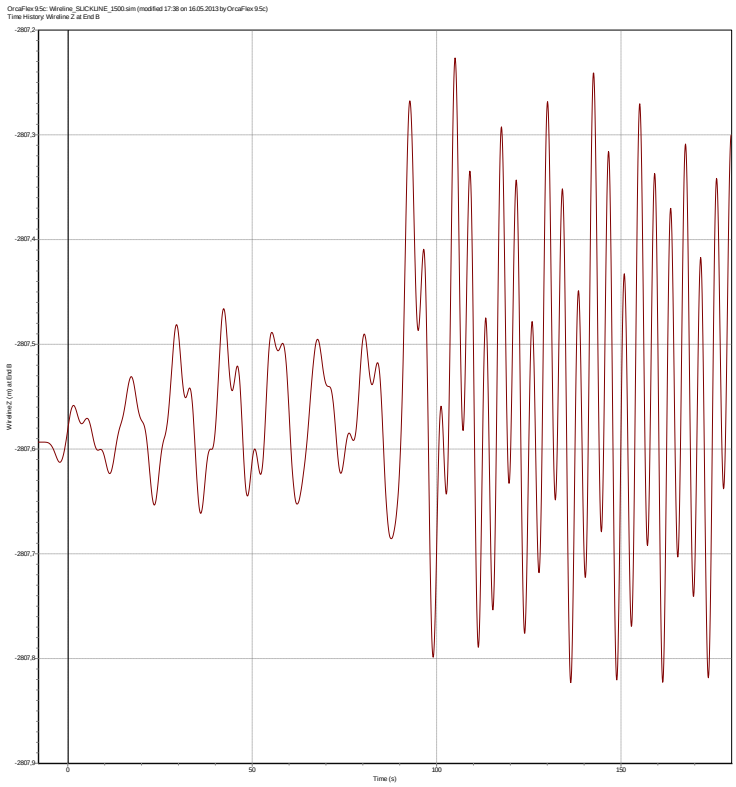

Case 1C: Range Graph for Wireline Solid Contact Force

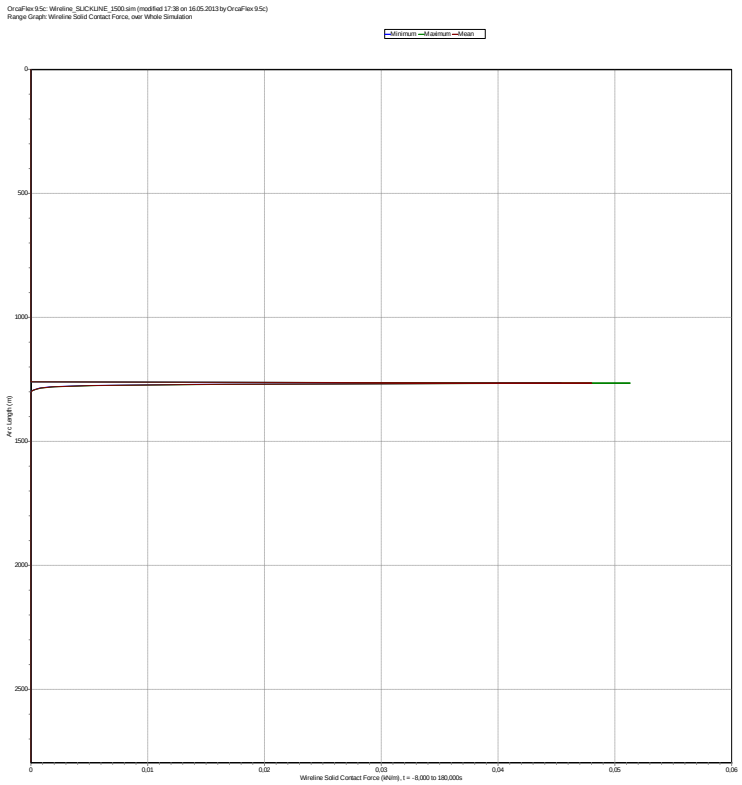

OrcaFlex Analysis Results of Case 2A for 100 meters Well Depth

Case 2A: Range Graph for Wireline Deflection

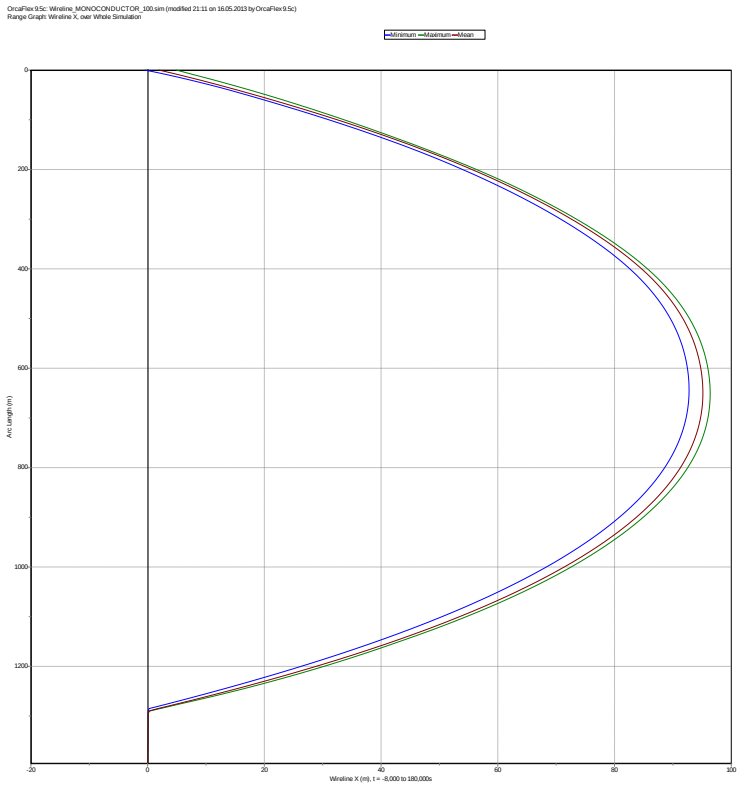

Case 2A: Range Graph for Wireline Effective Tension

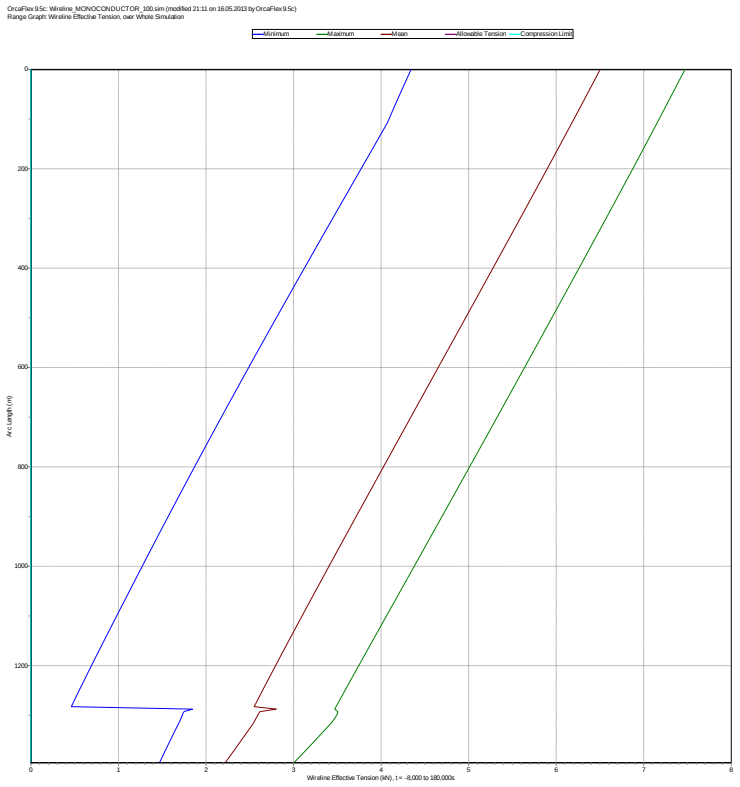

OrcaFlex Analysis Results of Case 2A for 100 meters Well Depth

Case 2A: Time History for Wireline Vertical Displacement at End B

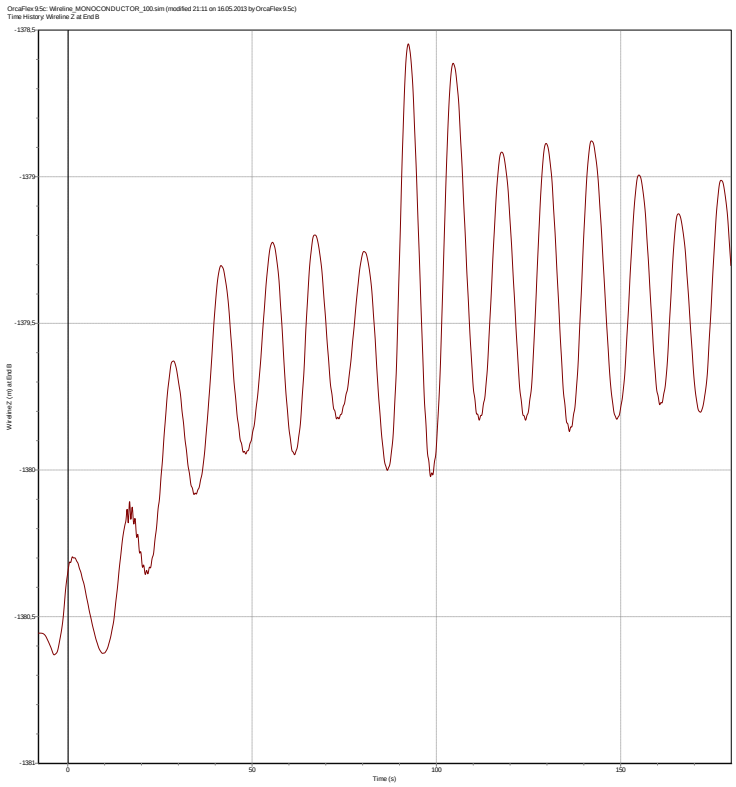

Case 2A: Range Graph for Wireline Solid Contact Force

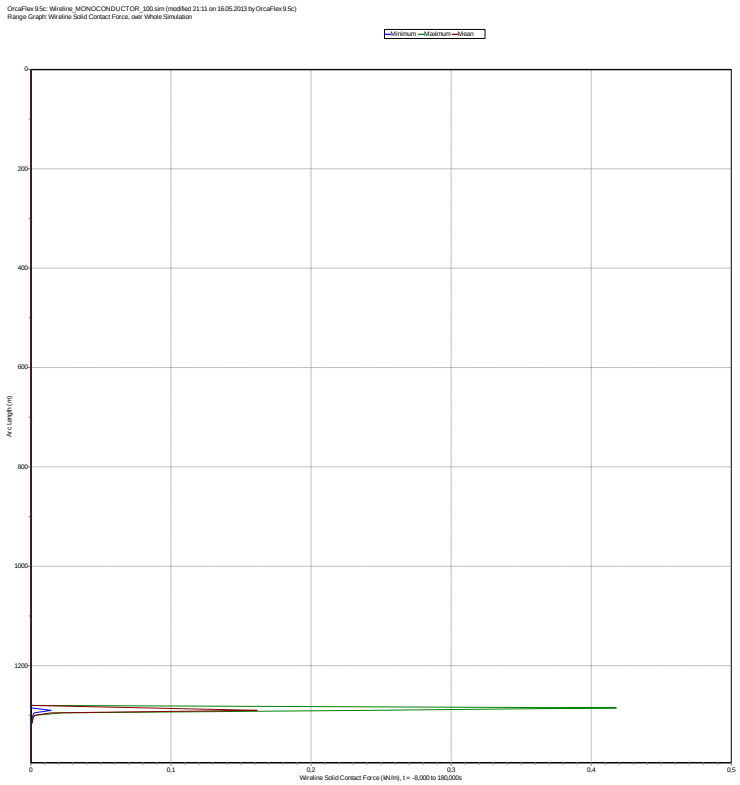

OrcaFlex Analysis Results of Case 2A for 1500 meters Well Depth

Case 2A: Range Graph for Wireline Deflection

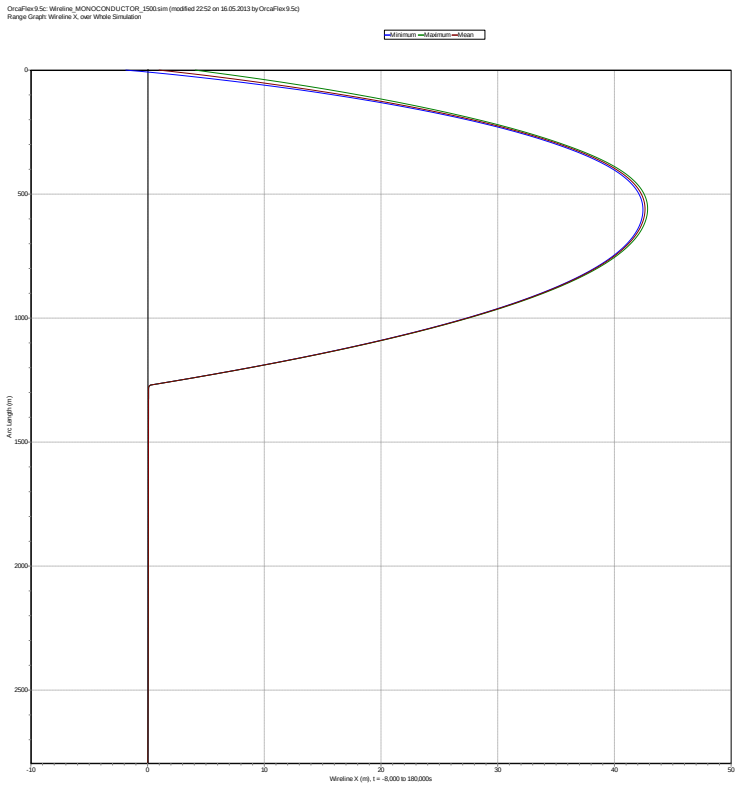

Case 2A: Range Graph for Wireline Effective Tension

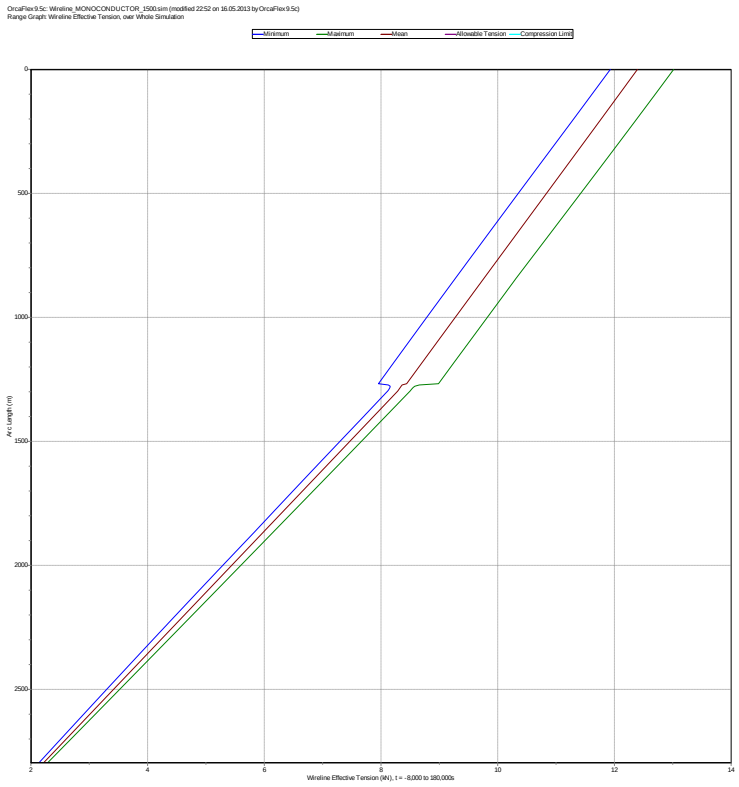

OrcaFlex Analysis Results of Case 2A for 1500 meters Well Depth

Case 2A: Time History for Wireline Vertical Displacement at End B

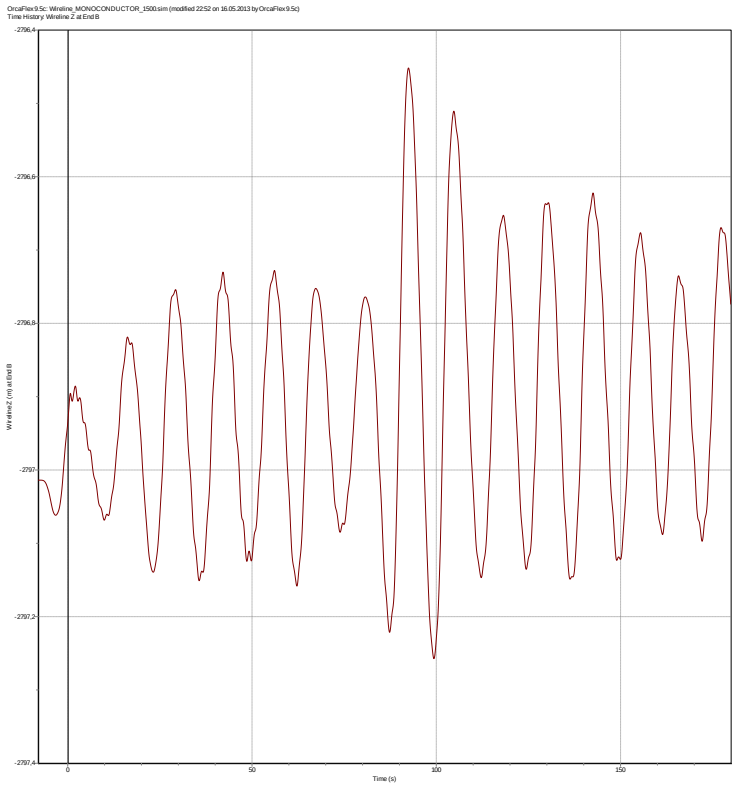

Case 2A: Range Graph for Wireline Solid Contact Force

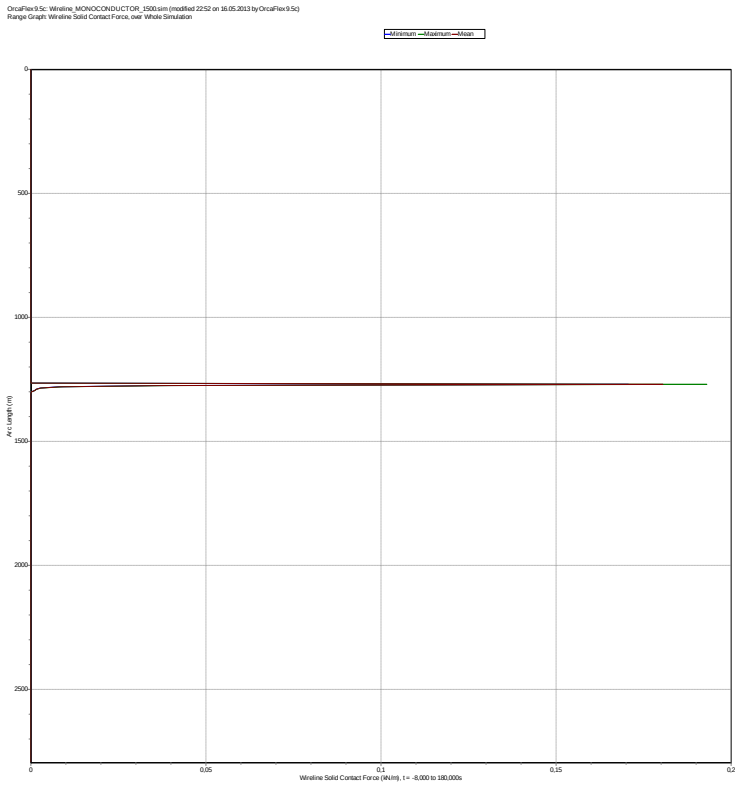

OrcaFlex Analysis Results of Case 2B for 100 meters Well Depth

Case 2B: Range Graph for Wireline Deflection

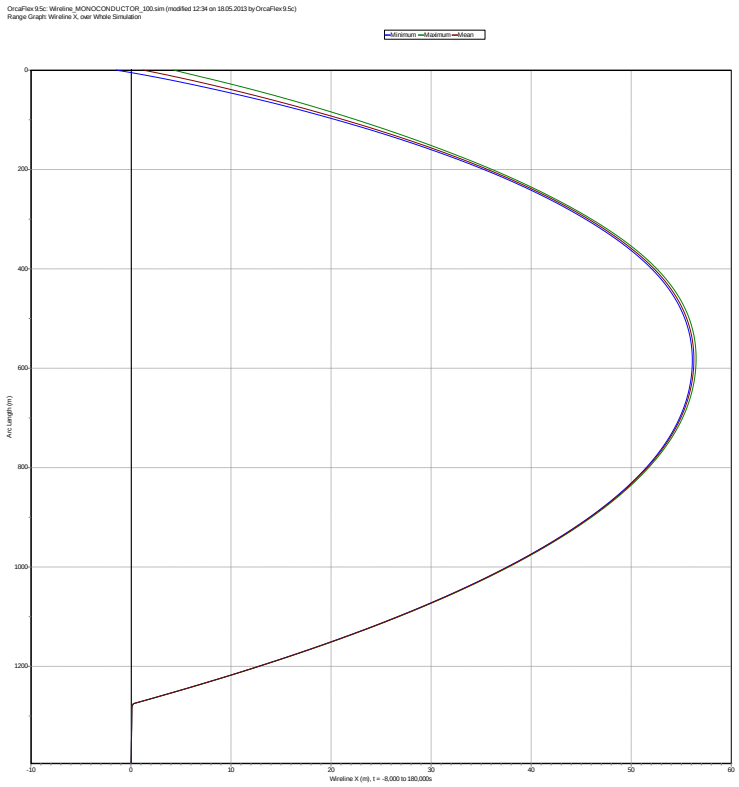

Case 2B: Range Graph for Wireline Effective Tension

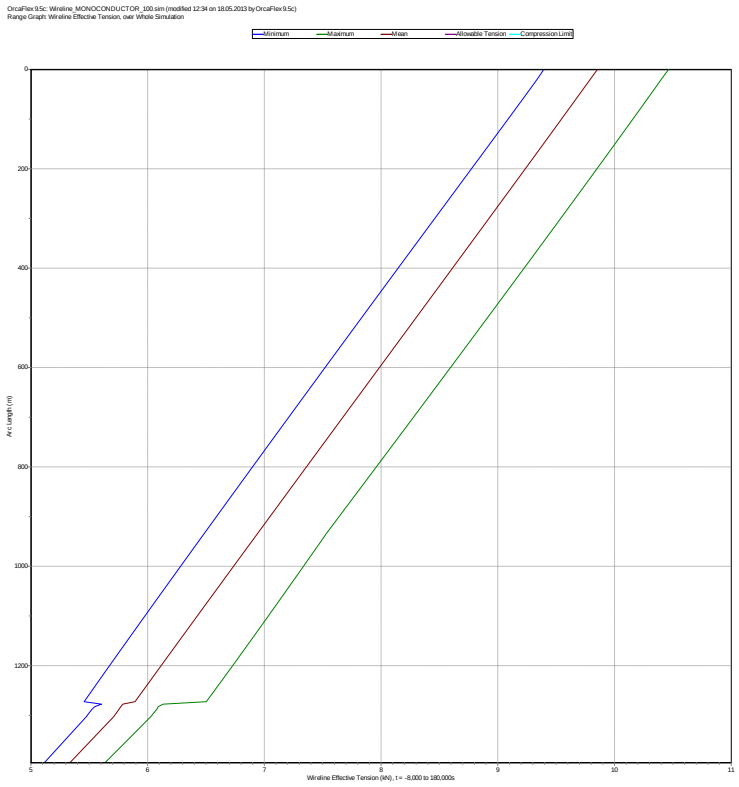

OrcaFlex Analysis Results of Case 2B for 100 meters Well Depth

Case 2B: Time History for Wireline Vertical Displacement at End B

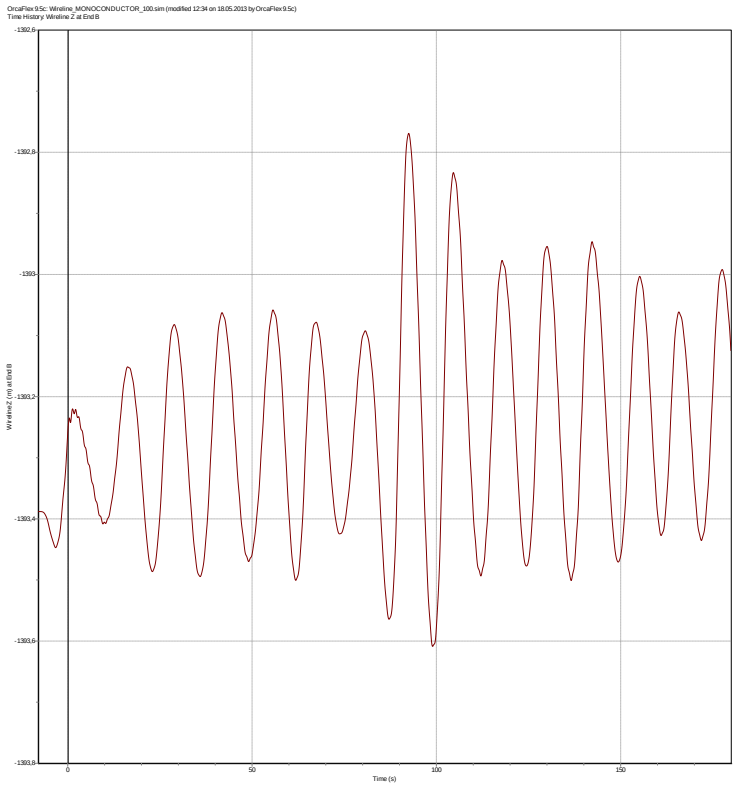

Case 2B: Range Graph for Wireline Solid Contact Force

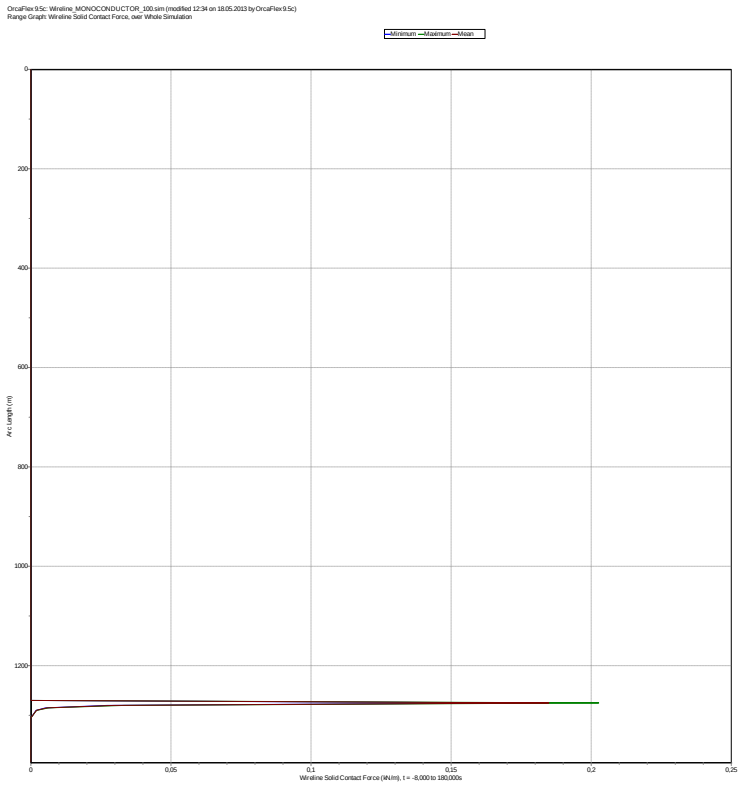

OrcaFlex Analysis Results of Case 2B for 1500 meters Well Depth

Case 2B: Range Graph for Wireline Deflection

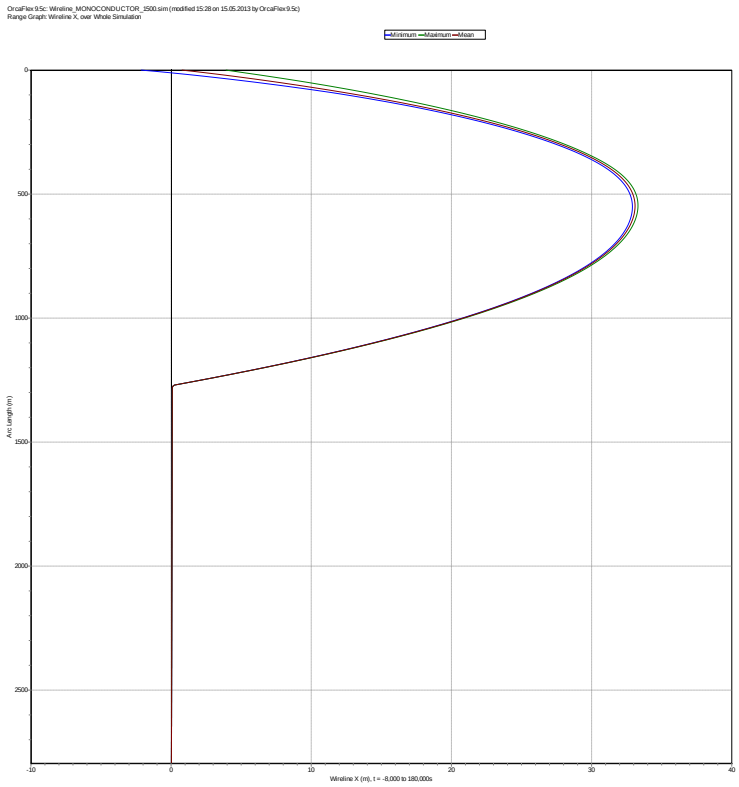

Case 2B: Range Graph for Wireline Effective Tension

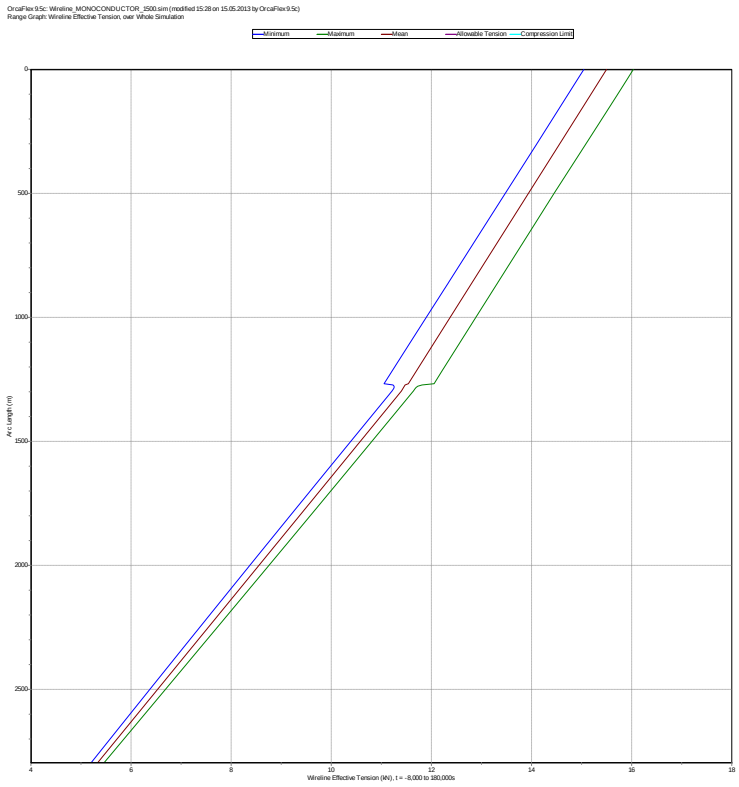

OrcaFlex Analysis Results of Case 2B for 1500 meters Well Depth

Case 2B: Time History for Wireline Vertical Displacement at End B

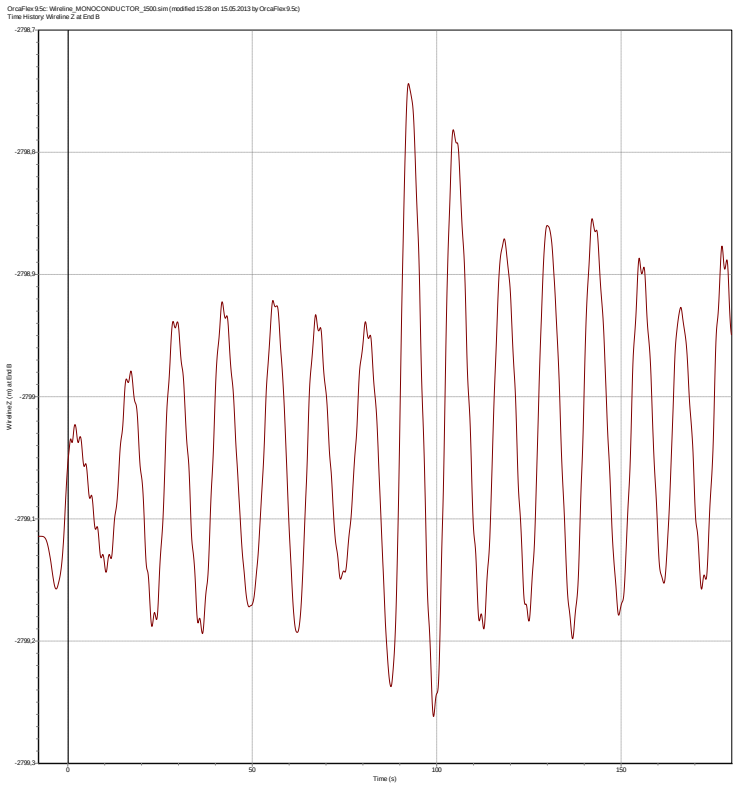

Case 2B: Range Graph for Wireline Solid Contact Force

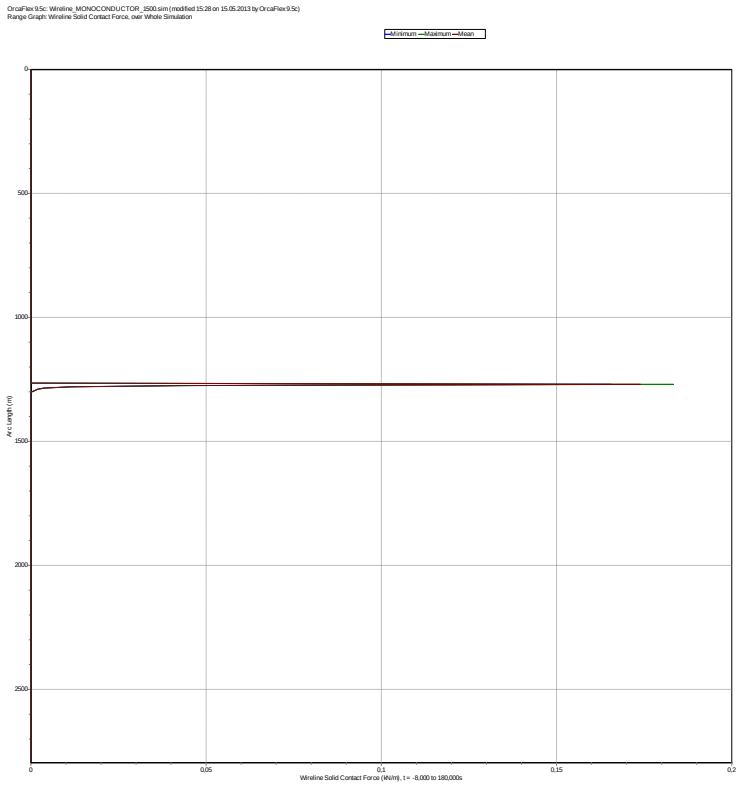

OrcaFlex Analysis Results of Case 2C for 100 meters Well Depth

Case 2C: Range Graph for Wireline Deflection

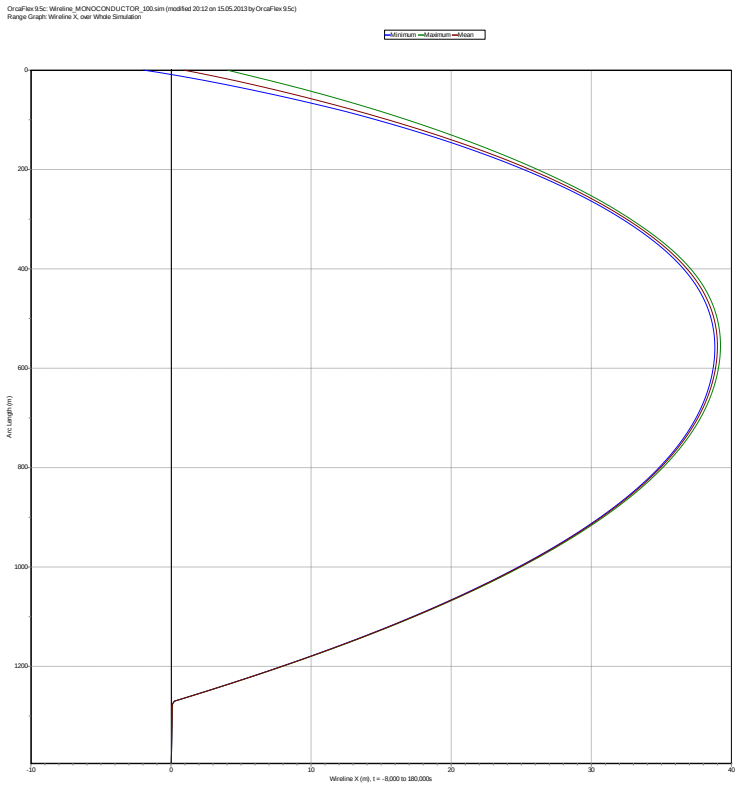

Case 2C: Range Graph for Wireline Effective Tension

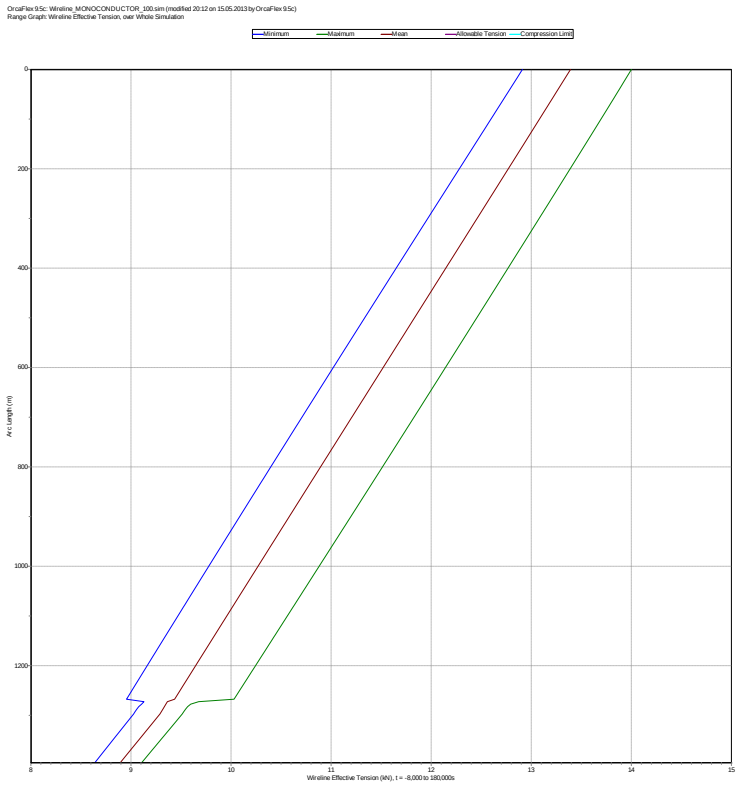

OrcaFlex Analysis Results of Case 2C for 100 meters Well Depth

Case 2C: Time History for Wireline Vertical Displacement at End B

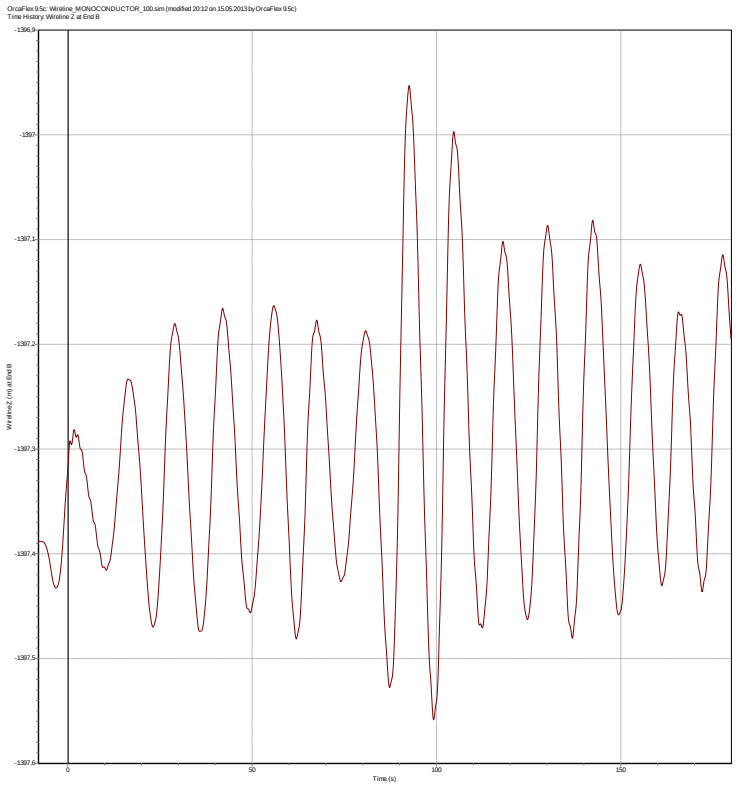

Case 2C: Range Graph for Wireline Solid Contact Force

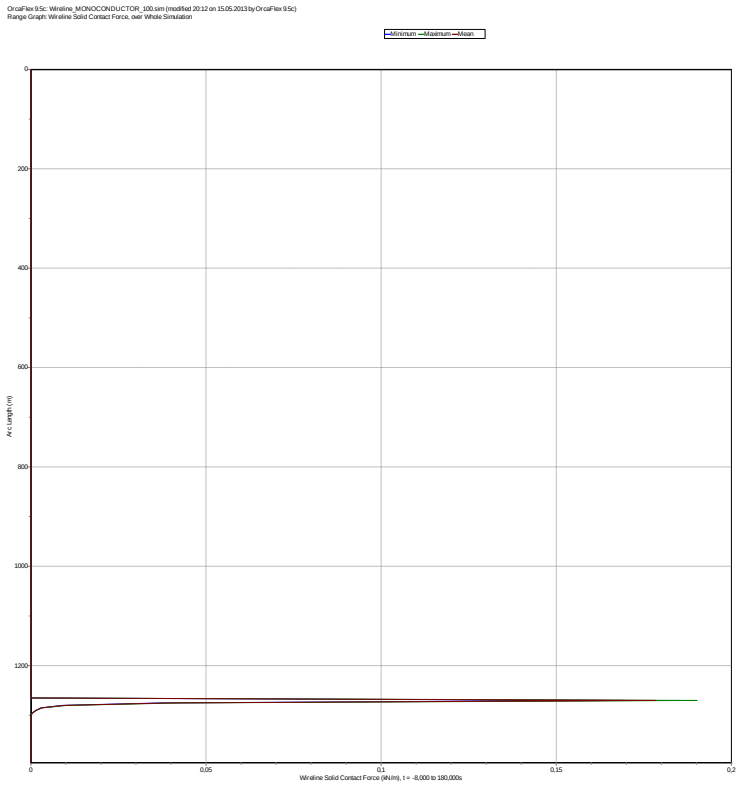

OrcaFlex Analysis Results of Case 2C for 1500 meters Well Depth

Case 2C: Range Graph for Wireline Deflection

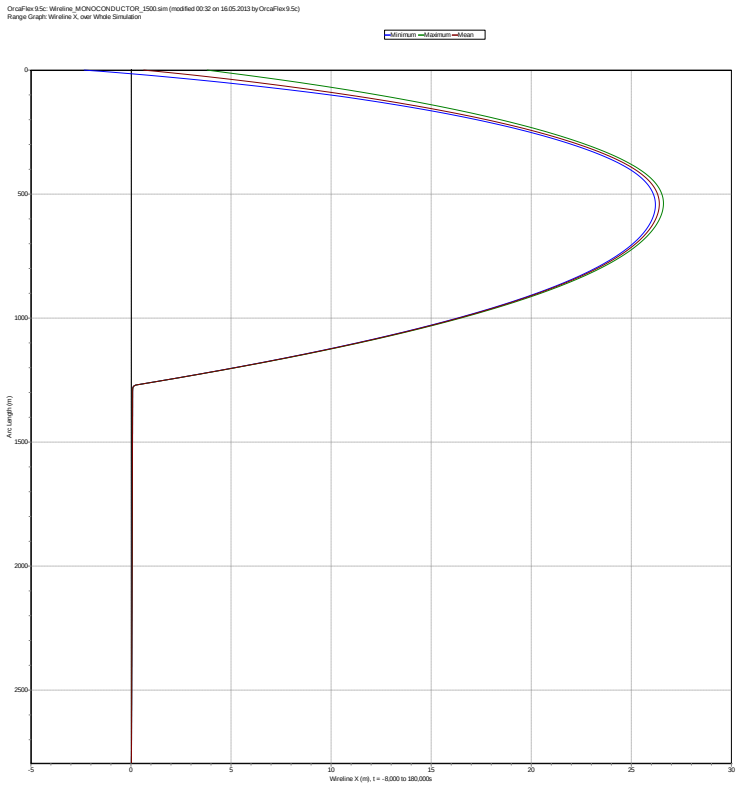

Case 2C: Range Graph for Wireline Effective Tension

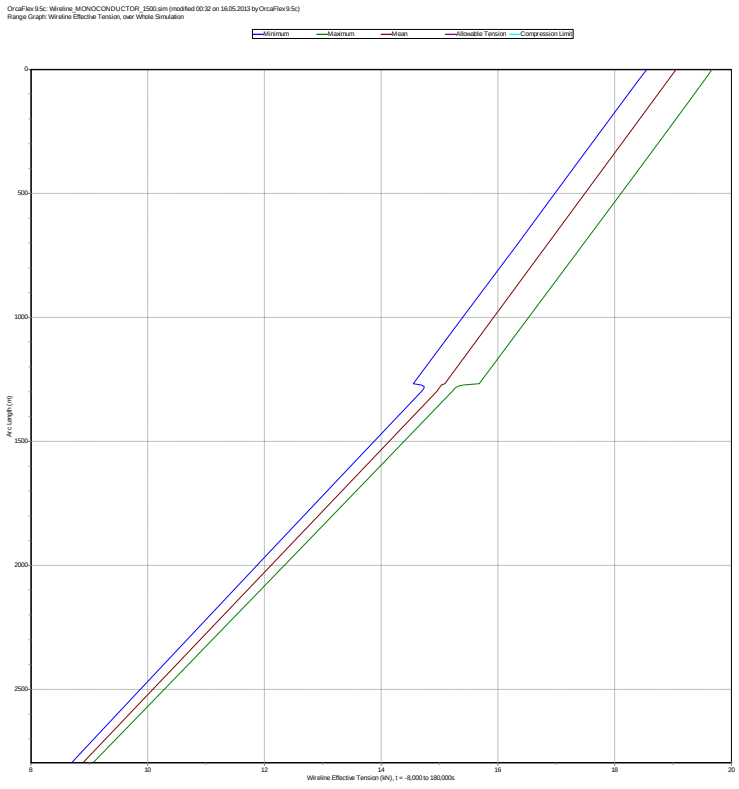

OrcaFlex Analysis Results of Case 2C for 1500 meters Well Depth

Case 2C: Time History for Wireline Vertical Displacement at End B

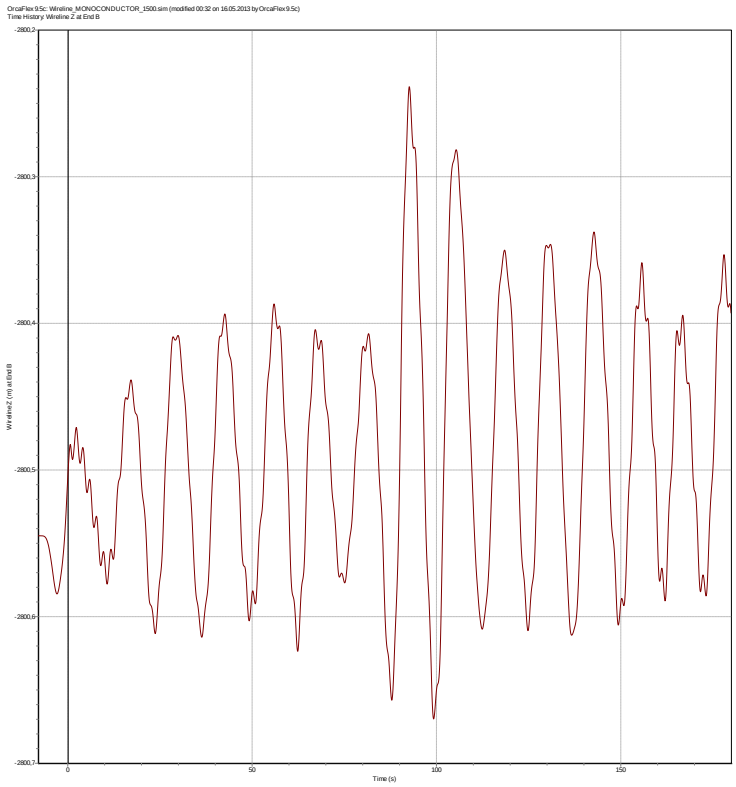

Case 2C: Range Graph for Wireline Solid Contact Force